Norwegian University
of Life Sciences

Master's Thesis 2021 60 ECTS
Faculty of Chemistry, Biotechnology and Food Science

Microbes meet real-life: understanding how denitrifying bacteria handle nutrient limitation – a prerequisite for novel N_2O mitigation options

Silje Kvist Simonsen
Biotechnology

Acknowledgements

During my work with this thesis, I have found great inspiration in comparing my experiences with Frodo Baggins' long journey to Mordor from The Lord of the Rings. Much like Frodo, I would not have gotten far without my trusted fellowship. Just as Gandalf and Aragorn were Frodo's most important advisors, Åsa Frostegård and Lars Bakken have been mine. They guided me onto my journey, and kept my course steady. I would like to offer a special thanks to Åsa Frostegård, my main supervisor. Not only have you offered me your knowledge and your passion for the field of research, but you have shown the amazing capability of giving me enough support to feel safe, whilst constantly pushing me to perform my best. Thank you.

Frodo also received help from a handful of skilled warriors – Legolas, Gimli and Boromir. I have likewise been so lucky as to work in the Nitrogen Group and the research group for Microbial Ecology and Physiology. Thank you all for welcoming me in, inviting me into the social life in the lab, and sharing your knowledge and support.

Frodo always had support from his own kin, the hobbits Merry and Pippin. I offer a sincere thank you to my housemates, friends, and family for believing in me and pushing me on, even though you did not understand what I was writing about.

Last, but certainly not least, Frodo would not have gotten far without Sam. I would like to offer a very warm thank you to Yuan Gao, aka Emma, my supervisor in the lab. You took me in with a smile, patiently answered all my questions and helped improve my laboratory techniques immensely. Thank you.

Samandrag

Dinitrogenoksid (N_2O) er den tredje viktigaste klimagassen etter CO_2 og metan, og er ein viktig bidragsyter til øydeleggingа av ozonlaget. Globale N_2O-utslipp er aukande, og mesteparten av utsleppa som er knytt til menneskeleg aktivitet kjem frå denitrifikasjon i landbruksjord. Denitrifikasjon er ein anaerob respirasjonsstrategi som finst hos mange mikroorganismar. Fullstendig denitrifikasjon er ein stegvis reduksjon av nitrat (NO_3^-) via nitritt (NO_2^-), nitrogenmonoksid (NO) og dinitrogenoksid (N_2O) til dinitrogengass (N_2). Kvart av reduksjonsstega er katalysert av ei gruppe denitrifikasjonsreduktaser, høvesvis Nar og/eller Nap, NirS eller NirK, Nor og NosZ klade I eller klade II. NosZ er det einaste enzymet som er kjend å kunne redusera N_2O til N_2, og det finst berre i prokaryotar. Bakteriar kan dermed tene som soldatar i kampen mot aukande N_2O-utslepp.

Det er fleire faktorar som verkar inn på ein organismes potensial for N_2O-reduksjon. Det genetiske potensialet for denitrifikasjon varierer mellom organismar, og det er berre nokre som har det genetiske potensialet for N_2O-reduksjon. Sjølv organismar som har *nosZ* genet har ulike potensial for å vere sterke N_2O-sluk, som mellom anna kan vere grunna metabolsk regulering. Ei slik regulering vart oppdaga i ein studie av bradyrhizobia-stammer som hadde det genetiske potensialet for komplett denitrifikasjon, men berre hadde Nap for dissimilatorisk reduksjon av nitrat. Under kultiveringar med både nitrat og N_2O tilgjengeleg reduserte cellene nesten utelukkande N_2O. Den komplette denitrifikanten *Paracoccus denitrificans*, med både Nar og Nap for dissimilatorisk nitratreduksjon, viste ikkje denne preferansen for N_2O. Det vart hypotetisert at dette kom av ein elektronkonkurranse mellom NapC og bc_1-komplekset, som donerer elektron til høvesvis Nap og NosZ. Det vart føreslådd at bc_1-komplekset var ein sterkare konkurrent for elektron enn Nap, i tillegg til at NosZ klade I kunne få ekstra elektron frå proteinet NosR. Dette førte i følgje hypotesa til at cellene med Nap som einaste dissimilatoriske nitratreduktase utviste ein sterk N_2O-reduksjon.

I mitt arbeide har eg studert denitrifikasjon i fire bakteriestammer. Tre av stammene, frå slekta *Thauera*, hadde Nap som einaste reduktase for dissimilatorisk nitratreduksjon, medan *Pseudomonas stutzeri* JM300 hadde både Nap og Nar. Alle stammene var komplette denitrifikantar. Gjennom detaljert overvaking av gasskinetikken til denitrifiserande celler har eg vist at elektronkonkurransen mellom NapC og bc_1-komplekset truleg er eit generisk fenomen funne i fleire slekter. Resultata mine indikerer òg at NosZ-kladen som er involvert i denitrifikasjon er essensiell for utfallet av elektronkonkurransen, og at NosZ klade I har eit

sterkare potensial for å motta elektron enn NosZ klade II, truleg grunna elektrontransport via NosR.

Komplette denitrifikantar med Nap som den einaste dissimilatoriske nitrat-reduktasen er verdfulle kandidatar for å redusere utsleppa av N_2O frå jord. Jordmikroorganismar lev ofte med svært avgrensa tilgang på næring, og vi veit lite om korleis dette påverkar utfallet av denitrifikasjon. Arbeidet mitt har derfor inkludert gassovervaking av denitrifiserande celler som var svelta for karbon. Resultata var optimistiske for bruk av mikroorganismar for å redusere N_2O-utslepp, og viste at sjølv svelta celler kan vere sterke N_2O-sluk.

Abstract

Nitrous oxide (N_2O) is the third most important greenhouse gas after CO_2 and methane, and it serves as an important destructor of the ozone layer. Global N_2O emissions are rising, and most of the anthropogenic N_2O comes from denitrification in agricultural soils. Denitrification is an anaerobic respiratory pathway found in many microorganisms. Complete denitrification is the stepwise reduction of nitrate (NO_3^-) via nitrite (NO_2^-), nitric oxide (NO) and nitrous oxide (N_2O), to dinitrogen gas (N_2). Each of the reduction steps are catalysed by a group of denitrification reductases, Nar and/or Nap, NirS or NirK, Nor and NosZ cladeI or clade II, respectively. NosZ is the only enzyme known to reduce N_2O to N_2, and it is only found in prokaryotes. Bacteria can therefore serve as important soldiers in the battle against increasing N_2O emissions.

There are several factors that contribute to an organism's potential for N_2O reduction. The genetic potential for denitrification varies between organisms, and only some carry the genetic potential for N_2O reduction. Even organisms that carry the *nosZ* gene have different potentials to serve as strong N_2O sinks, which can be due to metabolic regulation. One such regulatory mechanism was discovered in studies of bradyrhizobial strains which carried the genetic potential for complete denitrification, but had Nap as the only reductase for dissimilatory nitrate reduction. When cultivated in the presence of both N_2O and nitrate, the cells reduced N_2O almost exclusively. The complete denitrifier *Paracoccus denitrificans*, with both Nar and Nap for dissimilatory nitrate reduction, did not show this preference for N_2O. This was hypothesised to be due to an electron competition between NapC and the bc_1-complex, which donates electrons to Nap and NosZ, respectively. The bc_1-complex was proposed to be a better competitor for electrons, and it was proposed that NosZ clade I got additional electrons from the protein NosR. This was hypothesised to cause the preferred reduction of N_2O in cells with Nap as the only dissimilatory nitrate reductase.

In my work, I have studied denitrification in four bacterial strains. Three strains, from the genus *Thauera,* had Nap as the only dissimilatory nitrate reductase, whereas *Pseudomonas stutzeri* JM300 had both Nap and Nar. All strains were complete denitrifiers. Through detailed monitoring of the cells' gas kinetics during denitrification, I have shown that the electron competition between NapC and the bc_1-complex is likely a generic phenomenon found in several genera. My results also indicate that the NosZ clade involved in denitrification is

essential for the outcome of the electron competition, and that NosZ clade I has a stronger potential to receive electrons than NosZ clade II, likely due to electron transport via NosR.

Complete denitrifiers with Nap as the only dissimilatory nitrate reductase are valuable candidates for mitigating N_2O emissions from soils. However, soil microbes live under conditions with limited nutrients available. Very little is known about how this affects the outcome of denitrification. My work therefore included gas monitoring denitrification from cells that were starved for carbon. The results were optimistic with regards to using microorganisms to mitigate N_2O emissions, and showed that even starved cells can serve as powerful N_2O sinks.

List of abbreviations

CFU – colony forming units

DNRA – dissimilatory nitrate reduction to ammonium

GC – gas chromatograph

N_2 – dinitrogen gas

NH_4^+ - ammonium

NO – nitric oxide

NO_2^- - nitrite

NO_3^- - nitrate

N_2O – nitrous oxide

ON – over night

PBS – phosphate buffered saline

PHA - polyhydroxyalkanoates

PHB - polyhydroxybutyrate

PO – progressive onset of denitrification

RCO – rapid complete onset of denitrification

ROS – reactive oxygen species

RT – room temperature

Table of content

1. Introduction 1
1.1 Nitrous oxide - the forgotten threat 2
1.2 How can we use microorganisms to battle N_2O emissions? 4
1.3 Denitrification 6
1.3.1 Regulation of denitrification 10
1.3.2 Denitrification regulatory phenotypes 12
1.4 An electron tug of war 15
1.5 A life of feast and famine 16
1.5.1 Accumulation of internal carbon storages 16
1.5.2 Extremely slow growth 17
1.5.3 Feast, famine, and denitrification 17
1.6 Hypothesis 18
2. Materials and methods 20
2.1 An incubation system for monitoring denitrification gas kinetics 20
2.1.1 Transforming peak areas into gas concentrations 21
2.2 Bacterial strains 23
2.3 Medium and incubation conditions 23
2.4 Preparing incubation flasks for gas kinetics experiments 24
2.5 Experimental designs 24
2.5.1 Gas kinetics for well-fed cultures 24
2.5.2 Starvation bioassay 25
2.5.3 Determining the relationship between OD_{600} and cell number 28
2.5.4 Microscopic investigations of starved and well-fed cells 28
3. Results 30
3.1 Denitrification in well-fed cells 30
3.2 A microscopical portrait of *P. stutzeri* JM300 and *T.* sp. 27 34
3.3 Starvation strategies 37
3.3.1 The metabolic shutdown of *P. stutzeri* JM300 37
3.3.2 The starvation of *T.* sp. 27 45
4. Discussion 48
4.1 Denitrification phenotypes and the electron tug of war 48
4.1.1 NosZ-clades and their effect on denitrification 48
4.1.2 Technical discussion 49
4.2 Utilization of carbon sources in *P. stutzeri* JM300 51

4.3 A life of feast and famine ... 52
4.3.1 The transition from feast to famine ... 52
4.3.2 Starvation strategies ... 53
4.3.3 Technical discussion ... 56
4.4 Denitrification during starvation ... 58
4.5 Areas of application ... 60
4.5.1 The agricultural sector ... 60
4.5.2 Wastewater treatment ... 61
4.6 Further research ... 61
5. Concluding remarks ... 62
6. References ... 63
7. Appendix ... 70
7.1 Appendix A: Media for bacterial growth ... 70
7.1.1 Sistrom's medium ... 70
7.1.2 R2A medium ... 71
7.1.3 *Thauera* medium ... 72
7.1.4 Sistrom's buffer ... 72
7.1.5 Phosphate buffered saline (PBS) ... 72
7.2 Appendix B: R code for fitting a simple linear regression model in RStudio ... 73
7.3 Appendix C: Proteomics ... 74
7.3.1 Peptide extraction with gel separation ... 75
7.3.2 Peptide extraction using STrap tips ... 77
7.3.3 Chromatograms ... 79
7.4 Appendix D: Incubation of starved *P. stutzeri* JM300 ... 81
7.5 Appendix E: Calculating cell specific electron flow ... 82
7.6 Appendix F: Gas kinetics of discarded *Thauera* strains ... 84
7.7 Appendix G: Late expression of *narG* in *P. stutzeri* JM300 ... 85

1. Introduction

The microbial respiratory pathway of denitrification is a globally important process, and an important source of the potent greenhouse gas nitrous oxide (N_2O). It is an important part of the nitrogen cycle, where biologically available nitrogen (nitrate, NO_3^-) is reduced to dinitrogen gas (N_2), via three intermediates. Denitrification happens frequently in soils, and contributes greatly to the large N_2O emissions from the agricultural sector. Denitrification is also exploited in wastewater treatments as one of the microbiological processes used to remove ammonia from wastewater. However, because denitrifiers can accumulate N_2O, we must take care when selecting species for industrial use. An evaluation must be made based on genetics, the regulation of denitrification and the accumulation of intermediates. Many of the "knots and bolts" of denitrification are known, but there are many secrets yet to be discovered, and the variation between denitrifiers is vast. In addition to this, we hardly know anything about how real-life challenges, such as fluctuations in carbon availability, affects the regulation of denitrification. The leading belief today, according to my knowledge, is that denitrifying cells under carbon limitations are a source of N_2O, but this belief is based only on a single study. It is crucial that we learn more about how cells under more natural conditions denitrify, as this will have implication for mitigating N_2O emissions from both agricultural and industrial sectors.

In this thesis I will attempt to answer several questions regarding denitrification. I will explore a mechanism found in several bradyrhizobia with a certain denitrification genotype (6, 7), which seems to make the bacteria excellent at reducing N_2O to N_2. Is this mechanism found only among the bradyrhizobia, or is it found in other bacteria that have the same genetic potential? My studies will include strains of the genus *Thauera*, which are soil bacteria that are also abundant in wastewater treatments (8). I will also explore how some bacteria are affected by carbon starvation. How do the cells cope with a sudden lack of carbon? Will starved cells exhibit the same denitrification phenotypes as well-fed cells? To be able to fully understand the importance of this research, and to understand the results, I will first present the overhanging threats of N_2O-emissions and what might be done about this. I will then delve into the bacterial world to study the mechanisms of denitrification and some starvation strategies.

1.1 Nitrous oxide - the forgotten threat

Nitrous oxide (N_2O) is perhaps best known as laughing gas, but it is also the third most important anthropogenic greenhouse gas, after CO_2 and methane (CH_4) (9, 10). Even though the annual anthropogenic emissions of N_2O are lower than those of CO_2, N_2O has a heating potential that is 265-298 times larger than that for CO_2 in a 100 years perspective (11). This is partly due to the long lifetime (100-120 years) of N_2O in the atmosphere (10, 12). In addition, N_2O is today's most important contributor to the depletion of the ozone layer (13). If N_2O emissions continue as they are today, and no new methods for mitigation are implemented, the N_2O emissions are estimated to almost double by 2050, compared to the levels in 2005. This means that emissions would increase from 5.3 Tg N_2O-N per year (2005-2010) to 9.7 Tg N_2O-N per year by 2050, or from 3.3 Gt CO_2-equivalents per year (in 2020) to 4.5 Gt CO_2-equivalent per year in 2050 (10). If greenhouse gas emissions are not reduced, we will not reach the goal of a mean temperature increase of 1.5°C (14), and this will have dramatic global consequences (9, 14, 15). To increase our chances of reaching the 1.5°C goal, efforts need to be made in the sectors that are responsible for N_2O-emissions, which among others include both the agricultural sector and the wastewater treatment sector.

The most important source of anthropogenic N_2O is agricultural activities (10, 16), which are estimated to be responsible for 66 % of annual anthropogenic emissions (10). The need for biologically available nitrogen for food production has increased with a growing world population, and the invention of industrial nitrogen fixation for production of synthetic fertilizers made it possible to meet this need. Between 1860 and 2005, the creation of reactive (available) nitrogen increased from ~ 15 Tg N per year to 187 Tg N per year (17), which to a large extent has been used for synthetic fertilizers. Industrial nitrogen fixation is therefore one of the most important sources of reactive N entering terrestrial systems (18). Over the same period global soil N_2O emissions increased from 6.3 Tg N_2O-N per year to 10 Tg N_2O-N per year. Mineral N-fertilizing is estimated to be responsible for 54 % of the increase in terrestrial N_2O-emissions (19), and the relationship between N input to soils and N_2O emissions is believed to be non-linear, and possibly exponential (10, 20). Other sources of reactive N are manure, crop residues and biological nitrogen fixation, especially by legumes in symbiosis

with bacteria. In soils, N_2O is emitted primarily from the processes of denitrification (1, 5, 19, 21) and as a by-product from nitrification (4, 5) (see Box 1).

Box 1: The nitrogen cycle

The nitrogen cycle is a major biogeochemical cycle, driven mainly by microbial activities. Nitrogen is vital for life, but exists mainly as N_2 in the atmosphere, unavailable for most life forms. Nitrogen is made available through nitrogen fixation. Biological nitrogen fixation (Reaction 1 in Figure 1) can only be performed by prokaryotes, that are free living or living in mutualistic relationships with certain plant families. *Bradyrhizobium* is one of 18 genera in the bacterial group collectively called rhizobia, which are often found in nitrogen fixation symbioses with legumes. Fixed nitrogen exists as NH_4^+, and can be incorporated into biomass. It can also be oxidized to NO_3^-, in the aerobic process nitrification (Reaction 2). Further reactions in the nitrogen cycle include dissimilatory nitrate reduction to ammonium (DNRA) (Reaction 3), anaerobic ammonium oxidation to N_2 (anammox) (Reaction 4) and denitrification (Reaction 5). In the anaerobic process denitrification, nitrogen is brought back to the atmosphere as nitrogen containing gasses (NO, N_2O and N_2). Denitrification is regarded as the biggest source of N_2O in the nitrogen cycle (1-3), but N_2O is also released from nitrification, as a by-product. Nitrification is an important source of N_2O in wastewater treatment systems (4, 5).

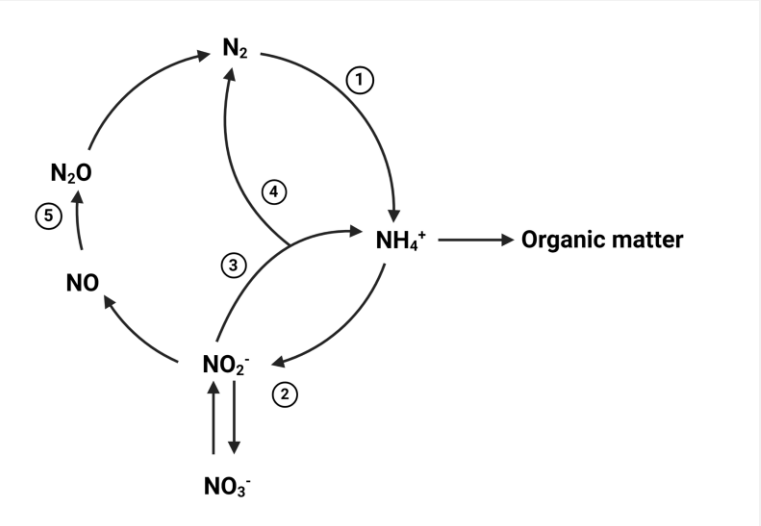

Figure 1: The nitrogen cycle. The microbial processes of the nitrogen cycle. (1) Nitrogen fixation. (2) Nitrification. (3) Dissimilatory nitrate reduction to ammonium. (4) Anaerobic ammonium oxidation, where NO_2^- and NH_4^+ are converted to N_2. (5) Stepwise denitrification of NO_3^- to N_2. (Created with BioRender.com)

Wastewater treatment plants (WWTP) are responsible for 3 % of anthropogenic N_2O emissions (10). One of the main goals in WWT technology is to remove nitrogen from wastewater. This is often done by using a combination of nitrification and denitrification, by which most of the ammonia is transformed to a nitrogen containing gas, which is released. Nitrification and denitrification are considered the main sources of N_2O from WWTP (4). Therefore, more knowledge on these processes are needed to efficiently remove nitrogen from waste water while reducing greenhouse gas emissions (22).

Both the wastewater industries and the agricultural industries face challenges when it comes to handling nutrients (in this case nitrogen) and reducing greenhouse gas emissions. Solving these challenges is crucial for the future of Planet Earth as we know it today (15). If we are to maintain a safe environment for future generations, we must take actions. Even if CO_2 emissions decline as predicted, the annual emissions of N_2O are predicted to continue to increase (23, 24), and new mitigation options must be found (10, 24). Luckily, new mitigation options are under development (25), and if they are implemented, we can stabilize the atmospheric levels of N_2O (10).

1.2 How can we use microorganisms to battle N_2O emissions?

If a collective job is done to mitigate N_2O emissions we may be able to reduce the annual emissions by 2050, and stabilize the atmospheric levels of N_2O at 340-350 ppm (10). If this is accomplished, from 2014 to 2050 we will have avoided emissions of 22 Tg N_2O-N per year, or 57 Gt CO_2-equivalents (these numbers will of course look a little different now in 2021) (10). Several strategies must be implemented, some of which should aim to reduce the greenhouse gas emissions from food production (14). We can use microorganisms to battle N_2O emissions from several sectors, especially agriculture!

Prokaryotes are important soldiers in the battle to reduce N_2O emissions because they are the only group of organisms were the enzyme NosZ is found. NosZ is the only enzyme that can reduce N_2O to harmless N_2 (more on this in Chapter 1.3). Many prokaryotes are soil dwelling bacteria, and can therefore play an important role in reducing N_2O-emissions from agricultural soils. However, only some prokaryotes carry the *nosZ* gene. Moreover, the organisms may not express the enzyme under all conditions, or the enzyme may have a reduced efficiency. This is a core problem when finding mitigation options that are based on microbial activities. We need to know more about the factors that control the production and reduction of N_2O in prokaryotes. Many of these factors lie hidden in the regulation of denitrification at different levels (genetic, transcriptomic, and metabolic). It is therefore crucial that the mechanisms and regulatory processes of denitrification are well understood. Research has already revealed that pH plays an important role in N_2O emissions, as NosZ is not assembled correctly under pH below ~ 6.8 (25, 26). Soil liming and the use of biochar has therefore been proposed as mitigation options to increase soil pH, and thus reduce N_2O emissions (25, 27, 28).

Research has been done to see if it is possible to engineer the soil microbiome by inoculating soils directly with efficient N_2O-reducers. This could be bacteria that perform complete denitrification or bacteria only capable of reducing N_2O to N_2 (25, 29) (more on denitrification in Chapter 1.3). The bacteria can be enriched in organic waste from methane production, called digestates. The digestates are rich in nitrogen and phosphate and can be used as fertilizers in agricultural soils (25, 29). This would secure a repeated inoculation of effective N_2O reducers into agricultural soils, as it has been shown that inoculation of microorganisms to soil must be repeated to obtain a significant effect (30, 31). Recent research has demonstrated that selected N_2O reducers can be inoculated into sterilized digestates, and that the N_2O emissions from soils treated with such digestates are reduced (29). However, the use of digestates is not the only inoculation strategy that has been explored.

The possibility of inoculating legumes with efficient N_2O reducers and N_2-fixers as a strategy to mitigate N_2O emissions from legume crops is under development. After a season of cultivating legumes is over, the plant residues and root nodules (housing the bacterial symbiont) are degraded in the soil. This process releases NH_4^+, which is oxidized to NO_2^- and NO_3^- during nitrification (see Box 1). The nitrifying bacteria consume oxygen, causing anoxia. Denitrifying bacteria can then reduce NO_3^- to nitrogen gasses. Both nitrification and especially denitrification can be important sources of N_2O, which makes the degradation of legume residues a potentially large source of N_2O (32, 33). Many commercial N_2-fixing strains used for legume inoculation lack the *nosZ* gene, and therefore contribute to this effect (25). Field studies have shown that inoculating root nodules with efficient N_2O reducers can reduce postharvest N_2O emissions (32). This could be a promising option for mitigating N_2O emissions, while ensuring an effective biological fixation of nitrogen.

If the mitigation options presented in this chapter are to be successful, more knowledge is required on the mechanisms of denitrification (24). We will now dive a little deeper into the process of denitrification and how it is regulated before we turn to see how bacteria can deal with conditions they meet in natural environments.

1.3 Denitrification

In the absence of O_2, many microorganisms can secure energy production through the anaerobic respiratory pathway of denitrification. Energetically, this is the second most favourable type of respiration, exceeded only by oxidative respiration. Denitrification is found in many facultative anaerobic bacteria and archaea, and in some fungal species (1, 2). It is defined as the reduction of NO_2^- to NO (34). However, in this thesis, complete denitrification is defined as the four-step reduction of nitrate to N_2 (Figure 2). The denitrification steps are catalysed by four groups of denitrification reductases, whose cellular orientation is illustrated in Figure 3. Many organisms are not complete denitrifiers, and lack one or several of the denitrification reductases.

Figure 2: Complete denitrification. Complete denitrification can be summarized in four steps. The catalytically active reductases are noted above the arrows. For the first three reactions there are different reductases that can catalyse the reaction. The reduction of N_2O to N_2 can only be performed by one enzyme, NosZ, which is divided into two clades, clade I and clade II. NO_3^- and NO_2^- are soluble in liquid, whereas NO, N_2O and N_2 are gasses at physiological temperatures.

Nitrate reductase: The dissimilatory reduction of nitrate to nitrite is catalysed by the dissimilatory nitrate reductases Nar and/or Nap. Periplasmic nitrate can be reduced to nitrite by the periplasmic enzyme complex NapAB, expressed from the *nap* gene cluster *napEDABC* (5). NapA has a [4Fe-4S]-centre and a molybdenium cofactor, whereas NapB is a cytocrome *c* (2, 5) . NapAB receives electrons from the membrane bound NapC, which in turn gets electrons from oxidation of the quinol pool (see Figure 3) (5).

Nitrate can also be dissimilatory reduced by NarG in the cytoplasm. Nitrate is first detected by nitrate sensors, activating nitrate transport through the membrane via the transporters NarK1 and NarK2 (5, 35). The dissimilatory reduction of cytoplasmic nitrate is catalysed by the membrane bound nitrate reductase complex NarGHI, encoded from the genes in the operon *narGHJI*. NarG is the catalytic subunit of NarGHI, and is located inside the cytoplasm. It contains a molybdenium cofactor in its active site. NarG receives electrons from the oxidation of the quinol pool, via NarI and NarH (Figure 3). The electron flow from NarI is mediated through two hemes *b* to NarH. Further on, the electrons are transported through Fe-S clusters (5). The flow of electrons from the membrane to the cytoplasm is associated with a translocation of protons, creating an electrochemical gradient across the membrane which is utilized for ATP-synthesis (5).

Nitrite reductase: Dissimilatory nitrite reduction takes place in the periplasm (gram negative bacteria) or in the "periplasm like" space (gram positive bacteria) (35). Nitrite is transported out of the cell after cytoplasmic dissimilatory nitrate reduction (in cells were this takes place). Nitrite is transported out via the NarK2 transporter, which is a nitrate/nitrite antiporter (5) and reduced to NO by nitrite reductase, NIR (Figure 3). This is the step that defines denitrification, as it leads to the production of a nitrogen containing gas (34, 36). There are two isofunctional versions of NIR, encoded by *nirS* and *nirK*, and denitrifiers typically have only one of them. However, some organisms, such as *Pseudomonas stutzeri* JM300, are reported to have both (37). *nirK* encodes a homotrimer with a copper centre (CuNIR), whereas *nirS* encodes a homodimer with a cytochrome *cd₁* (cd_1NIR) (5, 38). The electrons for nitrite reduction are obtained from quinol oxidation by the cytochrome bc_1 complex, via cytochrome *c* (Figure 3). During the oxidation of quinones, protons are translocated across the membrane to the periplasm (5).

Nitric oxide reductase: The reduction of NO is crucial to the cell, as NO is a radical and therefore a potent toxin**.** NO is reduced to N_2O by the membrane bound nitric oxide reductase, NOR (5). It is a heme copper oxidase, and there are several versions of it. cNor has two subunits, NorB and NorC. NorC is a type *c* cytocrome, and delivers electrons to NO reduction via the cytochrome bc_1 complex (Figure 3). The electrons are passed via a *b*-type heme to the binuclear centre in NorB were the catalytical site is found (1, 34). qNor has two functionally redundant subunits that receive electrons from the direct oxidation of the quinol pool (Figure 3) (1, 34). A third version of NOR has also been described. It is a dimer called qCuANor, and can receive electrons both from the quinol pool and from a cytochrome *c* (1, 34). The reduction of NO to N_2O is not associated with proton translocation (1, 5).

Nitrous oxide reductase: The last step in denitrification is the reduction of N_2O to N_2. Only one enzyme, nitrous oxide reductase (NosZ), is known to be able to reduce this potent greenhouse gas to N_2, and it is found only in prokaryotes (34). NosZ is a multicopper enzyme that is either membrane bound (gram-positive bacteria) or periplasmic (gram-negative bacteria) (5). The functional enzyme is a homodimer, the product of the *nosZ* gene (39). It has two copper centres (Cu_z and Cu_A with 4 and 2 copper ions, respectively) in each monomer (5,

39). The entire dimer has 12 copper ions (34). Electrons are obtained from the cytochrome bc_1 complex, via a cytocrome *c* (Figure 3). One electron is transferred through Cu_A to Cu_Z, were the reduction of N_2O occurs (5, 34, 39). The distance from Cu_A to Cu_Z in each monomer is 40 Å, which is too long for efficient electron transfer. The monomers are therefore arranged head-to-tail which reduces the distance for electron transfer to 10 Å (39), thus ensuring efficient electron transfer.

The NosZ protein can be divided into two groups, termed clade I and clade II. They differ in their architecture and secretion from the cytoplasm to the periplasm. Clade I proteins have the two domains (Cu_A and Cu_Z) as mentioned. The protein is exported into the periplasm via the twin-arginine translocation pathway (TAT-pathway) (39). The operon of clade I Nos also includes the gene *nosR*, which likely plays a part in electron donation to NosZ (1, 7, 40). Clade II proteins include a third domain, a cytochrome *c*. These proteins are transported by a Sec translocon (39), and are not associated with the NosR protein.

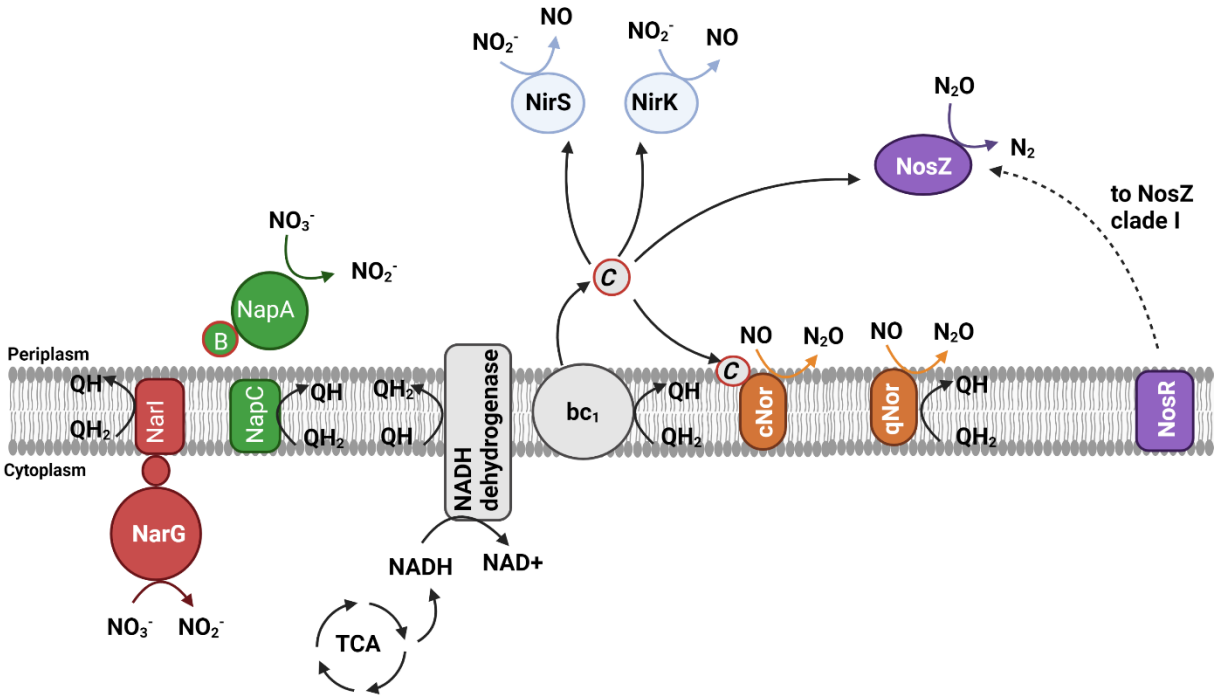

Figure 3: Denitrification reductases and electron pathways. The denitrification reductases are located either in the membrane or in the periplasm (gram negative bacteria). In the figure, the different reductases are colour coded based on the reaction they catalyse. The only exception is the two nitrate reductases Nar and Nap. These have different colours because the distinction between them will be important later in this thesis. Coloured arrows indicate a reductive step in denitrification. Black arrows indicate the electron flows to the different reductases, either directly from the quinol pool (QH_2 → QH) or via the cytochrome bc_1 complex. The dashed arrow represents the hypothesised electron flow from NosR to NosZ clade I. The circles lined with red represent small electron shuttle proteins, such as cytochrome *c*. Electrons to the quinol pool originate from the oxidation of NADH, which is provided from catabolic reactions such as the TCA-cycle. The NO reductase qCuANor is not included. The figure is heavily inspired by the works of Shapleigh (34) and Mania (7). Created with BioRender.com.

1.3.1 Regulation of denitrification

The expression of the denitrification reductases is transcriptionally regulated which is seen as a safeguard against accumulation of toxic intermediates (NO_2^- and NO) and as a way to secure that the most energetically favourable metabolism is used. However, the control mechanisms vary between organisms, leading to various "denitrification regulatory phenotypes" (41). If the regulation is not strict enough, the cell might "waste" energy by expressing a denitrification proteome when oxygen is abundant. However, if the regulation is too rigid, the cell might be trapped in anoxia without sufficient energy to express the denitrification

proteome. A poor regulation of denitrification can lead to the accumulation of NO to concentrations that are toxic for the cell.

The regulation of denitrification is an important factor in determining whether an organism is a source or a sink of N_2O. The regulation varies between species and strains, and has been studied in some model organisms. Although no universal regulatory mechanism has been found (1), it can be divided into layers that are shared between organisms. Regulatory signals from the environment, most importantly O_2 and NO, are detected by regulatory proteins (1, 42, 43). The regulatory proteins may vary between different organisms, but many belong to a family of transcriptional regulators called the Crp-Fnr family (1, 43). The regulatory proteins control the expression of the denitrification reductases, of which many are substrate regulated as well (1, 43). Because of the large variation in denitrification regulation mechanisms, I will present the regulation in *Pseudomonas stutzeri* as an example, illustrated in Figure 4.

The most important environmental signals that regulate the onset of denitrification are oxygen levels and respirable N-oxides, especially NO (1, 42, 43). Both of these signals are needed for the onset of denitrification (43). The Fnr-factors FnrD and DNR respond to the availability of O_2, and activate the transcription of *nir* and *nor* if O_2-levels are low (43). DNR will also serve as a transcriptional activator of *nir* and *nor* in the presence of NO (1), but will inhibit the transcription of the *nar* operon (1, 43). The activation of *nir* and *nor* are tightly connected, and the reduction of nitrite and NO are thus highly dependent on one another. This is essential to ensure the efficient reduction of the toxic NO. The reductions of nitrate and N_2O, on the other hand, are independent of the other denitrification steps (43). The presence of nitrogen oxides also plays an important part in regulating denitrification. NO is already mentioned through its effect on DNR. NO will also activate the transcription of *nir* and *nor* directly, and can induce the transcription of *nosZ* (1, 43). The increased transcription of *nir* leads to a positive feedback loop, in which more nitrite is reduced to NO, which will continue the activation of *nir* and *nor*, thereby securing the detoxification of nitrite and NO to N_2O. *nir* is also activated through the presence of nitrite, which in addition activates the transcription of *nor* and *nosZ* (43). The transcription of *nosZ* in *P. stutzeri* depends on the enzyme NosR, which may also be involved in electron transfer to NosZ (1, 40, 43). Apart from this, the transcription of NosZ is independent of the presence of nitrate and N_2O (1, 29, 43). Nitrate is

also plays a role in regulating denitrification, and activates the transcription of *nar* through NarXL proteins (1).

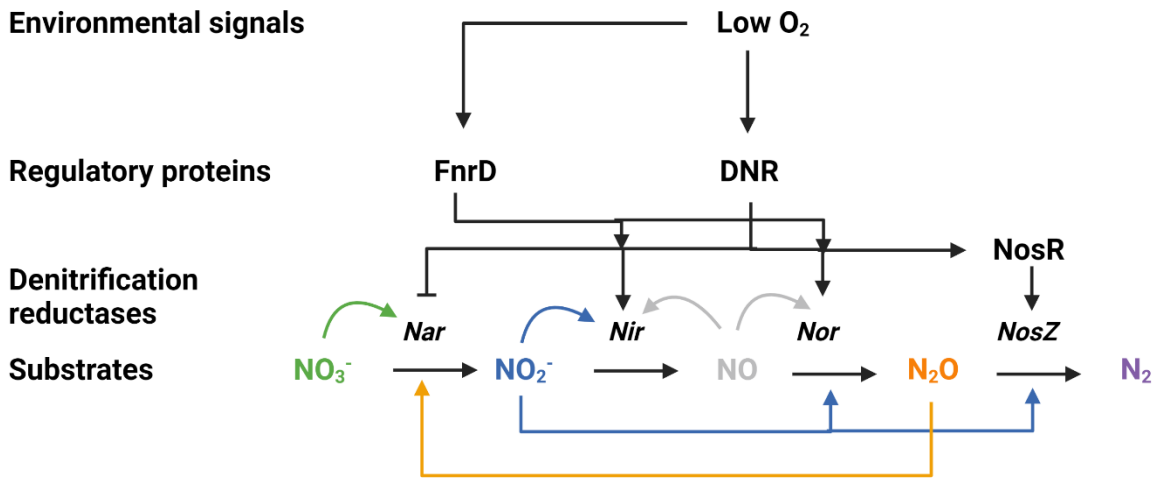

Figure 4: Regulation of denitrification in *Pseudomonas stutzeri*. Denitrification in *P. stutzeri* is controlled by several factors – the availability of O_2 and NO being the most important. When oxygen levels are low, the Fnr-factors FnrD and DNR are activated, and regulate the transcription of denitrification genes. Activation steps are marked as arrows, whereas inhibitory steps are marked with an upside-down "T". The different regulatory factors (both transcription factors and substrates) are coloured, and the arrows that show what steps they regulate are given the same colour. (Created with BioRender.com)

These are the main principles of the regulation of denitrification, but there are many other factors that contribute to different denitrification phenotypes between different organisms.

1.3.2 Denitrification regulatory phenotypes

Different denitrification phenotypes are important to consider when discussing microorganisms as sources or sinks for N_2O. The different phenotypes can be caused by different factors on the genetic, transcriptional, and metabolic level. Many organisms lack the *nosZ* gene, and are thus important sources of N_2O. Other organisms possess *nosZ*, either as the only or one of a few denitrification reductases, or as part of the entire set of denitrification

genes. These organisms may be important sinks for N_2O. However, even though an organism has *nosZ*, it may not be able to express the functional protein or use it efficiently. This will lead to no N_2O reduction, or a less effective N_2O reduction. Understanding denitrification phenotypes and why they differ is thus of great significance when finding ways to mitigate N_2O emissions.

Many organisms are full-fledged denitrifiers, which can reduce nitrate all the way to N_2. However, many organisms have truncated denitrification pathways (34). They may lack the genetic potential to perform complete denitrification, and have other end products than N_2 (34, 44). Studies by Lycus et al (44) revealed isolates with different denitrification pathways in soils, which was summarized in a figure that is reprinted here (Figure 5). The study found a high frequency of organisms with other end products than N_2, both in soils of neutral and low pH (44).

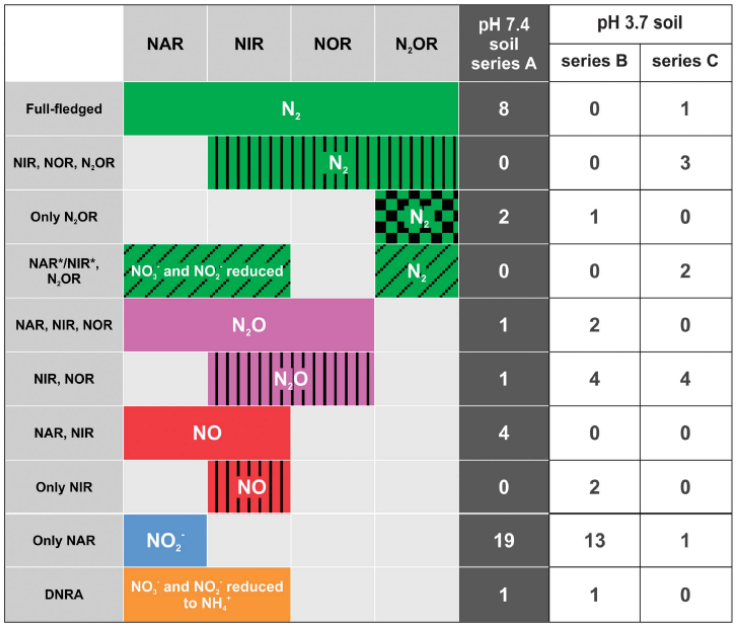

Figure 5: Denitrification phenotypes from soils. The figure is reprinted from Lycus et al (44). Organisms were isolated from two different soils (high and low pH) and grown in pH 7.3 or pH 5.7 (series B and C, respectively). The isolates are classified based on end-product analysis (coloured bars). The denitrification reductases required for each group are shown in the left column.

The studies by Lycus et al (44) revealed that denitrifiers with the potential for complete denitrification showed different regulatory phenotypes. This was also found in a different study of eight strains of complete denitrifiers from the genus *Thauera.* The *Thauera* strains showed two different strategies on handling the onset of denitrification (41). Some of the strains started denitrification before oxygen was depleted, and produced NO, N_2O and N_2 successively. In these strains, no accumulation of nitrite was observed, and all the nitrite produced through dissimilatory nitrate reduction was quickly reduced to NO. This phenotype was termed Rapid Complete Onset of denitrification (RCO) (41). The other strains showed a phenotype in which all the nitrate was first reduced to nitrite, which accumulated, before nitrite was further reduced to NO. This phenotype was named a Progressive Onset of denitrification (PO) (41). The two groups showed a different transcriptional regulation of denitrification. Organisms with the RCO phenotype showed a transcription of *nirS* and *nosZ* at an early stage when oxygen was still present. Organisms with the PO phenotype showed no transcription of *nirS* or *nosZ* before all nitrate was reduced to nitrite (41). This shows that strains with the same genetic potential for denitrification, grown under the same environmental conditions have different potentials for acting as strong N_2O-sinks. Organisms with a regulatory phenotype such as the RPO can reduce N_2O at an early stage in denitrification and are therefore valuable N_2O-sinks compared to organisms with the PO phenotype.

Differences on the metabolic level also affects the N_2O-reducing potential of strains with the same potential for complete denitrification. This will be introduced in the next chapter, and further studied in this thesis.

1.4 An electron tug of war

Recent studies have demonstrated a strong preference for N_2O over nitrate in a range of *Bradyrhizobium* strains that carried a complete set of denitrification genes, when grown anaerobically in the presence of both N_2O and nitrate (6, 7). This was also observed in a strain of *Thauera linaloolentis* (45) . Transcriptional analysis of the bradyrhizobia showed that the transcripts of both *nap* (the only dissimilatory nitrate reductase found in the strains) and *nosZ* were present during N_2O reduction, ruling out that transcriptional regulation of these genes was the cause of the observed phenotype (7). When all N_2O was consumed, and the reduction of nitrate had started, additional N_2O was added. This resulted in an instant switch were the bacteria started to reduce the added N_2O (7). It was thus clear that Nap was active during the reduction of N_2O. It was therefore proposed that the preferred reduction of N_2O was caused by a competition for electrons, much like a tug of war, and that Nos received considerably more electrons than Nap (7). This was further suggested to take place in complete denitrifiers with Nap as the only dissimilatory nitrate reductase (from here on referred to as Nap-Nos organisms), as the complete denitrifier *Paracoccus denitrificans,* with both Nar and Nap (organisms with this genotype are from here on referred to as Nar-Nos organisms), reduced nitrate and N_2O simultaneously (6).

Nos may have had an additional advantage in the electron competition. NosZ clade I, the nitrous oxide reductase found in bradyrhizobia, is associated with NosR (6). This association was speculated to increase the competitiveness of NosZ due to electron donations to NosZ clade I via NosR. This was supported by the finding that the competition between NapC and NirK was much more even than the competition between NapC and NosZ (7). As both NirK and NosZ receive electrons via the bc_1-complex (Figure 3), it was proposed that NosZ was more competitive due to additional electron donations from NosR.

Further experiments showed that if the electron flow to the cytochrome bc_1 complex, which donates electrons to Nir, Nor and Nos via cytochrome c, was blocked, nitrate was reduced more efficiently. If an external electron donor (TMPD) was added, nitrate was also reduced more efficiently (7). TMPD donates electrons directly to cytochrome *c*, thus leaving more electrons available for dissimilatory nitrate reduction via NapC. This led the authors to

hypothesise that the observed phenotype was due to a competition for electrons between NapC (which donates electron to NapA) and the cytochrome bc_1 complex (7).

Bacterial strains with a preference for N_2O over nitrate could serve as excellent sinks for N_2O, reducing both N_2O produced by themselves and other organisms. It makes them valuable candidates for soil inoculations. However, we need more research on how general this phenotype is, and how it is affected by starvation. The studies done on this electron tug of war are performed on bacteria grown in carbon rich medium. However, natural habitats such as soils often have low levels of carbon, and many organisms in soils thus suffer from semi-starvation or starvation (3, 46).

1.5 A life of feast and famine

There is a plethora of studies on starvation in bacteria, and there are many strategies that bacteria can use to survive. Upon starvation, most cells reduce cell size and volume, either through shrinking or fragmentation (cell division without growth), and the cells often take on a coccoid shape (47). To reduce energy consumption, cells can lower their metabolic rates. However, they must be able to maintain a minimum of metabolic activity for repair of essential biomolecules, the production of essential proteins, stabilizing mRNA transcripts and to maintain a membrane potential (46, 47). In this section, I will give a more detailed description of two strategies that can be used to handle starvation. I will also present the leading thoughts on denitrification during starvation.

1.5.1 Accumulation of internal carbon storages

One strategy that can be used to cope with starvation is the accumulation of polyhydroxyalkanoates (PHA), often in the form of polyhydroxybutyrate (PHB). PHAs serve as internal storages of carbon, and are found in more than 90 genera of bacteria, including the genus *Thauera* (8, 48). Experiments have shown that PHA/PHB can fill up to 80 % of the cell dry weight in *Eschericha coli* and *Ralstonia eutropha* when they are grown in a medium rich

in carbon (48, 49). Starved bacteria can use their store of PHA/PHB as a carbon source and an electron donor for respiration, and may thus be able to maintain some metabolic activity during periods of starvation (48, 50). Experiments with the denitrifier *T. aminoaromatica* showed that the cells degraded stored PHB to acetyl-CoA, which entered the TCA-cycle and provided reducing energy for the reduction of nitrate (8). The cells used reduction energy to accumulate PHB during periods where carbon was available, instead of reducing available nitrate to nitrite (8). This strategy of "preparing" for starvation may be found in other strains as well, and allows the cells to maintain a higher metabolism during starvation than cells without this strategy.

1.5.2 Extremely slow growth

Cells that lack internal carbon storages can survive starvation through extremely slow growth. Experiments on non-sporulating *Bacillus subtilus* showed the possibility of deep starvation (46). The cells showed signs of low metabolic activity, evident from the fact that they maintained a membrane potential. The cells showed no downregulation of genes related to cell division, which led to the conclusion that the cells were dividing, even though no increase in CFUs was observed (46). The cells likely got nutrients from lysed cells, leading to a rather constant number of living cells. This phenomenon, which was termed cryptic growth, is likely to occur in natural oligotrophic environments were nutrients are limited (46). Many denitrifiers dwell in oligotrophic environments, which may have implications for denitrification. However, to my knowledge there is only one study that has focuses on how starvation affects denitrification (50).

1.5.3 Feast, famine, and denitrification

The study, performed by Schalk-Otte and colleagues (50), was performed on *Alcaligenes faecalis*, a denitrifier with the genetic potential to reduce nitrite, but not nitrate, to N_2. *A. faecalis* showed an increase in the production of N_2O during starvation, as opposed to the production of N_2O when carbon was available. The increase in N_2O-production was hypothesised to be caused by an electron competition between Nos on the one hand and Nir and Nor on the other (50). Based on this single study, the current conception of denitrification during starvation is that it

leads to increased N_2O emissions. This clearly needs to be verified by other studies on other denitrifying organisms and should particularly include complete denitrifiers, having the genetic potential to reduce nitrate to N_2.

Increased knowledge on denitrification and N_2O reduction under natural conditions has been called for by several studies (1, 22, 42, 51), and will be essential for the continued effort to find microbial soldiers for the battle against N_2O emissions. The current knowledge gaps have led a research group at The Norwegian University of Life Sciences (NMBU) to direct their attention to how a life of feast and famine alters denitrification outcomes.

Studies by this research group show that strains from the genus *Bradyrhizobium*, which carry Nap and NosZ but lack Nar, retain their strong preference for reduction of N_2O over nitrate (see Chapter 1.4) after 20 hours of starvation (Gao and Frostegård, unpubl.). The results, which differ from what was found in *A. faecalis*, indicate that these organisms may act as strong sinks for N_2O under natural conditions where organisms regularly face reduced nutrient availability. However, this is a mostly unexplored field, and more studies on a wider range of denitrifying bacteria are needed if we are to understand how denitrification is controlled under natural conditions. This will be valuable knowledge also for various engineered systems such as wastewater treatment plants where nutrient levels fluctuate. Another area under development in newly started projects in our group is single cell production using denitrifying bacteria (L Bakken and L Bergaust) where upscaling of fermenters often leads to large substrate fluctuations. This thesis will break mostly unexplored ground in the field of starvation and denitrification in the search for a wider understanding of the subject.

1.6 Hypothesis

This thesis builds on the findings by Mania et al and Gao et al (6, 7) that denitrifying bradyrhizobia can act as strong sinks for N_2O. They hypothesised that the observed, preferred reduction of N_2O over nitrate is due to a competition for electrons between the electron pathway to NapA via Nap C and the pathway to NosZ via the bc_1 complex. Furthermore, they suggested that this phenotype is found in other NosZ-carrying organisms that have Nap as the only enzyme

complex for dissimilatory nitrate reduction. The present thesis investigates the validity of that suggestion by determining the denitrification phenotype in bacteria that are unrelated to bradyrhizobia. I hypothesize that:

1. The electron competition between Nap and Nos found in bradyrhizobia is a generic phenomenon that exists in bacteria belonging to other subphyla, and which carry Nap and Nos but lack the membrane-bound Nar.
2. The phenomenon is typical for bacteria having Nap and the clade I type of NosZ, since NosZ can receive electrons from NosR in addition to from the bc_1 complex. I do not expect the same strong N_2O reduction in organisms with the clade II type NosZ, since they lack the additional electron pathway through NosR.
3. I hypothesize that the strong preference for N_2O over nitrate as electron acceptor in Nap-Nos clade I bacteria will be retained under carbon starvation (electron limitation).

2. Materials and methods

2.1 An incubation system for monitoring denitrification gas kinetics

The denitrification gas kinetics of the different bacterial strains were monitored using a robotised incubation system (from here on referred to as the robot system) developed by Molstad et al (52). The system consists of a water bath, in which vials with the liquid bacterial culture are placed, a gas chromatograph (GC) and a chemiluminescence NO analyser (52). A schematic illustration of the system is presented in Figure 6. The headspace of the vials is filled with He-gas and a desired volume of other gasses (such as N_2O and O_2). A magnetic stirring plate in the water bath, and magnets in the vials, secure a constant stirring of the medium to minimize aggregation and optimize gas exchange between headspace and liquid. Samples are taken from the headspace with an autosampler that pierces the rubber septum of the flasks with a needle. The gas samples are passed through the GC and NO analyser, were the amount of N_2O, O_2, N_2, CO_2, CH_4 (in the GC) and NO (NO analyser) is determined. The volume sampled from the headspace is replaced with He-gas (52).

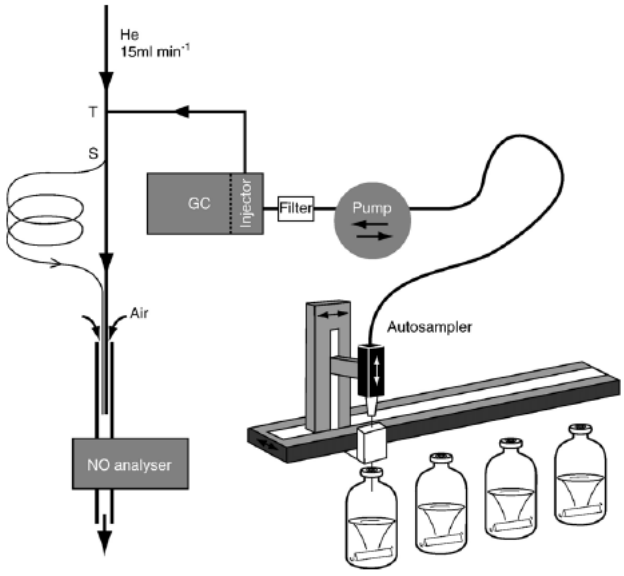

Figure 6: The robotized incubation system. A sample from the headspace of the vials is taken with an autosampler, which pumps an identical amount of He-gas back into the vials. The gas sample is analysed in a gas chromatograph (GC) or an NO analyser. The figure is taken from Molstad et al (52).

In addition to gas sampling, liquid samples can be taken manually to measure the concentrations of nitrite and nitrate in the liquid medium. Not more than 100 µl is sampled at several timepoints, using a needle that has been flushed with He-gas. Analysing the concentrations of nitrate and nitrite is done by reducing NO_3^-/NO_2^- to NO using saturated vanadium chloride (VCl_3) in 1 M hydrochloric acid or 1 % w/v sodium iodide (NaI) in acetic acid for nitrate and nitrite analysis, respectively. The NO concentration is measured using an NO analyser, and a standard curve ($R^2 > 0.99$) is used to find the nitrate/nitrite concentrations. Nitrite is measured shortly after sampling, whereas nitrate, which is more stable, can be kept at – 20°C over night (ON). If no accumulation of nitrite is observed, the concentrations of nitrate can be calculated based on mass balance, explained in Figure 12. This is a more credible alternative than measuring nitrate in the liquid.

2.1.1 Transforming peak areas into gas concentrations

The concentrations of headspace gasses are given as peak areas from the GC, and are converted to concentrations (ppmv) using an Excel sheet (KINCALC) (53). KINCALC is set with values of the solubilities of the different gasses, the transport rates between the headspace and the liquid, and the molar volume of the gasses (53). For these parameters to be correct, it is of crucial importance that the temperature and the pH for the experiment are noted in the sheet. The KINCALC sheet allows the user to calculate the concentrations of different gasses and their transformations. This is made possible due to three gas standards that are always included in empty vials in the experiment (Table 1). A response factor for each gas is calculated by dividing the concentration of the gas in the standard, with the first measured peak area of the gas. The response factors are used in addition with knowledge of the volume of the flasks and the medium. In addition to the response factors, some parameters must be set to obtain reliable data.

For the detection of N_2O, some robot systems use two detectors – ECD and TCD. The TCD-detector has a large linear range, and is therefore suitable for measuring high concentrations of N_2O. It is, however, unable to detect low concentrations of N_2O. The ECD-detector, on the other hand, is very sensitive and can detect very low concentrations of N_2O (< 0.1 ppmv). The

ECD-detector has a very short linear range, and is therefore not suited for measuring high concentrations of N_2O (53). A limit for when KINCALC is supposed to use ECD-values, and when to use TCD-values, is set (53). One of the robot systems often used in this work did not have an ECD-detector, and the limit was thus set to 0. However, the lack of an ECD-detector is not a problem for experiments were high concentrations of N_2O are used.

Table 1: Gas standards. Three different standards were used to calibrate the KINCALC-sheet. All concentrations are given in ppmv. Other trace gasses make up the missing parts of the standards.

Gas component	Air standard	High standard	NO standard
O_2	210 000	>500	-
N_2	780 000	>800	999 975
N_2O	0.58	150	-
NO	-	-	25
CO_2	361	10 000	-
CH_4	1.84	10 000	-
He	-	The rest	-

In the calculation of the KINCALC-sheet, the sampling volume needs to be adjusted. For each sample taken by the robot, there is a small leakage of O_2 and N_2 into the flasks. Additionally, some of the headspace gasses are lost during sampling. Setting the sample loss is done using data from the air standard. The leakage from this standard is negligible due to the high initial concentrations of O_2 and N_2, but the sampling loss is not. The sampling volume is set to a value which gives stable concentrations of O_2 and N_2 over time when leakages are adjusted for. The sampling losses are determined in the same way in the high standard, where the initial concentrations of O_2 and N_2 are low (53).

The last important parameter to set is the zero offset value for oxygen. Vials with actively growing aerobic cultures are needed for this. As the oxygen concentrations in a vial reaches minimal values, the peak areas measured by the GC will stabilise at a certain value. This is the zero offset value for oxygen, which may vary considerably between different incubation systems (53).

2.2 Bacterial strains

The bacterial strains used in this work can be divided into two genera. *Thauera aminoaromatica S2, T.* sp. 27, *T. terpenica* 58 Eu, *T.* DNT-1, *T. linaloolentis* 47 and *T.* sp. 63 were first selected. These have previously been described with regards to their denitrification phenotype (41). I failed in growing *T. aminoaromatica, T.* DNT-1 and *T. terpenica,* and therefore included *Pseudomonas stutzeri* strain JM300 (DSM 10701) in the study. The strains were either grown from stock cultures already available, or from purchased cultures from the German Collection of Microorganisms and Cell Cultures (DSMZ). Liquid cultures were based on single colony picks. All strains selected were complete denitrifiers, with different combinations of the denitrification reductases as presented in Table 2. All strains carried the genes for NosZ clade I, except *T. linaloolentis*, which had the genes for both NosZ clade I and clade II (45). The *Thauera* strains had Nap as the only dissimilatory nitrate reductase complex, and will from hereon be referred to as Nap-Nos organisms. *P. stutzeri* JM300 had both Nap and Nar for dissimilatory nitrate reduction, and is from here on referred to as a Nar-Nos organism.

Table 2: Denitrification genotypes of selected strains. The presence of a gene is marked with "X". The version of Nor present in the strain is not included.

Strain	Nar	Nap	NirS	NirK	Nor	NosZ
Thauera sp. 27		X	X		X	X
Thauera sp. 63		X	X		X	X
Thauera linaloolentis		X	X		X	X
Pseudomonas stutzeri JM300	X	X	X	X	X	X

2.3 Medium and incubation conditions

The initial strains were divided into two groups with regards to medium and incubation conditions. *P. stutzeri* JM300, *T.* sp. 27, *T.* sp. 63 and *T. linaloolentis* were grown in Sistrom's minimal medium (Appendix A) at 20 °C. *T. aminoaromatica, T.* DNT-1 and *T. terpenica* were grown both in *Thauera* medium (Appendix A) (41) and in R2A medium (Appendix A) at 28 °C. The pH in all media was 7.5. These conditions were used for all experiments unless else is

stated. The cultures were grown in 120 ml serum flasks with 50 ml liquid medium, covered with aluminium foil. A teflon covered magnet in each flask and magnetic stirring plates in the water baths ensured an even distribution of head space gasses into the medium. OD_{600} was kept low, ~ 0.3 – 0.4 or ~ 0.15 for incubations of well-fed and starved cultures, respectively. This was done to prevent the formation of local anoxic spots which could lead to the formation of a denitrification proteome.

2.4 Preparing incubation flasks for gas kinetics experiments

Special incubation flasks were prepared for the incubation experiments in the robot system. The flasks were the same type used for growing precultures; 120 ml serum bottles with 50 ml liquid medium. For experiments where nitrate was used as an electron acceptor, KNO_3 was added to the medium. The flasks were sealed with butyl rubber septa and aluminium crimps, to avoid gas leakage. The headspace gasses in the flasks were removed through a series of evacuation and He-filling steps, referred to as a He-wash. During the He-wash, the flasks were kept on magnetic stirring plates to ensure a homogenisation of the liquid/gas phase. After the He-wash, the headspace in all the flasks was filled with He-gas. The overpressure was balanced out, and the desired volumes of other gasses were added using a special gas tight syringe. Before inoculation, the flasks were kept ON to create an equilibrium between nitrogen in the medium and the head space gasses.

2.5 Experimental designs

2.5.1 Gas kinetics for well-fed cultures

Well-fed cultures were grown in their respective media with a low OD (0.3 - 0.4) for several generations. The incubation flasks were premade with medium with 100 µmol KNO_3 and 1 ml N_2O (~ 90 µmol) and 0.7 ml O_2 (~ 60 µmol) in the headspace. The incubation flasks were inoculated with a volume equalling 1ml of culture with OD_{600} = 0.1 (~ $1.67 \cdot 10^7$ cells), and incubated in the robot system at temperatures suited for each strain (20 °C or 28 °C). Liquid samples for nitrite measurements were harvested during the first hours of denitrification. A minimum of three replicates were used for each treatment in the experiments.

2.5.2 Starvation bioassay

A "starvation bioassay" was developed to examine the effect of severe carbon limitation (i.e. electron donor limitation) on denitrification phenotypes. A buffer derived from Sistrom's medium without any carbon sources was used as medium (Appendix A). Two strains (*P. stutzeri* JM300 and *T.* sp. 27) with complete denitrification pathways were compared. They carry the same type of Nir, Nor and Nos but differ with respect to their denitrification nitrate reductases. *P. stutzeri* JM300 has both Nar and Nap for dissimilatory nitrate reduction, while *T.* sp. 27 has only Nap (Table 2). The cells were starved aerobically for 20 hours before being transferred to anoxic conditions. The starvation workflow is visualised in Figure 7.

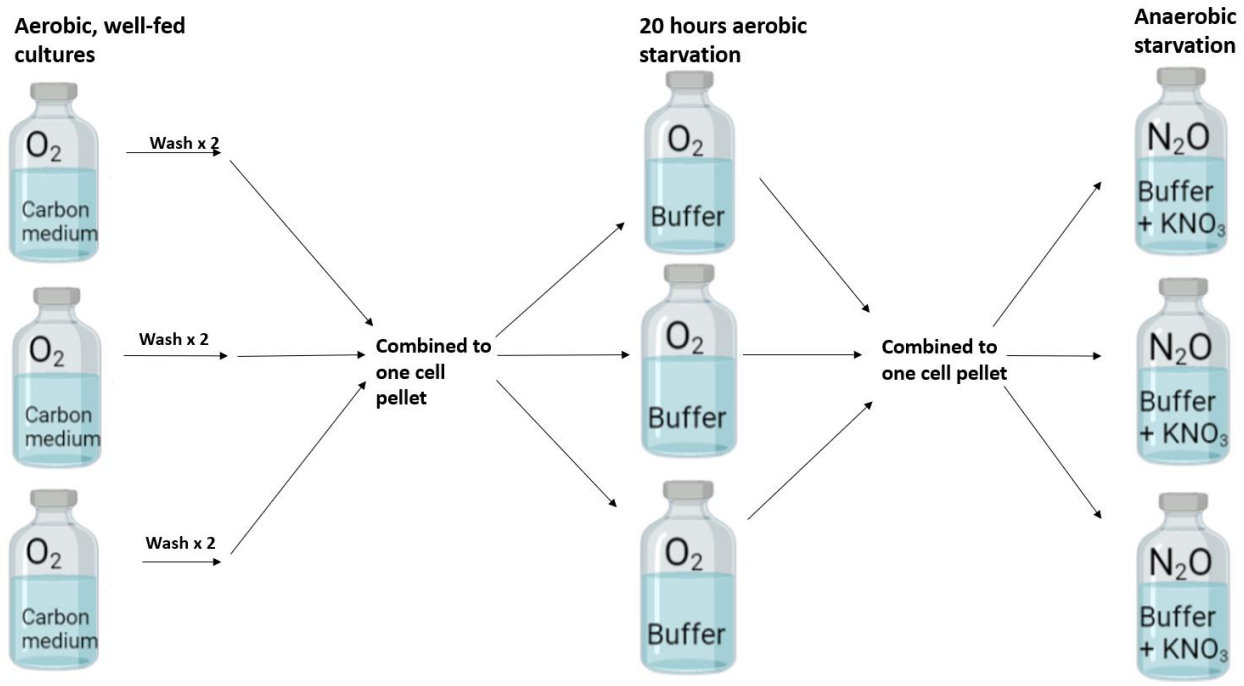

Figure 7: Starvation bioassay workflow. Cells were cultivated aerobically in Sistrom's medium up to OD_{600} ~ 0.15, before being transferred to oxic buffers and starved for 20 hours. After starvation, the cells were transferred to anoxic flasks with buffer and KNO_3 and N_2O as electron acceptors. In the visualization, cells from three precultures are combined to one cell pellet through centrifugation, and equally distributed to three flasks with buffer. This set up was used frequently, but four or five flasks were combined in one cell pellet in other experiments, depending on the total number of flasks in the experiment. Created with BioRender.com.

Precultures of cells were first grown aerobically in carbon rich medium, with $OD_{600} < 0.15$ for several generations. Portions of culture were regularly transferred to new medium to prevent too dense cultures and anoxic conditions, which would lead to de novo synthesis of denitrification reductases. Several precultures were made. The entire cell pellet from a preculture was transferred to aerobic, carbon free buffer after undergoing the first steps seen to the left in Figure 7. The cells were centrifuged (10,000 g, 15 min, 4 °C) and washed twice with autoclaved ddH_2O. Cell pellets from different precultures were combined to one cell pellet. This pellet was resuspended in carbon free buffer (1 ml per cell pellet in the combination), and equally distributed to oxic incubation flasks with buffer (1 ml cell suspension per flask). This ensured homogeneity between the replicates. The cells were kept at 20 °C with stirring for 20-21 hours. During this time, the cells were starved for electrons as they performed oxic respiration.

After 20-21 hours, the cultures were centrifuged, and cell pellets were combined and resuspended in buffer as described above. 1 ml cell suspension was transferred to premade anoxic incubation flasks with buffer and electron acceptors (100 µmol KNO_3, 1 ml N_2O). For the incubations of *P. stutzeri*, I was afraid of trapping the cells in anoxia, without sufficient energy for the de novo synthesis of denitrification reductases. To give the cells a more gradual transition to anoxic conditions, I added a small volume of oxygen to the incubation flasks (166 µl or ~ 7 µmol). Liquid samples for nitrite measurements were taken when denitrification started, seen as a reduction of N_2O and a production of N_2.

After starving the cells of *T.* sp. 27, the flasks were He-washed. This left the cells without electron- donors or acceptors. I suspected that this would keep the cells inactivated ON, before they were transferred to anoxic incubation flasks (100 µmol KNO_3, 1 ml N_2O). Due to the long period of oxygen reduction in *P. stutzeri* (115 hours) (see Figure 12), no oxygen was added to the incubation flasks of *T.* sp. 27. Some oxygen (2.3 µmol flask $^{-1}$) was still present in the flasks, partly from the buffer used to resuspend the cell pellets. No nitrate samples were taken, as the strain is reported not to accumulate nitrite (41).

2.5.2.1 Providing starved cells with carbon

I wanted to examine how the starved cells responded to a sudden access of carbon after a period of starvation. This was examined in starved cells of *P. stutzeri* JM300. Four ml of a carbon solution containing the carbon sources found in ~50 ml Sistrom's medium (0.055 g ml^{-1} succinate, 0.001375 g ml^{-1} L-glutamic acid, 0.00055 g ml^{-1} L-aspartic acid, 0.00275 g ml^{-1} nitrilotrioacetate) was added to three of the incubation flasks after ~140 hours of starvation. This led to a slight pH decrease in the buffer from 7.5 to 7.35. Additional N_2O (0.5 ml or ~ 43 µmol) was added to ensure that enough electron acceptors were present during the more rapid metabolism that was expected to follow. Liquid samples for nitrite measurements were taken.

Three flasks of *P. stutzeri* JM300 were kept for a longer period of starvation. After being starved according to the starvation bioassay (Figure 7), they were kept under anoxic conditions for 19 days, with regular additions of N_2O. After 19 days, the septas covering the flasks were replaced by aluminium foil, and the cells were starved under oxic conditions for an additional 92 days. After a total of 113 days of starvation, 100 µmol KNO_3 was added to the flasks, and they were He-washed. Additional electron acceptors and donors in the form of 1 ml N_2O and 4 ml carbon solution was added, which led to a small decrease in pH from 7.5 to 7.25. Liquid samples were taken for nitrite measurements.

2.5.2.2 The transition from feast to famine

Due to the extremely slow metabolism observed in *P. stutzeri* JM300, a new starvation experiment was designed to study how the cells handled the shift from well-fed to carbon limited conditions. The cells were grown in two different modified versions of Sistrom's medium, both with 0.086 g l^{-1} succinate. One type of media contained the D-glutamic acid and D-aspartic acid found in Sistrom's medium (0.1 g l^{-1} and 0.04 g l^{-1}, respectively), whereas the other type lacked glutamic acid and aspartic acid altogether. This medium was used to determine if *P. stutzeri* JM300 depends on the extracellular availability of these two amino acids for growth. The shift to starvation was studied using the robot system under oxic (0.26 mmol O_2 as electron acceptor) and anoxic (0.52 mmol N_2O as electron acceptor) conditions. The cells were provided with 0.037 mmol succinate as an electron donor, which should

provide 0.52 mmol electrons. Twice as many electrons, 1.04 mmol, are needed to completely reduce the electron acceptors. This setup allowed me to study how the cell's respiration was affected by a sudden lack of electrons.

2.5.3 Determining the relationship between OD_{600} and cell number

The relationship between OD_{600} and cell number (Colony Forming Units (CFU)/ml) was determined for *P. stutzeri* JM300. A preculture was grown to OD_{600} = 0.54 and diluted with 0.9 % NaCl in a five-fold dilution series. OD_{600} of the different dilutions was measured and 100 µl of the cultures that were diluted 5^{-6}, 5^{-7} and 5^{-8} times were spread onto Sistrom's agar plates (pH = 7.5) with a drigalski spatula. The plates were incubated at 28 °C until visible colonies appeared. Three dilution series were made, and the plating of the dilutions was done in triplicates. The number of CFU/ml was used to determine the amounts of cells in the original culture and the dilutions. A simple linear regression model was assumed, and a regression line was fitted in RStudio (Appendix B).

2.5.4 Microscopic investigations of starved and well-fed cells

To determine the effects of starvation on cell size, morphology, and internal stores of PHB in *P. stutzeri* JM300 and *T.* sp.27, cells were examined using confocal microscopy. Starved and well-fed cells were compared after growth both under oxic and denitrifying conditions.

Well-fed cells were grown in Sistrom's medium. Aerobic cultures were grown with vigorous stirring up to an OD_{600} between 0.1 and 0.4. Anaerobic precultures were made by adding 100 µmol KNO_3 to aerobic cultures, He-washing the flasks and adding 0.7 ml O_2 and 1 ml N_2O, and leaving them ON. Aerobic cultures were He-washed without adding any electron acceptors, to prevent further growth and possibly anoxic conditions due to increased cell densities.

Starved cultures were prepared as described for the starvation bioassay (Figure 7). After 20 hours of aerobic starvation, some flasks were He-washed, and 100 µmol KNO_3 and 1

ml N_2O was added to induce denitrification. The cultures were left for 4.5 – 5 hours. The other cultures were kept oxic.

All cultures were fixed simultaneously. Cell cultures were mixed with a fixing solution (2 % paraformaldehyde [wt/vol] and 2.5 % glutaraldehyde [vol/vol] in phosphate-buffered saline, pH = 7.4) at a 1:1 ratio. The cells were vortexed, and left for fixing for 1 hour at room temperature, and later ON at 4 °C. Afterwards, the cells were washed thrice with PBS and kept in 30 µl PBS at 4°C for four months until microscopy.

The cells were stained with 0.5 µl nilered (0.1 mg/ml) and 0.5 µl dapi (0.5 mg/ml), and 0.5 µl of each sample was spread onto a thin layer of 1.2 % agarose (Biorad, diluted in PBS). The microscopy was performed by using a Zeiss AxioObserver microscope with ZEN Blue Software. Microscopic images were taken using an ORCA-Flash4.0 V2 Digital CMOS camera (Hamamatsu Photonics) through a 100 x PC objective. An HPX 120 Illuminator (Zeiss) was used as a light source for fluorescence microscopy. The images were analysed using the ImageJ software.

3. Results

The results presented in this thesis include a comparison of the denitrification phenotypes of four bacterial strains (*P. stutzeri* JM300, *T. linaloolentis*, *T.* sp. 63 and *T.* sp. 27) that are all full-fledged denitrifiers, but differ in the types of genes encoding the denitrification reductases. Two strains, *P. stutzeri* JM300 and *T.* sp. 27, were studied in greater detail and their phenotypes and morphologies were compared when grown with sufficient carbon source (well-fed) *vs* with a lack of carbon source (starved).

3.1 Denitrification in well-fed cells

The denitrification phenotype of well-fed cells was studied for all four strains (Figure 8 A-D). The strains belonging to the genus *Thauera* carry the genes for Nap as the only dissimilatory nitrate reductase complex, thus lacking genes coding for Nar. *P. stutzeri* JM300 carries genes for both Nar and Nap. All four strains carry the genes for NosZ clade I, except *T. linaloolentis*, which carries genes for both NosZ clade I and II (Table 2).

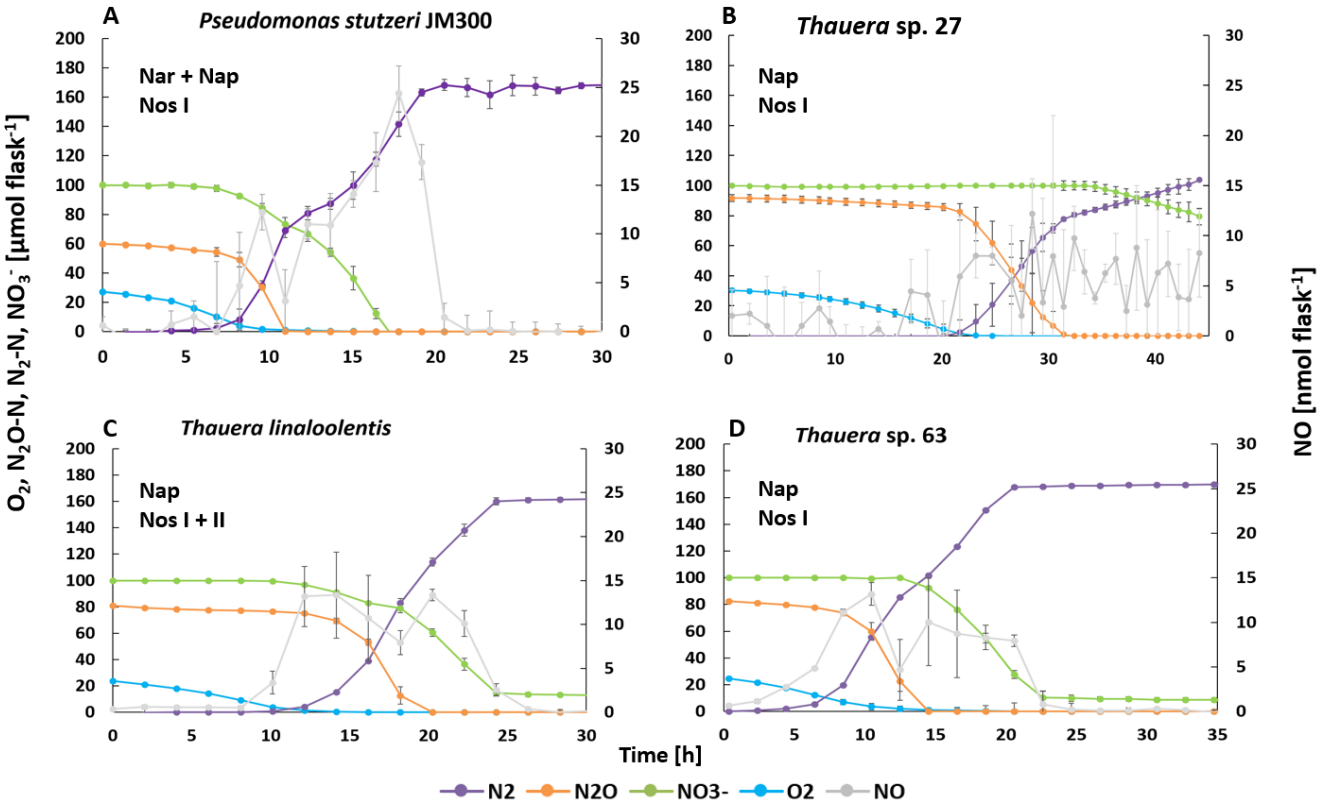

Figure 8: Denitrification phenotypes in four denitrifying strains. The strain's genetic potential for the denitrification steps NO_3^- reduction and N_2O reduction is shown in the top left corner of each figure. All strains are complete denitrifiers. *P. stutzeri* JM300 carries both Nar and Nap for dissimilatory nitrate reduction, whereas the remaining strains only carry Nap as the dissimilatory nitrate reductase. All strains carry NosZ clade I, except *T. linaloolentis*, which carries both NosZ clade I and clade II. The cells were grown in Sistrom's medium at 20 °C with vigorous stirring throughout the incubation. The flasks initially contained ~ 25 µmol O_2, 60 - 90[1] µmol N_2O-N and ~ 100 µmol NO_3^-. The concentrations of O_2, N_2O-N, N_2-N and NO_3^- are given as µmol flask^{-1} on the left-hand axis, whereas the concentration of NO is given as nmol flask^{-1} on the right-hand axis. Standard deviations are given as vertical bars (n = 3 for all cultures except *T.* sp. 27 (n = 2)). Some standard deviations are too small to be visible. The cycle times for gas sampling varied between the experiments. The kinetics were followed beyond the point where all N added to the system was recovered as N_2, except for the incubation of *T.* sp. 27 (Panel B). The incubation of *T.* sp. 27 was ended after all exogenous N_2O was reduced, and the reduction of NO_3^- had started.

[1] The low concentration of N_2O-N in the incubation of *P. stutzeri* (60 µmol flask^{-1}) was likely caused by a low partial pressure of N_2O in the syringe used to transfer gas to the incubation flasks.

The fours strains (Figure 8, A-D) showed some differences in their denitrification phenotypes. All the strains respired oxygen at first, and denitrification started when oxygen was close to depleted (~ 5 µmol flask^{-1}). At the onset of denitrification, all strains reduced N_2O, which led to an accumulation of N_2 in the flasks. However, the strains differed in the reduction of nitrate. Both *P. stutzeri* (Figure 8 and 9 A) and *T. linaloolentis* (Figure 8 and 9 C) reduced nitrate and N_2O simultaneously. The two strains continued to reduce nitrate once N_2O was depleted.

In contrast to this, the reduction of nitrate lagged behind in *T.* sp. 27 (Figure 8 and 9 B) and *T.* sp. 63 (Figure 8 and 9 D). Nitrate reduction was seen towards the end of N_2O reduction in *T.* sp. 63 (Figure 8 and Figure 9). When N_2O was depleted, the concentration of N_2-N (~ 85 µmol flask^{-1}) exceeded the N added to the system as N_2O (~ 82 µmol flask^{-1}). This indicated that about 3 µmol of the N_2-N arose from the reduction of nitrate. In *T.* sp. 27, on the other hand, no nitrate reduction was seen before N_2O was completely depleted. The incubation was ended before all exogenously added N was retrieved as N_2.

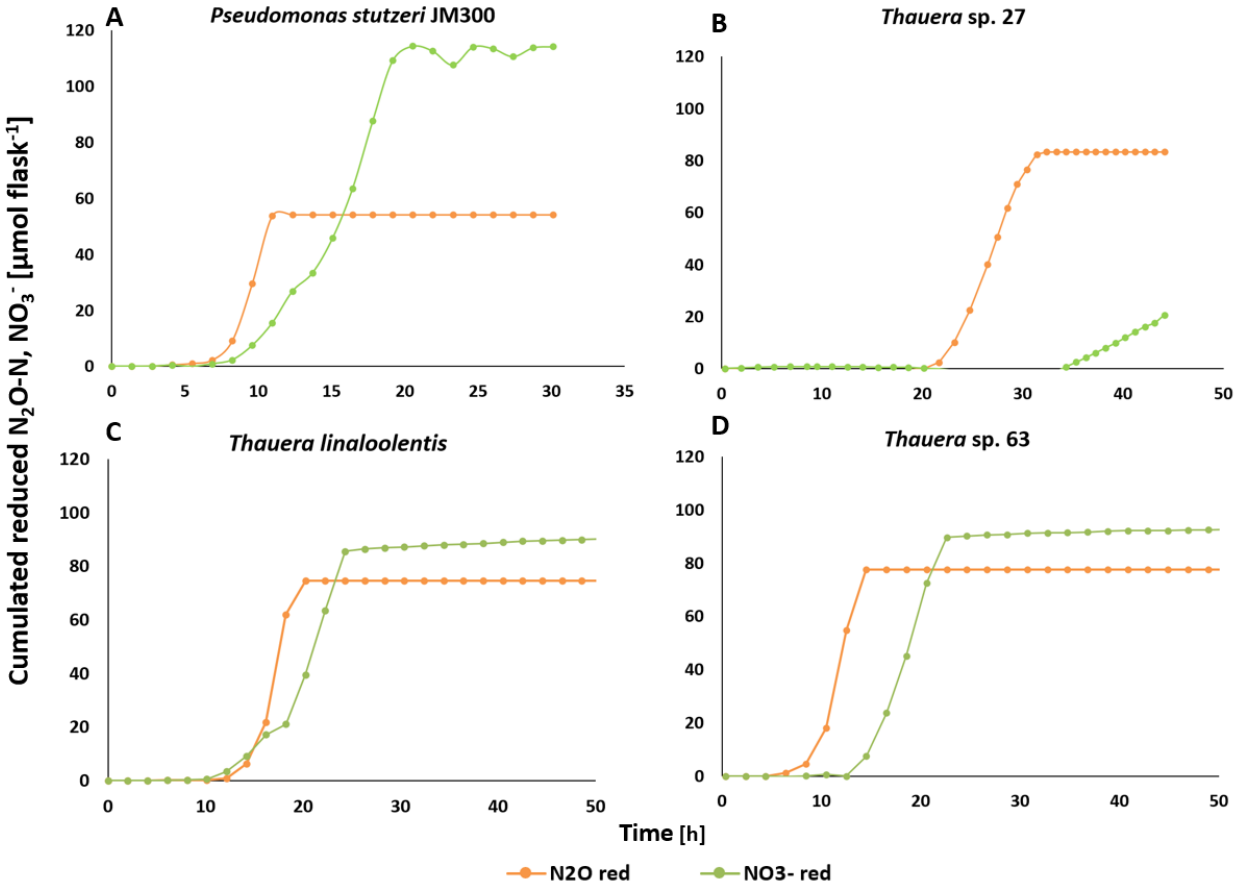

Figure 9: Cumulated reduction of NO_3^- and exogenous N_2O for four denitrifying strains. The cumulated values were calculated from the same dataset used to determine the denitrification phenotypes (Figure 8). The cumulated reduced N_2O (orange) arose from externally provided N_2O, added initially to the headspace. The cumulated reduced NO_3^- (green) consisted of all N from NO_3^- retrieved as N_2. The reduction of exogenous N_2O-N is calculated based on the N_2O-reduction rates from timepoint to timepoint. The production of N_2-N (not included here) is likewise calculated based on the N_2-production rates from timepoint to timepoint. NO_3^- values are based on mass balance calculations were the difference between N_2-N produced and N_2O-N reduced is assigned to NO_3^--reduction. This is shown in more detail in Figure 12.

Ideally, the gas kinetics should have been accompanied by analyses of the proteome of *T.* sp. 27 and *P. stutzeri* JM300, but the results could not be obtained. Even though the peptide extractions for some samples were successful, the results were not reliable (Appendix C). The problems may be caused by the production of exopolysaccharides (slime). A more thorough discussion of the proteome analysis and what went wrong can be found in Appendix C.

After determining the denitrification phenotypes of the four strains, more extensive research was performed on *T.* sp. 27 and *P. stutzeri* JM300. The morphology of the strains will first be presented before I delve deeper into their denitrification and explore how they handled starvation.

3.2 A microscopical portrait of *P. stutzeri* JM300 and *T.* sp. 27

Cells of *P. stutzeri* and *T.* sp. 27 from different treatments (oxic and anoxic, starved and well-fed cells) were studied microscopically (Figure 10 A-G), which showed rodformed cells with a length of ~ 2 µm. The cells of *P. stutzeri* (Figure 10 A, C and E) appeared slimmer than the cells of *T.* sp. 27 (Figure 10 B, D, F and G), which showed a more ovococcoid shape. The well-fed cells of *P. stutzeri* were not noticeably different under oxic conditions (Figure 10 A) compared to anoxic conditions (Figure 10 C), whereas the well-fed cells of *T.* sp. 27 took on a more coccoid shape under anoxic conditions (Figure 10 D) compared to oxic conditions (Figure 10 B). Starved cells under both oxic and anoxic conditions (Figure 10 E-G) differed from the well-fed cells (Figure 10 A-D) by having darker areas towards the cell poles. This was particularly evident for cells of *T.* sp. 27 (Figure 10 F and G). No anaerobically starved cells of *P. stutzeri* were found in the microscopic investigations after fixation. The reason for this is unclear.

The cells were also stained with dapi and nile red to investigate the presence of intracellular storages of carbon in the form of PHB. The results are presented in Figure 11 A-G. Nile red (red) stains lipids, such as PHB and the cell membrane, whereas dapi (blue) stains DNA. Many of the well-fed cells of *T.* sp. 27 showed areas with increased nile red signals (indicated with arrows in Figure 11 B and D), from here on referred to as granules. Such granules were not found in starved cells (Figure 11 F and G). The areas dominated by granules showed weaker dapi signals than the surrounding areas (not shown). The nile red granules were not found in well-fed cells of *P. stutzeri* (Figure 11 A and C), were the cells expressed an even, low signal of nile red. This was likely caused by staining of cell membrane lipids.

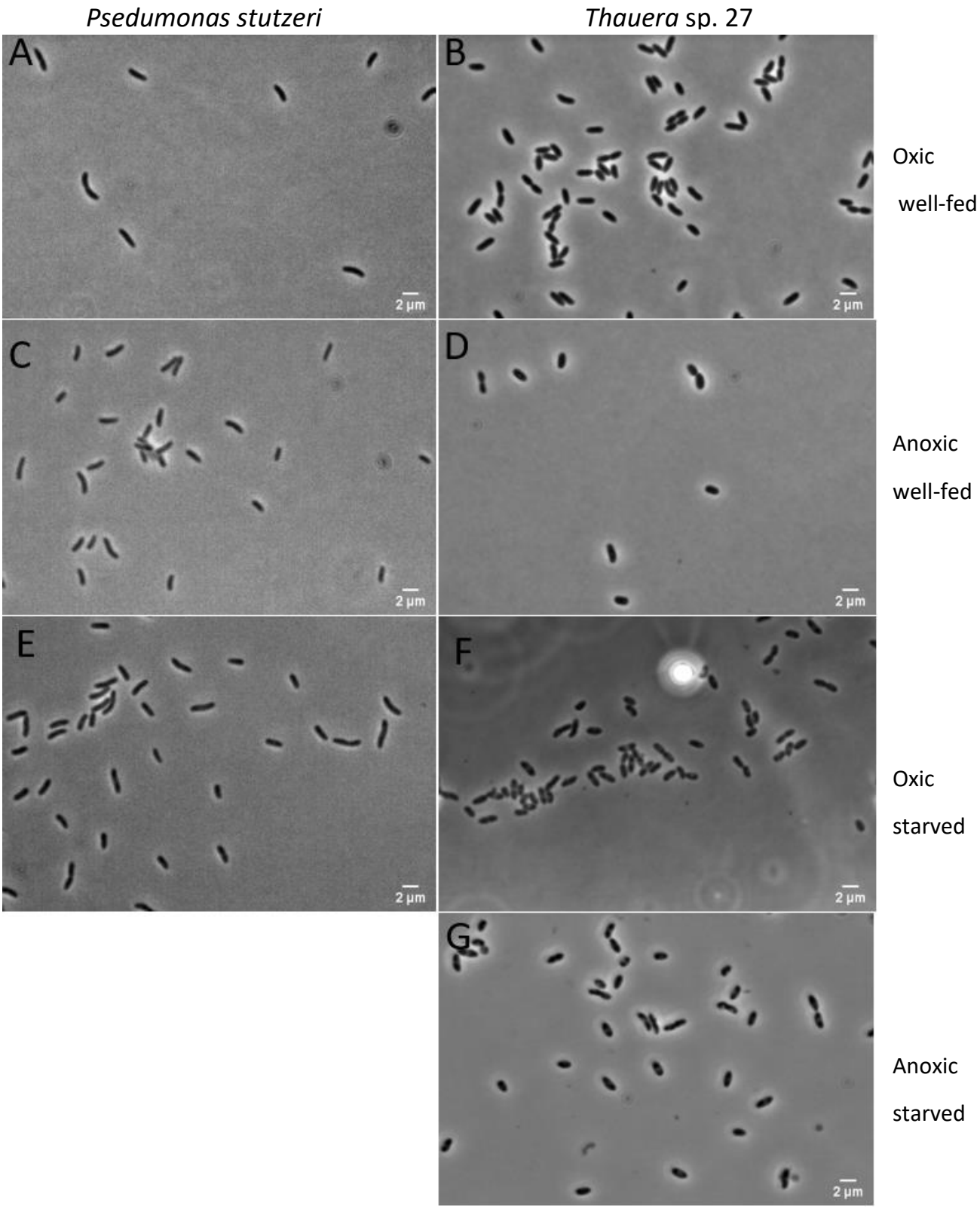

Figure 10: Morphology of well-fed and starved cells of *P. stutzeri* JM300 (A, C and E) and *T.* sp. 27 (B, D, F and G). The cells were subjected to both oxic conditions (A, B, E and F) and anoxic conditions (C, D and G). The cells in pictures A-D were well-fed, whereas the cells in pictures E-G were starved. No anaerobic starved cells of *P. stutzeri* were obtained after fixation, for unknown reasons. The cells were studied using phase contrast. Two replicates for each treatment were investigated.

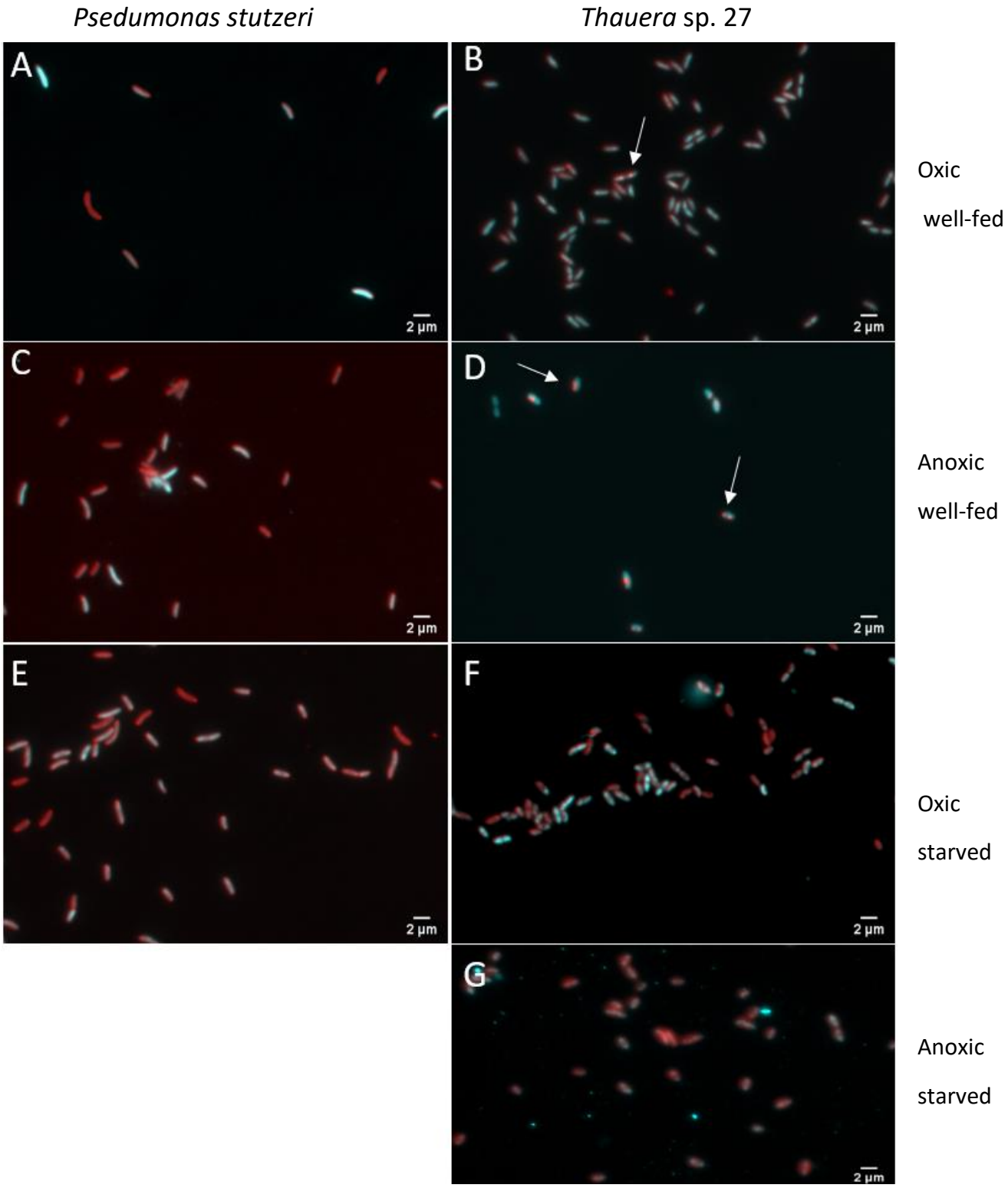

Figure 11: Microscopic investigations of cellular PHB content. Cells of *P. stutzeri* (A, C and E) and *T.* sp. 27 (B, D, F and G) were stained with dapi (blue) and nile red (red). Both well-fed cells (A-D) and starved cells (E-G) were investigated, under oxic conditions (A, B, E and F) and anoxic conditions (C, D and G). Dapi stains DNA, while nile red stains PHB and the cell wall. Strong signals of nile red in well-fed cells of *T.* sp. 27 are indicated with arrows. No anaerobic starved cells of *P. stutzeri* were obtained after fixation, for unknown reasons. The pictures are the same as the phase contrast pictures in Figure 10. Two replicates for each treatment were investigated.

3.3 Starvation strategies

The consequences of starvation on denitrification were studied in *P. stutzeri* JM300 and *T.* sp. 27. The cells were starved according to the starvation bioassay from chapter 2.5.2, Figure 7. The transition from well-fed conditions to carbon limited conditions was studied in *P. stutzeri*.

3.3.1 The metabolic shutdown of *P. stutzeri* JM300

The first starvation experiments in this thesis were conducted on *P. stutzeri*, as presented in Figure 12 and 13, A and B. A small amount of oxygen (~ 7 µl) was added to the incubation flasks, as described in chapter 2.5.2. It took the cells > 115 hours to deplete this oxygen. The first 95 hours of aerobic respiration have been cut from the figures, which now include the depletion of oxygen and the onset of denitrification. It should be noted that the concentration of N_2O-N decreased with ~ 15 µmol flask^{-1} during the first 95 hours of the incubation, while the concentration of N_2-N during this period increased with only ~ 3.3 µmol flask^{-1}. This suggests that the decrease in N_2O-N was caused by headspace dilution during sampling (see Appendix D).

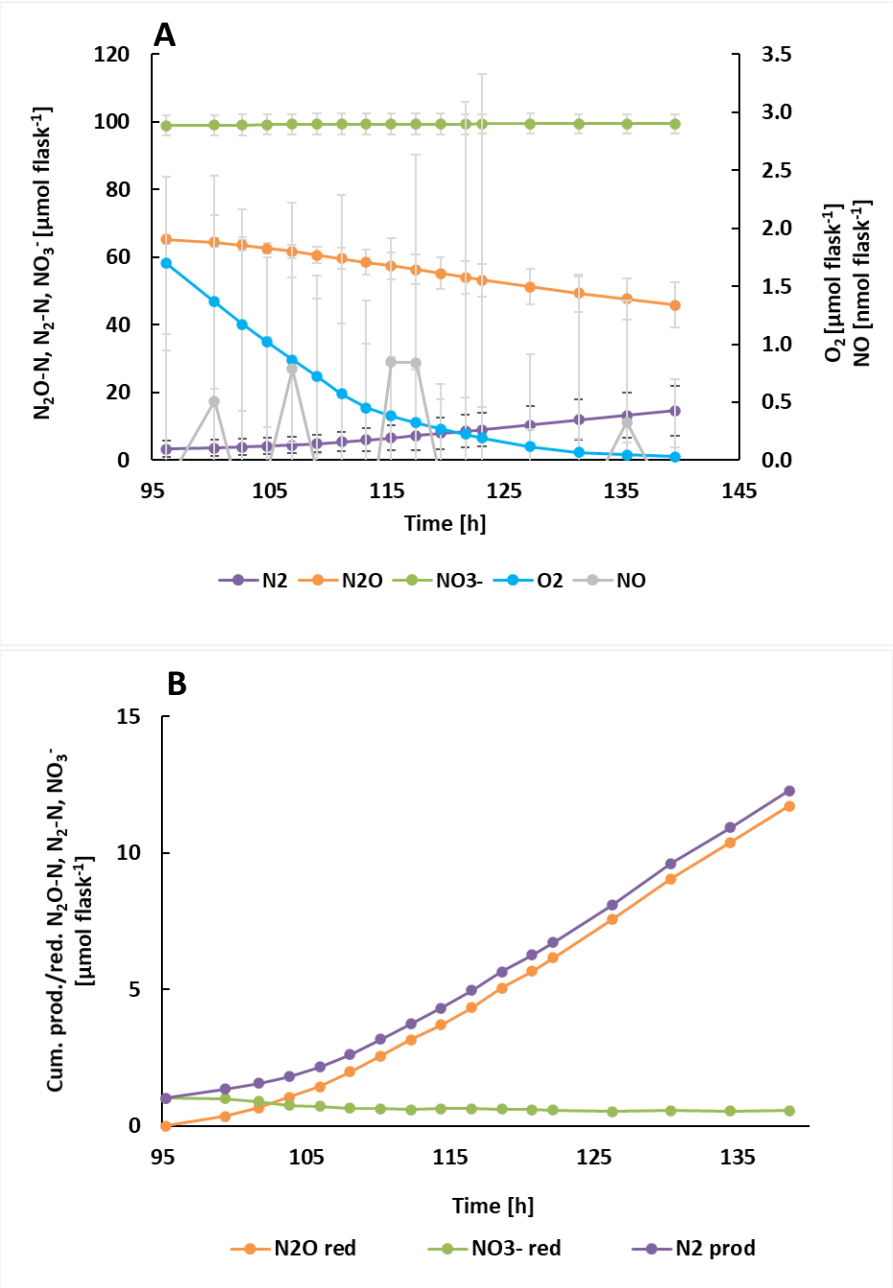

Figure 12: Denitrification in starved *Pseudomonas stutzeri* JM300. The cells were starved following the starvation bioassay (Figure 7) with 0.23 % initial O_2, and kept at 20 °C with vigorous stirring throughout the incubation. The flasks initially contained ~ 7 µmol O_2, ~ 65 µmol N_2O-N and ~ 100 µmol NO_3^-. Due to the very slow respiration of oxygen during the first 115 hours, the first 95 hours of the incubation are not shown. **Panel A** shows the denitrification phenotype of starved cells. The concentrations of N_2O-N, N_2-N and NO_3^- are given as µmol flask^{-1} on the left-hand axis, whereas the concentrations of O_2 and NO are given as µmol flask^{-1} and nmol flask^{-1}, respectively, on the right-hand axis. Standard deviations are given as vertical bars (n = 9). **Panel B** shows the cumulative reduction of N_2O and NO_3^- and the cumulative production of N_2 for the same cultures as in panel A. The reduction of exogenous N_2O-N (orange) is calculated based on the N_2O-reduction rates from timepoint to timepoint. The production of N_2-N (purple) is likewise calculated based on the N_2-production rates from timepoint to timepoint. NO_3^- values are based on mass balance calculations were the difference between N_2-N produced and N_2O-N reduced is assigned to NO_3^--reduction (green).

The metabolism of starved *P. stutzeri* was extremely slow with a cell specific respiration of 1.37 +/- 0.934 fmol e^- $cell^{-1}$ h^{-1} (mean +/- sd), equalling 1 % of the respiration of well-fed denitrifying cells. Oxygen was depleted after about 115 h (Figure 12 A). Denitrification started about 5 h before that (at 110 hours), seen as a slight decrease in N_2O, accompanied by a corresponding increase in N_2. At the same time, the cumulative reduction of externally added N_2O-N increased (Figure 12 B). No reduction of nitrate was observed in most of the flasks. However, in one flask, a gradual decrease of nitrate was calculated (Figure 13 A and B) to occur at the same time as N_2O reduction.

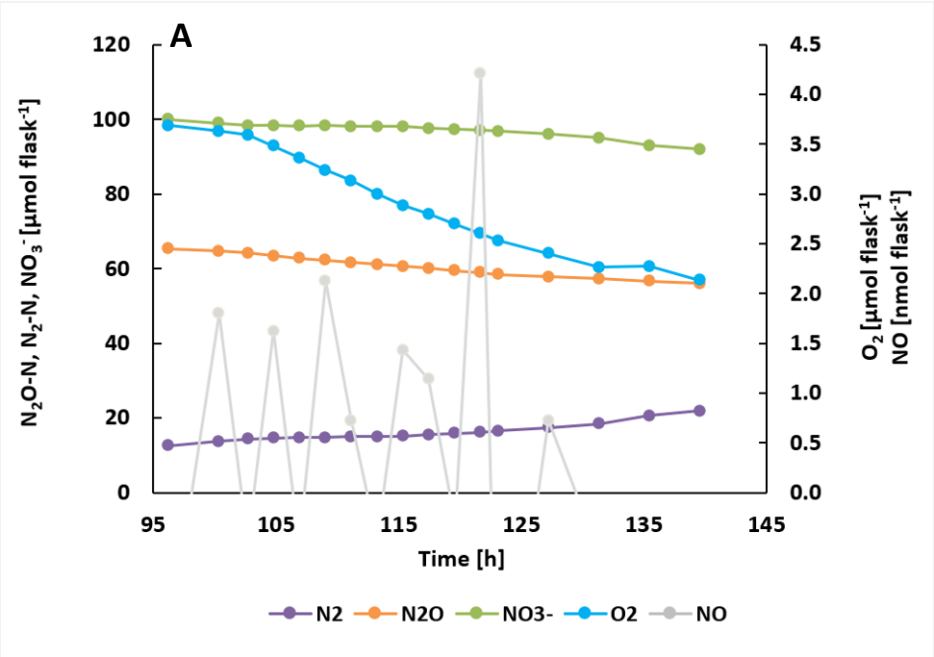

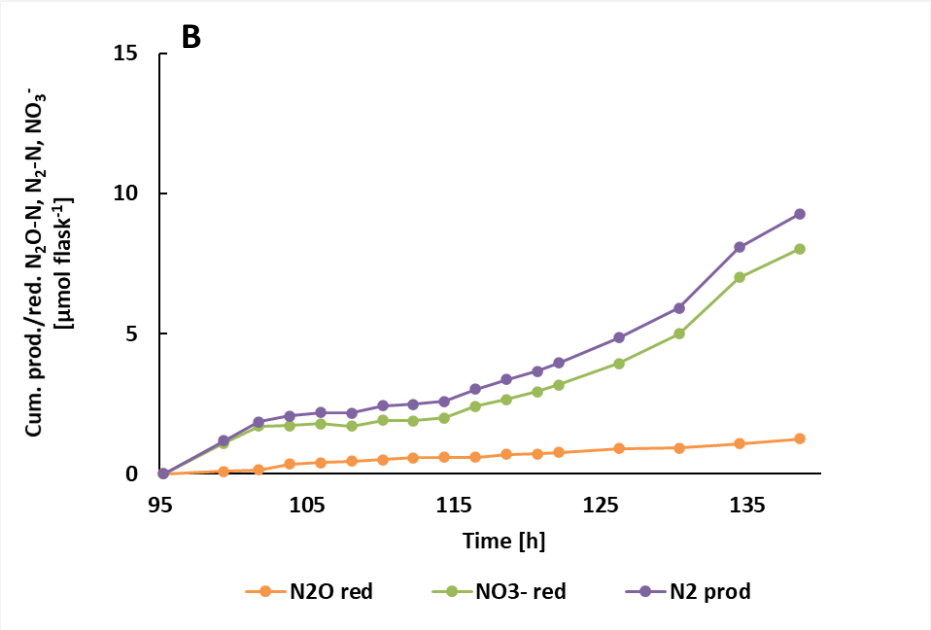

Figure 13: Denitrification in starved *Pseudomonas stutzeri* JM300 with nitrate reduction. The cells were starved following the starvation bioassay (Figure 7) with 0.23 % initial O_2, and kept at 20 °C with vigorous stirring throughout the incubation. The flasks initially contained ~ 7 µmol O_2, ~ 65 µmol N_2O-N and ~ 100 µmol NO_3^-. Due to the very slow respiration of oxygen during the first 115 hours, the first 95 hours of the incubation are not shown. **Panel A** shows the denitrification of starved cells. Note that the concentrations of N_2O-N, N_2-N and NO_3^- are given as µmol flask^{-1} on the left-hand axis, whereas the concentrations of O_2 and NO are given as µmol flask^{-1} and nmol flask^{-1}, respectively, on the right-hand axis. This phenotype was only observed in one flask; hence no standard deviations are given. **Panel B** shows the cumulative reduction of N_2O and NO_3^- and the cumulative production of N_2 for the same culture as in panel A.

One culture reduced nitrate towards the end of oxygen respiration, as shown in Figure 13 A. Figure 13 B illustrates that most of the accumulated N_2-N did in fact originate from the reduction of nitrate. The reduction of exogenous N_2O-N only accounted for 1.25 µmol flask^{-1} of the total 9.3 µmol flask^{-1} of accumulated N_2-N. This culture also showed a slower respiration of oxygen, and had a final O_2 concentration of ~ 2 µmol flask^{-1} at the end of the experiment, compared to a final O_2 concentration of ~ 0 µmol for the other cultures (Figure 12 A). Despite the slower aerobic respiration, the overall cell specific respiration was 5.60 +/- 0.968 fmol electrons cell^{-1} h^{-1}, which is 2 % of the cell specific respiration of well-fed denitrifying cells. Since no carbon was provided in the medium, the calculations of cell specific respiration were based on the assumption that the cell number was constant throughout the incubation time.

3.3.1.1 The transition from feast to famine

Due to the extremely slow metabolism of starved *P. stutzeri*, an experiment was conducted to study the metabolic response when the cells entered starvation. Cells were grown in carbon restricted media with (S1) or without (S2) glutamic and aspartic acid (See Table 3). The metabolic activity is portrayed in Figure 14 A-D and Figure 15. The cells showed a fast metabolism (217 and 237 fmol electrons cell^{-1} h^{-1} under oxic and anoxic conditions, respectively) during the first 10-15 h when a carbon substrate was still available in the medium. The fast metabolism was seen as a rapid consumption of the electron acceptor (O_2 or N_2O), and a corresponding production of CO_2 (Figure 14 A-D). For the cells grown with glutamic acid and aspartic acid (Figure 14 A and C), the respiration rate decreased after about 10 and 15 h, respectively. After approximately 50 h, all electron acceptors were consumed (Figure 14 A and C), and the CO_2 production ceased.

Table 3: Two versions of Sistrom's medium with low concentrations of succinate. The media used (S1 and S2) were derived from Sistrom's medium, but the concentration of succinate was restricted. Only one of the media (S1) contained glutamic - and aspartic acid.

Medium	Succinate [g/l]	L - aspartic acid [g/l]	L - glutamic acid [g/l]
S1	0.086	0.04	0.1
S2	0.086	-	-

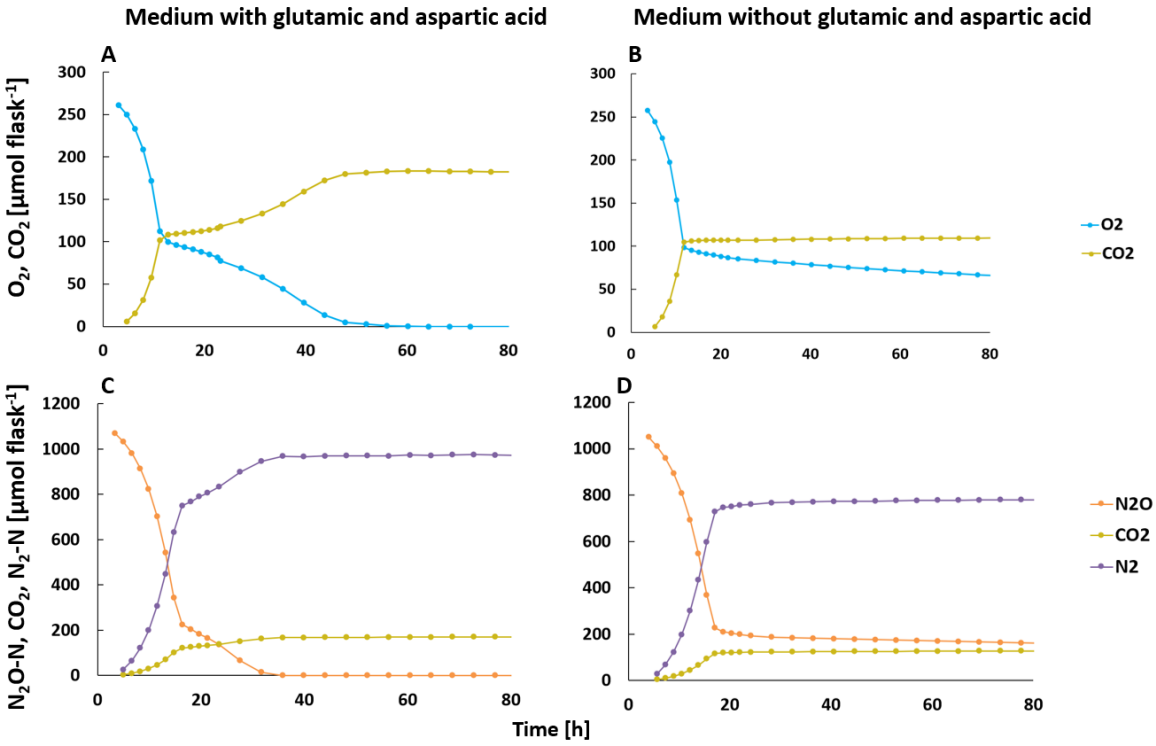

Figure 14: Metabolic activity of cells in carbon restricted medium, with and without glutamic and aspartic acid. Cells of *P. stutzeri* were grown in Sistrom's medium with 0.086 g/l succinate, with (A and C) or without (B and D) glutamic and aspartic acid (0.1 g/l and 0.04 g/l, respectively). The metabolic activity is shown as the respiration of available electron acceptors (O_2 for panels A and B or N_2O for panels C and D), and as the production of CO_2 and N_2 (for cells under anoxic conditions). The provided amounts of carbon source and electron acceptor (O_2 or N_2O) were chosen so that the electron acceptors would be depleted before the carbon source. This was not the case for cells were glutamic acid and aspartic acid were present in the medium.

For the cells grown without glutamic and aspartic acid (Figure 14 B and D), the metabolism came to a halt after 10-15 h. The consumption of electron acceptor decreased significantly, and O_2-levels and N_2O-levels stabilized at about 100 µmol flask^{-1} and 200 µmol flask^{-1}, respectively. At this point the cells were expected to have used all the carbon provided in the medium, and to have entered starvation. Following the transition to starvation, the cell specific respiration fell considerably, as visualized in Figure 15.

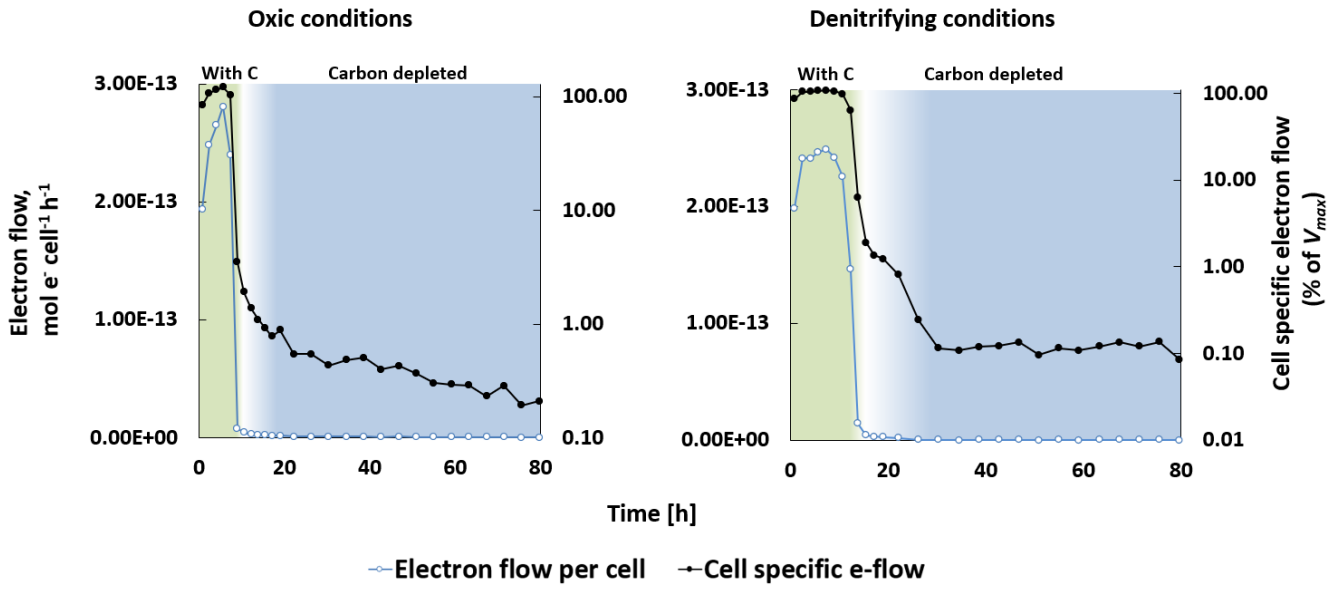

Figure 15: Cell specific respiration during the transition from feast to famine in *P. stutzeri* JM300. The figures show the transition from a phase with carbon available ("With C", green phase) to a phase where all carbon provided in the medium was assumed to be depleted ("Carbon depleted", blue phase) under oxic and anoxic (denitrifying) conditions. The metabolic activity of the cells is shown as electron flow (mol e^- cell^{-1} h^{-1}) on the right axis, and as cell specific respiration on the left axis. The cell specific respiration is given as percent of maximum respiration of the cells (V_{max}). Note that the values for cell specific electron flow are logarithmic, and that the right figure has a minimum value of 0.1, whereas the left figure has a minimum value of 0.01.

As the cells assumedly depleted their carbon sources, the electron flow per cell dropped to 0.62 +/- 0.18 fmol electrons cell^{-1} h^{-1} for cells under oxic conditions, and 0.28 +/- 0.03 fmol electrons cell^{-1} h^{-1} for cells under denitrifying conditions (mean +/- sd). In Figure 15, the depletion of carbon is seen as a transition from the green phase to the blue phase. When carbon substrate (succinate) was available, the cells respired at a maximum rate (V_{max}). As they entered starvation, the cell specific electron flow fell to 2.4 % and 1.2 % of V_{max} under

oxic and denitrifying conditions, respectively. The respiration rate was a stable low throughout the rest of the incubation time.

3.3.1.2 The recovery of starved *P. stutzeri* JM300

To investigate the possible recovery from starvation, some cultures of *P. stutzeri* received carbon substrate and additional N_2O after starvation. Three cultures had been starved under oxic conditions for 115 h (+ 20 h prior to incubation, see Figure 7) and then under anoxic conditions for an additional 25 h. The response to carbon addition is shown in Figure 16. Prior to carbon addition, no nitrate had been reduced (Figure 12).

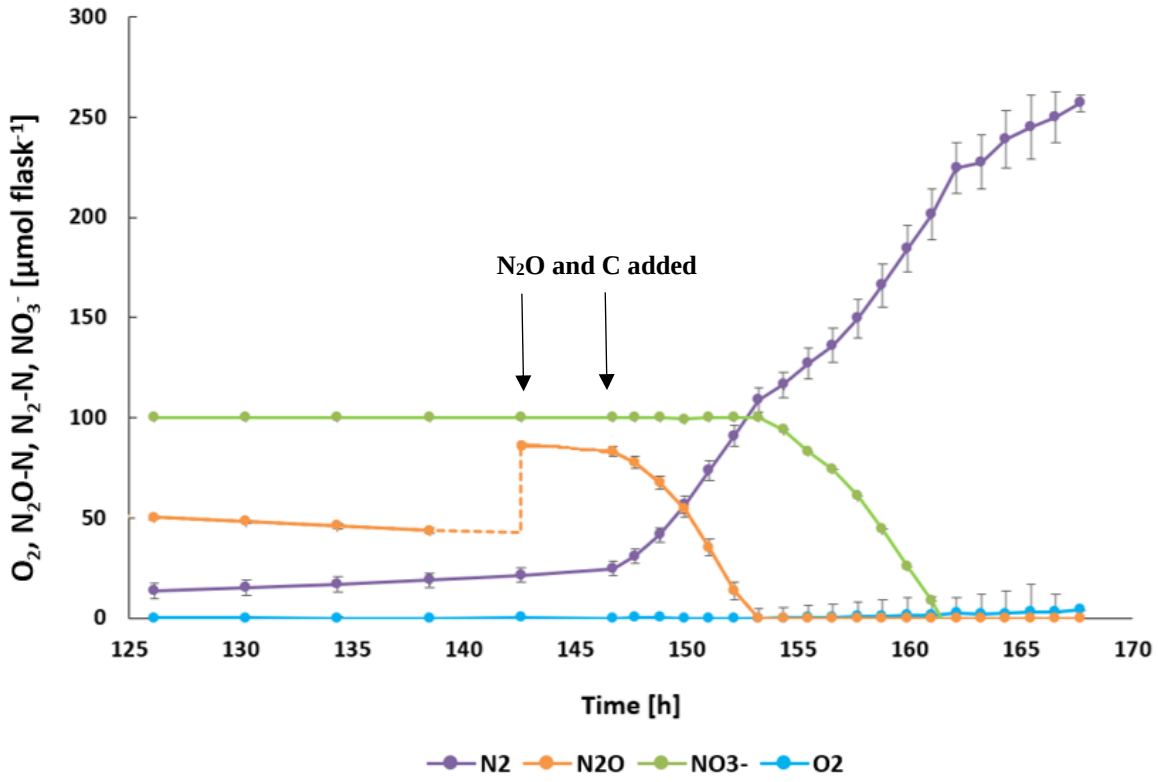

Figure 16: Providing starved cells of *P. stutzeri* with carbon. After 115 hours of oxic starvation and 25 hours of anoxic starvation, an amount of carbon equal to 50 ml Sistrom's medium was added to the incubation flasks. 43 µmol N_2O-N was added to provide the cells with sufficient electron acceptors prior to the carbon addition (at 146 h). The addition of N_2O is shown with a dashed line. The cycle time for gas sampling was reduced to get a higher resolution. The concentrations of NO did not exceed 1 nmol, and are therefore not shown in the figure. Standard deviations are given as vertical bars (n = 3).

The addition of carbon to starved cells led to an increased rate of N_2O reduction and N_2 production, as evident from Figure 16. Following the principles presented in Appendix E, it was calculated that 1-2 % of the initial cells responded to the addition of carbon. Less than 10 h after carbon addition, the cells had reduced all externally provided N_2O. The total accumulated concentration of N_2-N when N_2O was depleted (~ 87.6 µmol flask^{-1}) corresponded to the N_2O-N reduced (~ 86.8 µmol flask^{-1}) at the same time. This suggested that almost no nitrate was reduced before N_2O was depleted, as is also illustrated in Figure 16. Nitrate was reduced after the depletion of N_2O. The cells showed a different nitrate reduction strategy than what was seen for well-fed *P. stutzeri* (Figure 8 A), were N_2O and nitrate were reduced simultaneously.

Cells that were starved further, first under anoxic and then under oxic conditions for a total of 113 days also showed a recovery after carbon addition. The share of viable cells after this long period of starvation was between 0.25 % and 1.56 % (n = 3).

3.3.2 The starvation of *T.* sp. 27

Since oxygen reduction was extremely slow in starved *P. stutzeri*, starved cells of *T.* sp. 27 were added directly to anoxic incubation flasks (as explained in the starvation bioassay in Chapter 2.5.2 and Figure 7). The incubation flasks contained a small amount of oxygen (2.3 µmol), which was reduced within 15 h (Figure 17 A). Once oxygen was depleted, the cells reduced N_2O to N_2 for approximately 15 h. The reduction rate of N_2O increased from ~ 0.24 µmol N_2O-N h^{-1} to ~ 0.76 µmol N_2O-N h^{-1} during this time (Figure 17 B). After 30-35 h, the N_2O-reduction and N_2-production stopped, and the cumulated reduced N_2O stabilized after the reduction of approximately 20 µmol N_2O. Based on the assumption that no nitrite was accumulated it was concluded that no reduction of nitrate took place.

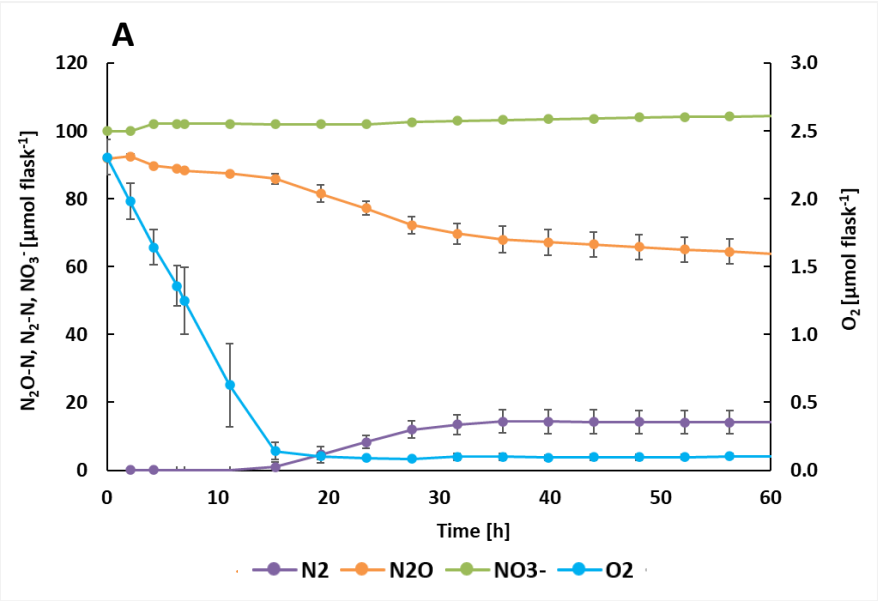
A
120
100
80
60
40
20
0
3.0
2.5
2.0
1.5
1.0
0.5
0.0
0
10
20
30
40
50
60
Time [h]
N2
N2O
NO3-
O2

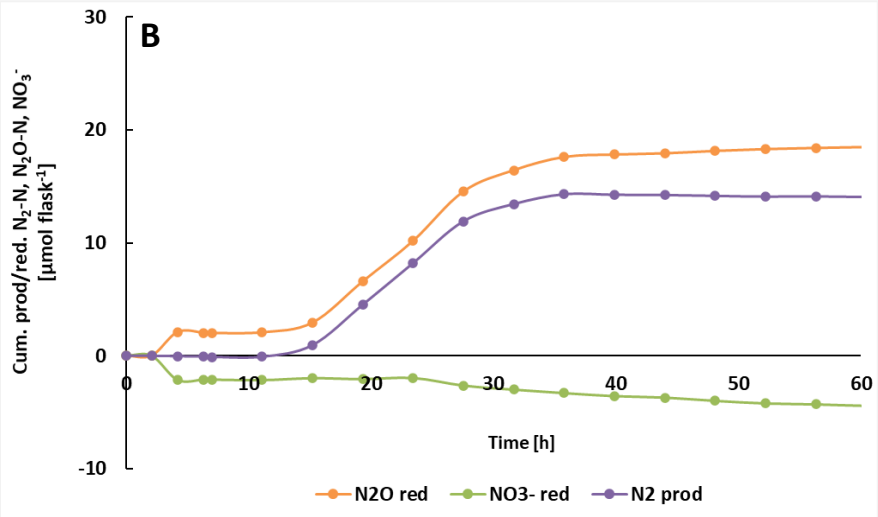
B
30
20
10
0
-10
0
10
20
30
40
50
60
Time [h]
N2O red
NO3- red
N2 prod

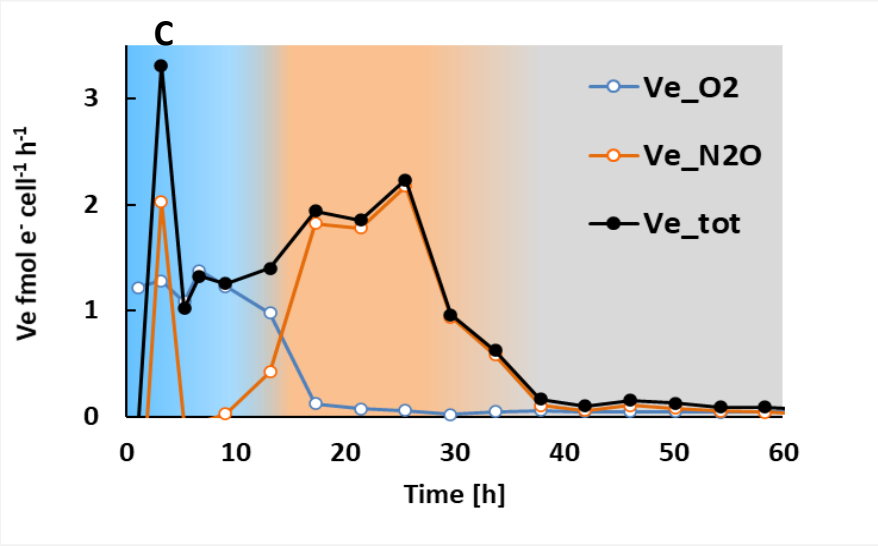
C
3
2
1
0
0
10
20
30
40
50
60
Time [h]
Ve_O2
Ve_N2O
Ve_tot

Figure 17: Denitrification in starved *Thauera* sp. 27. The cells were starved according to the starvation bioassay described in Chapter 2.5.2 (Figure 7), and kept at 20 °C with vigorous stirring throughout the incubation. The flasks initially contained ~ 2.3 µmol O_2, ~ 90 µmol N_2O-N and ~ 100 µmol NO_3^- as electron acceptors. **Panel A** shows the denitrification kinetics of starved cells. Note that the concentrations of N_2O-N, N_2-N and NO_3^- are given as µmol flask^{-1} on the left-hand axis, whereas the concentration of O_2 is given as µmol flask^{-1} on the right-hand axis. The concentrations of NO are left out of the figure because they were considered as noise. Standard deviations are given as vertical bars (n = 5). **Panel B** shows the accumulated reduction and production of N_2O and NO_3^-, and N_2, respectively. **Panel C** illustrates the cell specific electron flow (V_e) (fmol e$^-$ cell^{-1} h^{-1}) to O_2 (blue line), N_2O (orange line) and the total electron flow (black line) throughout the incubation time. The electron flow was divided into three phases of oxic respiration, denitrification and a "metabolic pause", which are presented as a blue, an orange and a grey phase, respectively. The electron flow calculations were based on O_2 reduction rates, N_2O reduction rates and the cell number per vial, estimated via OD_{600} measurements.

The electron flows to the utilized electron acceptors, O_2 and N_2O, were calculated as an estimate for cell specific respiration throughout the incubation time. The electron flows are presented in Figure 17 C, together with the total electron flow to both electron acceptors. The total electron flow was highest at the start of the incubation time, with a maximum of 3.31 fmol electrons cell^{-1} h^{-1}, due to a peak in the electron flow to N_2O. The total electron flow dropped from this point, but the electron flow to O_2 remained stable at 1.24 +/- 0.11 fmol electrons cell^{-1} h^{-1} throughout the phase of aerobic respiration (blue).

During the transition from aerobic respiration to denitrification (blue to orange phase) after about 15 h, the electron flow to O_2 decreased to an average of 0.05 +/- 0.02 fmol electrons cell^{-1} h^{-1}. The electron flow to N_2O increased to a maximum of 2.17 fmol electrons cell^{-1} h^{-1} after 30 h. During the last stages of denitrification, before the cells entered the "metabolic pause" (grey phase), the electron flow to N_2O (and thus also the total electron flow) dropped significantly. From 40 h and onwards, the total electron flow stabilised at 0.1 +/- 0.04 fmol electrons cell^{-1} h^{-1}. During this phase, the cells showed no significant metabolic activity based on gas kinetics (Figure 17 A). The electron flow calculations were based on the assumption of a constant cell number throughout the incubation period.

4. Discussion

4.1 Denitrification phenotypes and the electron tug of war

The results from Figures 8 and 9 support the first hypothesis postulated (originally by Mania et al and Gao et al (6, 7)) in this thesis; that there is indeed an electron competition between NapC and the bc_1-complex. As shown for diverse strains of bradyrhizobia in those studies, the two organisms *T.* sp. 27 and *T.* sp. 63 with Nap as the only dissimilatory nitrate-reductase complex and NosZ clade I studied in this thesis both showed a strong preference for N_2O over nitrate. However, the preference was not absolute, and a small reduction of nitrate was seen towards the end of N_2O-reduction for *T.* sp. 63 (Figures 8 and 9). This suggested that both reductases were present during N_2O reduction, as indicated by transcription analysis (7) and confirmed by proteomics (Gao and Frostegård, unpublished results) in bradyrhizobia. A small leakage of electrons to NapC is coherent with previous investigations in bradyrhizobia (6, 7), and does not discard the hypothesis. *P. stutzeri* JM300, with the genetic potential for both Nar and Nap, reduced nitrate and N_2O simultaneously, in accordance with the hypothesis. Ideally, my results should have included proteomic investigations, to confirm the presence of the denitrification reductases. This could have confirmed that the preferred N_2O reduction in Nap-Nos-organisms is due to metabolic regulations, had both Nap and NosZ been detected during N_2O reduction. Unfortunately, the proteome extraction of *P. stutzeri* was unsuccessful, as was the mass spectrometric analysis of the proteome of *T.* sp. 27. This is discussed in Chapter 4.1.2.3. However, other factors than the presence of Nar and/or Nap seem to play an important role in the electron allocation between denitrification reductases. This was evident from one of my tested strains, *T. linaloolentis*, which did not show the expected phenotype.

4.1.1 NosZ-clades and their effect on denitrification

T. linaloolentis has the genetic potential for Nap as the only dissimilatory nitrate reductase complex, and was thus expected to reduce N_2O prior to nitrate. However, the strain showed a phenotype similar to a Nar-Nos organism, such as *P. stutzeri* (Figures 8 and 9). I have two possible explanations for this divergent phenotype. First, it may be that the electron competition between NapC and the bc_1-complex, and its implications for N_2O reduction in Nap-Nos organisms, is not as generic as hypothesised. The second explanation is that this is

caused by *T. linaloolentis* potential for both NosZ clade I and clade II (45). I hypothesised that NosZ clade II organisms with Nap, but not Nar, would not show the same strong preference for N_2O reduction, due to the lack of NosR. If NosZ clade II was the dominant NosZ version in denitrification in *T. linaloolentis,* this could explain why the strains showed a simultaneous reduction of nitrate and N_2O.

Some of the properties of NosZ clade I and clade II support the idea that NosZ clade II was dominant during denitrification in *T. linaloolentis*. NosZ clade II is found to have a higher affinity for N_2O than NosZ clade I (54). I therefore speculate that even though both clades may have been present during the incubation, NosZ clade II dominated N_2O reduction. Even though NosZ clade II had the highest affinity for N_2O does not necessarily make it a strong competitor for electrons. Without the aid in electron transfer for NosR, the possibility to reduce N_2O may have been limited, resulting in a simultaneous reduction of nitrate and N_2O. A study by Semedo et al (45) suggest that NosZ clade II is inhibited by high concentrations of nitrate, by the nitrate concentration used in my experiments (2 mM) were likely too low to cause this inhibition. I therefore propose that N_2O reduction was dominated by NosZ clade II in my incubation of *T. linaloolentis.* However, this is based purely on speculations. Further studies, combined with transcriptome and/or proteome investigations are needed to understand the effect of NosZ clades on denitrification.

4.1.2 Technical discussion

4.1.2.1 The case of the slow growing Thauera *strains*

Three of the *Thauera* strains originally included in this thesis, *T. terpenica, T. DNT-1* and *T. aminoaromatica,* were excluded from my work. They were reported as being slow growing cells with the genetic potential for complete denitrification, including the genes for Nar, Nap and Nos (41). Initially, they were grown in R2A medium under oxic conditions (Appendix A), as suggested by the culture collection they originated from (DSMZ). Prior to incubation, they were inoculated into a medium earlier designed for culturing these strains (41) referred to as *Thauera*-medium (see Appendix A). However, none of the strains showed any detectable denitrification activity (Appendix F). This was also the case when R2A was used during the

incubation (Appendix F). Similarly, no aerobic growth was detected in *Thauera*-medium, even though three different batches of media were tested. Since time was limited, I could not invest more effort into getting those strains to grow, and they were replaced by *Pseudomonas stutzeri* JM300, which had the same genetic potential for denitrification.

4.1.2.2 Calculating the relationship between OD_{600} and cell number

The factor describing the relationship between OD and cell number for *P. stutzeri* was determined through plate spreading and a simple linear regression analysis (Appendix B). Although the R^2-value was very high (0.999), the number is associated with some uncertainty. The CFU/ml was only decided for three cell densities, so a large part of the standard curve is based on interpolation. However, the linear relationship between OD and cell number up to certain densities is well known, so I do not consider this to be of major concern. More importantly, the variation between replica plates was huge, varying from 100 to > 800 colonies per plate for the least diluted series. Additionally, the factor was only determined for *P. stutzeri*. The relationship between OD and cell number should have been determined for *T.* sp. 27 as well, but no colonies appeared on the plate after plate spreading. The cells originated from an actively growing culture, and had previously grown on the agar I used. It therefore remains a mystery to me why this was unsuccessful.

Despite the variation associated with the relationship between OD and cell number, it was still used while analysing data. The factor was never used to determine the number of cells present at a certain time, but was always used in comparisons. In all the comparisons, the same factor was used to determine cell number, thus discarding the importance of the factor itself. The factor could therefore also be used on starved cells and anaerobically grown cells, even though the true relationship between OD and cell number was not likely to be the same for different treatments or strains.

4.2 Utilization of carbon sources in *P. stutzeri* JM300

The utilization of three different carbon sources was neatly demonstrated in an experiment with *P. stutzeri* JM300, as illustrated in panels A and C of Figure 14. The cells were given access to succinate, aspartic acid, and glutamic acid. The cells showed a classic diauxic growth, were the cells first exploited one carbon source before synthetising enzymes to utilize the next carbon source (55).

I suspect that during the first period of exponential growth (the first 10 to 15 hours for oxic and anoxic growth, respectively), the cells used succinate and glutamic acid as their carbon sources. The cells were grown on Sistrom's medium with succinate as the main carbon source in between incubations, and were therefore expected to possess the enzymes necessary for succinate degradation from the start of incubation. Additionally, as succinate is an intermediate in the TCA-cycle, one can assume that cells would rather grow on succinate than aspartic acid. Studying the kinetics in Figure 14 also indicates that succinate is utilized prior to aspartic acid, as the first period of exponential growth in panels A and C resemble the growth in panels B and D, where the cells only had access to succinate. It is likely that enzymes for the uptake glutamic acid were also expressed. Glutamic acid is an intermediate in the TCA-cycle, and is involved in the formation of most of the cell's nitrogen-containing metabolites as an amino-group donator (56). I therefore assume that the cells utilized succinate and glutamic acid prior to aspartic acid.

After the depletion of succinate and glutamic acid, as seen by decreased rates of O_2- and N_2O reduction as well as of CO_2- and N_2 production, the cells entered a lag phase. During this phase, the cells were metabolically active and respiring, though at a much slower rate than during succinate/glutamic acid growth. During the lag phase, new enzymes for the utilization of aspartic acid were likely synthesised. Once the cells had adapted to grow on aspartic acid, the metabolism increased, and the cells entered a new stage of exponential growth. However, the cells quickly depleted their electron acceptors (O_2 and N_2O) before they could grow further. None the less, the experiment is a textbook example of the enzymatic adaptation and diauxic growth that Monod described in the 1940-1960's (55). Additionally, it showed that cells of *P. stutzeri* JM300 did not depend on a supply of aspartic acid or glutamic acid to grow.

4.3 A life of feast and famine

4.3.1 The transition from feast to famine

The transition from feast to famine in *P. stutzeri* JM300 is a dramatic story of sudden change. The transition was studied by growing cells in a medium with a shortage of electron donors (0.52 mmol electrons from succinate) compared to electron acceptors (1.04 mmol electrons from O_2 or N_2O). As seen in Figure 14 B and D, the cells responded almost immediately to the lack of carbon sources by reducing their metabolic activity considerably. Based on gas kinetics (Figure 14) the metabolism of the cells seemed to shut down completely, as no increase in CO_2 was seen. There was a small decrease in O_2 and N_2O concentrations after succinate was depleted, but as this was not seen in conjunction with an increase in CO_2, it may well have been caused by headspace dilution during sampling. None the less, the cells still sustained a low metabolic activity.

The metabolic activity sustained during the "metabolic shutdown" was seen as cell specific electron flow (Figure 15). Upon starvation, the electron flow quickly dropped, and eventually stabilised at a rate equal to 0.1-0.2 % of V_{max} (cell specific electron flow seen during succinate utilization). Interestingly, the cell specific respiration under oxic conditions was twice as high as the respiration under denitrifying conditions. This is not unreasonable. Cells living in oxic environments must constantly face the dangers posed by reactive oxygen species (ROS), such as H_2O_2 and O_2^-. ROS can cause damages to enzymes, particularly Fe-S centres, and nucleic acids. In order to prevent and repair such damages, the cells must have scavenging enzymes to control the intracellular concentrations of ROS, and a variety of repair systems at the ready (57). Cells in anoxic environments, on the other hand, do not face these challenges, and it is likely that they can settle at a lower metabolic rate.

4.3.2 Starvation strategies

Cells of *P. stutzeri* that had been starved according to the starvation bioassay in Figure 7 seemed to be in a "metabolic shutdown", as expected from the results in Figures 14 and 15. The cells therefore performed oxic respiration for about 120 hours to reduce the 7 µmol O_2 added to the flasks. At the same time, a considerable loss of N_2O was seen, which was assigned mostly to headspace dilution due to sampling (Appendix D). However, a slight increase in N_2 occurred during this time. This could either be due to a small leakage of atmospheric air into the incubation flasks, or it could suggest that some denitrification took place during oxygen reduction, which is not unreasonable (58). Even though the presence of oxygen is one of the most important repressors of denitrification (1, 43), cells are seen to start N_2O reduction at low O_2 tensions (Figure 8) (41, 58). It is advantageous for cells to express a part of the denitrification proteome before the oxygen tension gets too low. If the oxygen tension gets too low, the cells might be trapped in anoxia, without sufficient energy to synthesise the denitrification proteome. Synthesising a part of the proteome early enables the cells to start respiring anoxically once oxygen is depleted, providing energy to synthetise the remaining denitrification proteome (59, 60). Additionally, *nosZ* is hypothesised to be transcribed constitutively for *T.* sp. 27, also under oxic conditions (41), and this may also be the case for *P. stutzeri*. This argumentation supports the idea that a small reduction of N_2O to N_2 may have taken place from the onset of incubation. After oxygen was depleted, the slow metabolism continued, and the cells start to denitrify, keeping a cell specific electron flow of about 1.37 fmol electrons $cell^{-1}$ h^{-1}.

The cells of *T.* sp. 27 seemed to show a different strategy to handle starvation than *P. stutzeri*. During the first hours of starvation, *T.* sp. 27 kept a relatively stable electron flow of 1-2 fmol electrons $cell^{-1}$ h^{-1} (Figure 17 C). During this time, oxygen was depleted, and some N_2O was reduced to N_2. After about 30 hours, the reduction of N_2O ceased, and the cell specific electron flow dropped significantly to 0.1 fmol electrons $cell^{-1}$ h^{-1} (Figure 10 C). Even though the cell specific electron flow during respiration was in the same order as the cell specific electron flow in starved *P. stutzeri* (calculated from Figures 12 and 13), the reduction of O_2 and N_2O was much faster for *T.* sp. 27. Additionally, the results on the transition from feast to famine of *P. stutzeri* (Figure 15) showed that the starved cells had a cell specific electron flow of 0.28 fmol electrons $cell^{-1}$ h^{-1}. This supports the idea that starvation in *T.* sp. 27 is divided

into an active face of low, but noticeable, respiration, and a “metabolic pause”. Cells of *P. stutzeri*, on the other hand, showed a stabile low metabolism over a long period of time, with a slow respiration rate. This idea is further supported by the microscopic investigations performed on well-fed and starved cells.

Microscopic investigations of *T.* sp. 27 and *P. stutzeri* (Figures 10 and 11) suggested that *T.* sp. 27 accumulates PHB as an internal carbon storage, whereas *P. stutzeri* does not. The nile red granules in *T.* sp. 27 can reasonably be assumed to be PHB, since strains from this genus have previously been reported to accumulate PHB (8, 48). The grains occurred only in well-fed cells, and were randomly spread across the cells. The areas dominated by grains showed a much lower signal of dapi, which stains DNA. This indicated that the grains were located in between DNA, which is a logical assumption for lipid-containing granules. Another argument that the grains were in fact PHB is the fact that they seemed to be absent from starved cells. I believe that upon starvation, the cells used the extra carbon available in the granules (PHB) to maintain a higher metabolism for a longer time. It should be noted that this is a speculation based only on visual examinations, and needs to be confirmed by quantitative analyses of PHB content.

I further believe that the cells of *P. stutzeri* did not accumulate PHB, as no granules were found in the microscopic investigations (Figure 11), and no strains of *P. stutzeri* are reported to accumulate intracellular carbon storages in the form of PHB (61, 62). However, the possibility that *P. stutzeri* accumulates other carbon storages, such as glycogen, cannot be rejected. Based on my results, it is difficult to evaluate whether this is the case. Based on the transition from feast to famine (Figure 15), the cells seem to enter a state of “metabolic shutdown” from the moment external carbon sources are depleted, seen as a constant decrease in cell specific electron flow. However, starved cells that respired oxygen for 115 hours showed a clear increase in N_2 once denitrification was initiated. This suggests that the cells remained active for a longer time than *T.* sp. 27, where the cells did not show any noticeable respiration after 40 hours (+ 20 hours of oxic respiration prior to incubation and 16 hours as He-washed, see Chapter 2.5.2). Due to the slightly different experimental setups for *P. stutzeri* and *T.* sp. 27, an accurate comparison is difficult. The precise starvation strategies for *P. stutzeri* and *T.* sp. 27 remain unknown. However, some well-known starvation strategies were observed in both strains.

Both *P. stutzeri* and *T.* sp. 27 showed some typical morphological changes when subjected to starvation. As seen in Figure 10, starved cells of *T.* sp. 27 (panels F and G) had a rounder shape and were possibly smaller than well-fed cells, although the size change was difficult to determine with the naked eye. These morphological changes were not unexpected, as energy starved cells are often seen to take on a more coccoid shape (47). Both strains showed an accumulation of dark matter towards the cell poles, which is most evident in panel G (anaerobically starved cells of *T.* sp. 27). The dark matter was likely cellular material, and the accumulation towards the poles suggested that these cells were fragmenting, which in turn results in smaller cells. I suspect that if the cells were starved for a longer time, the size reduction would be more prominent. The morphological changes lead to both smaller cell sizes and a reduced surface area to volume ratio. This increases the diffusion rates in the cells and facilitates the uptake of nutrients from the environment.

The efficiency of nutrient uptake by starved cells was shown for *P. stutzeri* (Figure 16). After about 140 hours of starvation under both oxic and anoxic conditions, a small fraction of the original population (1-2 %) was revived. Even in cultures that had been subjected to various periods of oxic and anoxic starvation for a total of 113 days, about 0.1 – 0.2 % of the cells were still viable. The experiment shows that bacterial cells can persist and survive over long periods of time by shutting down their metabolism to a minimum, still ensuring vital cellular functions. When the cells experience a flux of nutrients, only a small fragment of the population needs to be viable, thus securing the population to rise again. My results are in agreement with Gray et al, who found that cells of non-sporulating *B. subtilis* were viable after 100 days of starvation (46). In addition, I showed that cells can survive even longer, and under more drastically changing conditions, than *B. subtilis* was subjected to.

4.3.3 Technical discussion

4.3.3.1 Differences in cell specific electron flow

The cell specific electron flow for starved *P. stutzeri* was calculated based on two different incubations, seen in Figures 12, 13 and 15. The cell specific electron flow was about 10 times higher in the incubations from Figures 12 and 13, compared to the incubation in Figure 15. First, this indicates that the washing of cells according to the starvation bioassay (Figure 7) did not reduce the cells' ability to respire. This increases the reliability of the results from incubations of starved cells.

Secondly, the electron flows in Figures 12 and 13 were calculated differently than in Figure 15. In Figures 12 and 13, the electron flow was calculated by using the rate of N_2O-reduction and O_2-reduction at different timepoints. The reduction of 1 mol O_2 requires 4 mol electrons, whereas the reduction of 1 mol N_2O requires 1 mol electrons. Based on the cell number at the onset of incubation, the cell specific electron flow was calculated. This method was also used to calculate cell specific electron flow for starved *T.* sp. 27 (Figure 17 C). The method assumes that the cell number remains constant throughout the incubation time, due to the lack of carbon substrate. It is theoretically possible that the cell number did in fact increase throughout the incubation period, either through fragmentation, growth on internal carbon sources, or both. If so, the cell specific electron flow would in fact be lower than the calculated electron flow. The cell specific electron flow in Figure 15 was calculated based on simulated cell growth, as explained in Appendix E. Thus, the differences calculated between different samples may not be as large as estimated.

Nevertheless, the cells were severely starved and had a metabolic activity not higher than 2 % of the metabolic activity of well-fed cells. The discussion of denitrification during starvation (Chapter 4.4) is therefore not affected by the observed differences.

4.3.3.1 Microscopic investigations

The microscopic investigations of well-fed and starved cells could have been performed differently to obtain more reliable results. The anaerobic cells, both well-fed and starved, should have stayed under anoxic conditions for much longer than 4-5 hours. With a generation time of 2.5-3 hours for both strains, the cells were subject to anoxic conditions for no more than two generations. This is not necessarily enough for the cells to show an altered morphology. The cells were expected to shrink upon anoxia, due to a considerable reduction observed in OD in cultures that transitioned from oxia to anoxia. However, shrinking was not supported by the microscopic investigations, possibly because the cells had not been under anoxic conditions for long enough. Another suggestion for the reduction in optical density could be cell aggregation. Even under constant stirring, anaerobic cells, and especially starved cells of *T.* sp. 27, tended to form biofilms on the glass wall of the culture flask, thus efficiently removing the cells from the suspension. Increased surface adhesion is found as a starvation response in many strains (47). A tendency of increased aggregation was indeed observed in the microscopic investigation of anaerobic well-fed *T.* sp. 27, but not in the anaerobic starved, as would have been expected.

As mentioned in chapter 2.5.4, some cultures were He-washed prior to fixation, without any electron acceptors present. Starved cells of *T.* sp. 27 were kept like this with neither electron acceptors nor electron donors available. This was done to stabilize the cells over the weekend, to avoid working during the weekend. I suspected that the cells would be immobilized in this state with little chances to grow. Low amounts of oxygen were likely left in the flasks, as seen from other starvation experiments. However, this would only support a little growth to the well-fed cells, whilst subjecting the starved cells to a deeper starvation, forcing them to sacrifice more of their restricted electron donors. A minimum of metabolism in the starved cells must have been present regardless, as discussed previously. One could argue that He-washing the starved cells over the weekend was unnecessary, and that the period of aerobic starvation could simply have been extended.

The well-fed cells were He-washed to prevent excessive growth. The main reason that the starved cells were He-washed was to investigate cells that had undergone the same treatment as the cells used in the incubation experiments (20 hours of oxic starvation). The

prolonged starvation after He-washing may be a reason for why the morphological changes in starved cells were more distinct for *T.* sp. 27 than for *P. stutzeri*. It can take up to several weeks for a starvation-induced change in morphology to appear (47). One could therefore argue that all the cells should have been starved for a longer time.

4.4 Denitrification during starvation

My results on denitrification in starved cells were surprising, and they showed that starved cells can be strong sinks for N_2O. Based on my hypothesis regarding denitrification and starvation, cells of *T.* sp. 27 were expected to reduce N_2O prior to nitrate due to the electron competition between NapC and the bc_1-complex. The results in Figure 17 show that the cells did indeed reduce N_2O almost exclusively. For the same reason, cells of *P. stutzeri* were expected to reduce nitrate and N_2O simultaneously. Interestingly, this was not the case.

Despite the observation that *P. stutzeri* showed no preference for N_2O over nitrate in well-fed incubations (Figure 8 A), 9 out of 10 starved cultures showed a strong preference for N_2O (Figure 12). Only one starved culture reduced nitrate to a larger extent than N_2O (Figure 13). This could suggest that there is a degree of stochasticity regarding the expression of the denitrification reductases in *P. stutzeri*, as has been observed in other strains as well (60). Such a degree of stochasticity is supported by previous investigations of denitrification in *P. stutzeri* JM300 (Milligan and Frostegård, unpublished results) (Appendix G). The study included analyses of the transcriptome of cells that transitioned from oxic to anoxic (denitrifying) conditions in well-fed cultures, and it showed that *narG* was expressed much later than *napA*. My incubations of well-fed cultures indicate that *narG* was expressed, as the cells showed the phenotype of a typical Nar-Nos organism. This indicates that the transcription of *narG* in *P. stutzeri* JM300 is stochastic. This offers a possible explanation for the two phenotypes observed in incubations of starved cells.

The nine starved cultures which exhibited a preference for N_2O reduction might have had a late expression of *nar*, compared to *nap*. With time, the cells entered a deeper starvation, and might have been too starved to express *nar* at a later stage. The cells would

then act as if they were Nap-Nos cells, and thus expected to reduce N_2O prior to nitrate, as observed. The one culture which had nitrate reduction (Figure 13) might have had an early expression of *nar*, and thus shown a phenotype that can be expected for a Nar-Nos organism.

This argumentation is supported by the fact that "resurrected" *P. stutzeri* cells, which had previously showed a preferred N_2O reduction when starved, kept this preference for N_2O when carbon was provided (Figure 16). This supports the thought that these cells had not expressed *nar*, and that they did not express it during the first hours after carbon supply, when N_2O was available. However, the mechanism behind this proposed stochastic expression of *nar* is unknown. Further studies should include analyses of the transcriptome and/or proteome of both well-fed and starved cultures of *P. stutzeri* to get a better picture of the regulation of the expression of *nar*.

Regardless of why starved cells of *P. stutzeri* showed two phenotypes, I can conclude that starvation does not necessarily lead to increased emissions of N_2O, as previously suggested (50). I have shown that Nap-Nos clade I organisms that are strong N_2O sinks due to their preferred reduction of N_2O, can retain this phenotype under nutrient limitations. However, there are probably several factors that affect the outcome of denitrification under nutrient limitations. More research is needed to unravel these mysteries and understand more about what factors lead to increased N_2O-emissions during starvation, and what factors lead to cells being good N_2O-sinks during starvation. This knowledge will be crucial for developing efficient microbiological mitigation options to reduce N_2O-emissions.

4.5 Areas of application

The results in this thesis contribute to knowledge that is of interest for several reasons. The results increase our understanding of the mechanisms behind denitrification, through studying the allocation of electrons between NapC and the bc_1-complex. It also casts some much-needed light on the regulation of denitrification under natural conditions, in this case under carbon limitation. The fact that starved cells functioned as N_2O-sinks in the presence of nitrate is optimistic for the possibility of using microorganisms to mitigate N_2O-emissions. This can be valuable both in the agricultural sector and in wastewater treatment technologies.

4.5.1 The agricultural sector

The potential of using microbes to battle N_2O-emissions from the agricultural sector is large. Microorganisms can be inoculated into the soil to engineer the soil microbiome through vectors such as waste water digestates (25, 29) or via seeds (such as from legumes) that are coated with efficient N_2-fixing and N_2O-reducing bacteria (25, 32). My work has investigated the hypothesis that organisms with Nap as the only nitrate reductase will show a preferred reduction of N_2O prior to nitrate, and that this is caused by an electron competition between NapC and the bc_1-complex. Organisms with a preferred reduction of N_2O could slow down the removal of nitrate from soils, leaving more available for plant growth, whilst limiting the emissions of N_2O from soils. While the electron competition appears to exist in organisms beyond bradyrhizobia, it also appears to be influenced by more factors than just the presence of Nar and/or Nap. The genetic potential for the NosZ clade seems to be of special importance. Additionally, other N-oxides present in soils, such as nitrite, could influence the allocation of electrons to Nos, and thus possibly hamper the strong N_2O reduction potential of the cells. My results show that Nap-Nos clade I organisms are potential agricultural inoculants, though their denitrification phenotype should be screened under natural conditions to verify that they will contribute to the desired effect of N_2O reduction.

4.5.2 Wastewater treatment

Increased knowledge of microbial N-transformation will always be valuable to the wastewater treatment sector, where such transformations are actively used. My work has contributed to this sector by exploring denitrification mechanisms in the genus *Thauera*, which are commonly found in wastewater microbial communities (8). I have shown that fluctuations in carbon availability, which occur in wastewater communities, does not necessarily lead to increased emissions of N_2O. This knowledge is also interesting for biological phosphate removal, were a feast-famine regime can combine phosphate removal, through accumulation of PHB, and nitrogen removal, through denitrification during famine with PHB as an electron source (63). My results show that the possibility of using strong N_2O sinks in wastewater communities is not limited by nutrient fluctuations, and the potential to reduce greenhouse gas emissions from wastewater treatments is large.

4.6 Further research

My results also show some of the knowledge gaps that still exist regarding microbial N-transformations. The role of the NosZ-clades should be assessed further, to unravel their role in making an organism a strong N_2O-sink. The bioenergetics of different enzymes should also be studied. The discovery of the low K_m of NosZ clade II (54) shows that this enzyme might be a much more efficient scavenger of N_2O in natural environments were N_2O concentrations may be fluctuating. Similarly assessing the bioenergetics of other denitrification reductases might lead to similar discoveries. Studies on the competitiveness between the denitrification reductases should be performed, as soils are complex environments where organisms will not only have nitrate and N_2O available, as in my experiments. The competition between Nir, Nor and NosZ is perhaps of special interest, based on starvation studies suggesting that Nir is a stronger competitor than NosZ when carbon is limited (50). Transcriptome and proteome analyses should also be performed to increase our understanding on how different conditions affect the expression of denitrification reductase genes, and other genes associated with denitrification, such as the bc_1- complex and cytochrome *c*. Expanding our knowledge on these areas would be valuable to further use microbes in N_2O mitigation strategies.

5. Concluding remarks

Being able to efficiently use bacteria as N_2O-sinks will be a valuable tool in the fight against climate change in different sectors such as agriculture and wastewater treatments. The results obtained in this thesis have strengthened the hypothesis that there is a general electron competition between NapC and the bc_1-complex which affects the denitrification phenotype of bacterial strains. Furthermore, at least for some strains, the results support that this electron competition is not altered when cells are starved. My results also reveal knowledge gaps with regards to the role of the NosZ-clade on denitrification. Last, but not least, my work has shown that starvation is not necessarily associated with increased emissions of N_2O, contrary to popular belief. Many mysteries of denitrification under natural conditions remain to be solved. More research on the metabolic regulation and electron allocations between the denitrification reductases is needed to provide the best options for microbial mitigation of N_2O-emissions. Nevertheless, my results are optimistic with regards to using microbial soldiers in natural environments to fight alongside us in the battle against N_2O emissions!

6. References

1. Spiro S. Nitrous oxide production and consumption: regulation of gene expression by gas-sensitive transcription factors. Philos Trans R Soc Lond B Biol Sci. 2012;367(1593):1213-25.

2. Richardson D, Felgate H, Watmough N, Thomson A, Baggs E. Mitigating release of the potent greenhouse gas N2O from the nitrogen cycle – could enzymic regulation hold the key? Trends Biotechnol. 2009;27(7):388-97.

3. Pepper IL, Gerba CP, Gentry TJ. Environmental Microbiology. Third ed. United States of America: Elsevier; 2015.

4. Massara TM, Malamis S, Guisasola A, Baeza JA, Noutsopoulos C, Katsou E. A review on nitrous oxide (N2O) emissions during biological nutrient removal from municipal wastewater and sludge reject water. Sci Total Environ. 2017;596-597:106-23.

5. Kraft B, Strous M, Tegetmeyer HE. Microbial nitrate respiration – Genes, enzymes and environmental distribution. J Biotechnol. 2011;155(1):104-17.

6. Gao Y, Mania D, Mousavi SA, Lycus P, Arntzen M, Woliy K, et al. Competition for electrons favors N2O reduction in denitrifying Bradyrhizobium isolates. Environ Microbiol. 2021;23(4):2244–59.

7. Mania D, Woliy K, Degefu T, Frostegård Å. A common mechanism for efficient N2O reduction in diverse isolates of nodule-forming bradyrhizobia. Environ Microbiol. 2020;22(1):17-31.

8. Zhang Z, Zhang Y, Chen Y. Comparative metagenomic and metatranscriptomic analyses reveal the functional species and metabolic characteristics of an enriched denitratation community. Environ Sci Technol. 2020;54(22):14312-21.

9. Pachauri RK, Allen MR, Barros VR, Broome J, Cramer W, Christ R et al. Climate change 2014 synthesis report. contribution of working groups I, II, and III to the fifth assessment report of the Intergovernmental Panel on Climate Change. IPCC, 2014. 1 p.

10. Davidson EA, Kanter D. Inventories and scenarios of nitrous oxide emissions. Environ Res Lett. 2014;9(10):105012.

11. IPCC. Climate Change 2013: The Physical Science Basis. Contribution of Working Group I to the Fifth Assessment Report of the Intergovernmental Panel on Climate Change. [Stocker TF, Qin D, Plattner G-K, Tignor M, Allen SK, Boschung J et al. (editors)]. Cambridge University Press, United Kingdom and New York, NY, USA; 2013.

12. Volk C, Elkins J, Fahey D, Dutton G, Gilligan J, Loewenstein M, et al. Evaluation of source gas lifetimes from stratospheric observations. J Geophys Res Atmos. 1997;102(D21):25543-64.

13. Ravishankara AR, John SD, Robert WP. Nitrous oxide (N2O): The dominant ozone-depleting substance emitted in the 21st century. Science. 2009;326(5949):123-5.

14. Clark MA, Domingo NGG, Colgan K, Thakrar SK, Tilman D, Lynch J, et al. Global food system emissions could preclude achieving the 1.5° and 2°C climate change targets. Science. 2020;370(6517):705-8.

15. Rockström J, Steffen W, Noone K, Scheffer M. A safe operating space for humanity. Nature. 2009;461(7263):472-5.

16. Smith K, Crutzen P, Mosier A, Winiwarter W. The global nitrous oxide budget: a reassessment. In: Smith K, editor. Nitrous oxide and climate change. 1st ed. London: Routledge; 2010. p. 63-84.

17. Galloway JN, Townsend AR, Erisman JW, Bekunda M, Cai Z, Freney JR, et al. Transformation of the nitrogen cycle: Recent trends, questions, and potential solutions. Science. 2008;320(5878):889-92.

18. Herridge DF, Peoples MB, Boddey RM. Global inputs of biological nitrogen fixation in agricultural systems. Plant Soil. 2008;311(1-2):1-18.

19. Montzka SA, Dlugokencky EJ, Butler JH. Non-CO2 greenhouse gases and climate change. Nature. 2011;476(7358):43-50.

20. Iurii S, Neville M, Robertson GP. Global metaanalysis of the nonlinear response of soil nitrous oxide (N2O) emissions to fertilizer nitrogen. Proc Natl Acad Sci U S A. 2014;111(25):9199-204.

21. Tian H, Yang J, Xu R, Lu C, Canadell JG, Davidson EA, et al. Global soil nitrous oxide emissions since the preindustrial era estimated by an ensemble of terrestrial biosphere models: Magnitude, attribution, and uncertainty. Glob Chang Biol. 2019;25(2):640-59.

22. Garrido-Amador P, Kniaziuk M, Vekeman B, Kartal B. Learning from microorganisms: using new insights in microbial physiology for sustainable nitrogen management. Curr Opin Biotechnol. 2021;67:42-8.

23. Tian H, Xu R, Canadell JG, Thompson RL, Winiwarter W, Suntharalingam P, et al. A comprehensive quantification of global nitrous oxide sources and sinks. Nature. 2020;586(7828):248-56.

24. Rogelj J, Shindell D, Jiang K, Fifita S, Forster P, Ginzburg V. Mitigation pathways compatible with 1.5 °C in the context of sustainable development. In: Masson-Delmotte V, Zhai P, Pörtner H-O, Roberts D, Skea J, Shukla PR, editor. Global warming of 1.5 °C. An IPCC special report on the impacts of global warming of 1.5 °C above pre-industrial levels and related global greenhouse gas emission pathways, in the context of strengthening the global response to the threat of climate change, sustainable development, and efforts to eradicate poverty. 2018. In press.

25. Bakken LR, Frostegård Å. Emerging options for mitigating N2O emissions from food production by manipulating the soil microbiota. Curr Opin Environ Sustain. 2020;47:89-94.

26. Bergaust L, Mao Y, Bakken LR, Frostegård Å. Denitrification response patterns during the transition to anoxic respiration and posttranscriptional effects of suboptimal pH on nitrogen oxide reductase in Paracoccus denitrificans. Appl EnvironMicrobiol. 2010;76(19):6387-96.

27. Aamer M, Shaaban M, Hassan MU, Guoqin H, Ying L, Hai Ying T, et al. Biochar mitigates the N2O emissions from acidic soil by increasing the nosZ and nirK gene abundance and soil pH. J Environ Manage. 2020;255:109891.

28. Agegnehu G, Bass AM, Nelson PN, Bird MI. Benefits of biochar, compost and biochar–compost for soil quality, maize yield and greenhouse gas emissions in a tropical agricultural soil. Sci Total Environ. 2016;543(Pt A):295-306.

29. Jonassen KR, Hagen LH, Vick S, Arntzen M, Eijsink VG, Frostegard A, et al. Bacteria in biogas digestates for reduced climate forcing. bioRxiv. 2020.

30. Gilbert E, Crowley D. Repeated application of carvone-induced bacteria to enhance biodegradation of polychlorinated biphenyls in soil. Appl Microbiol Biotech. 1998;50(4):489-94.

31. Mallon CA, Le Roux X, Van Doorn G, Dini-Andreote F, Poly F, Salles J. The impact of failure: unsuccessful bacterial invasions steer the soil microbial community away from the invader's niche. ISME J. 2018;12(3):728-41.

32. Akiyama H, Hoshino YT, Itakura M, Shimomura Y, Wang Y, Yamamoto A, et al. Mitigation of soil N2O emission by inoculation with a mixed culture of indigenous Bradyrhizobium diazoefficiens. Sci Rep. 2016;6(1):32869.

33. Woliy KJ. Rhizobia in climate-smart agriculture - N_2 fixation effectiveness and N_2O reduction capacity of phylogenetically diverse Bradyrhizobium and Ensifer strains [PhD] Ås: Faculty of Chemistry, Biotechnology and Food Sciences, Norwegian University of Life Sciences; 2019.

34. Shapleigh JP. Denitrifying prokaryotes. In: Rosenberg E, DeLong EF, Lory S, Stackebrandt E, Thompson F, editors. The prokaryotes: Prokaryotic physiology and biochemistry. Berlin, Heidelberg: Springer Berlin Heidelberg; 2013. p. 405-25.

35. Sharma V, Noriega CE, Rowe JJ. Involvement of NarK1 and NarK2 proteins in transport of nitrate and nitrite in the denitrifying bacterium Pseudomonas aeruginosa PAO1. Appl Environ Microbiol 2006;72(5):3802.

36. Tiedje JM. Ecology of denitrification and dissimilatory nitrate reduction to ammonium. In: Zehnder AJB, editor. Biology of anaerobic microorganisms. New York: Wiley; 1988. p. 179-244.

37. Wittorf L, Jones CM, Bonilla-Rosso G, Hallin S. Expression of nirK and nirS genes in two strains of Pseudomonas stutzeri harbouring both types of NO-forming nitrite reductases. Res Microbiol. 2018;169(6):343-7.

38. Bothe H, Ferguson S, Newton WE. Biology of the nitrogen cycle. Amsterdam: Elsevier; 2007.

39. Schneider LK, Wüst A, Pomowski A, Zhang L, Einsle O. No laughing matter: The unmaking of the greenhouse gas dinitrogen monoxide by nitrous oxide reductase. In: Kroneck PMH, Torres MES, editors. The metal-driven biogeochemistry of gaseous compounds in the environment. Dordrecht: Springer Netherlands; 2014. p. 177-210.

40. Wunsch P, Zumft W, G. Functional domains of NosR, a novel transmembrane iron-sulfur flavoprotein necessary for nitrous oxide respiration. J Bacteriol. 2005;187(6):1992-2001.

41. Liu B, Mao Y, Bergaust L, Bakken LR, Frostegård Å. Strains in the genus Thauera exhibit remarkably different denitrification regulatory phenotypes. Environ Microbiol. 2013;15(10):2816-28.

42. Mania D, Heylen K, van Spanning RJM, Frostegård Å. Regulation of nitrogen metabolism in the nitrate-ammonifying soil bacterium Bacillus vireti and evidence for its ability to grow using N2O as electron acceptor. Environ Microbiol. 2016;18(9):2937-50.

43. Zumft WG. Cell biology and molecular basis of denitrification. Microbiol Mol Biol Rev. 1997;61(4):533-616.

44. Lycus P, Bøthun KL, Bergaust L, Shapleigh JP, Bakken LR, Frostegård Å. Phenotypic and genotypic richness of denitrifiers revealed by novel isolation strategy. ISME J. 2017;11:2219 - 32.

45. Semedo M, Wittorf L, Hallin S, Song B. Differential expression of clade I and II N2O reductase genes in denitrifying Thauera linaloolentis 47LolT under different nitrogen conditions. FEMS Microbiol Lett. 2020;367(24):fnaa205.

46. Gray DA, Dugar G, Gamba P, Strahl H, Jonker MJ, Hamoen LW. Extreme slow growth as alternative strategy to survive deep starvation in bacteria. Nat Commun. 2019;10(1):890-.

47. Lever MA, Rogers KL, Lloyd KG, Overmann J, Schink B, Thauer RK, et al. Life under extreme energy limitation: a synthesis of laboratory- and field-based investigations. FEMS Microbiol Rev. 2015;39(5):688-728.

48. Poirier Y, Nawrath C, Somerville C. Production of polyhydroxyalkanoates, a family of biodegradable plastics and elastomers, in bacteria and plants. Nat Biotechnol. 1995;13(2):142-50.

49. Juengert JR, Bresan S, Jendrossek D. Determination of polyhydroxybutyrate (PHB) content in Ralstonia eutropha using gas chromatography and nile red staining. Bio Protoc. 2018;8(5):e2748.

50. Schalk-Otte S, Seviour RJ, Kuenen JG, Jetten MSM. Nitrous oxide (N2O) production by Alcaligenes faecalis during feast and famine regimes. Water Res. 2000;34(7):2080-8.

51. Hein S, Simon J. Bacterial nitrous oxide respiration: electron transport chains and copper transfer reactions. Adv Microb Physiol. 2019;75:137-75.

52. Molstad L, Dörsch P, Bakken LR. Robotized incubation system for monitoring gases (O2, NO, N2O, N2) in denitrifying cultures. J Microbiol Methods. 2007;71(3):202-11.

53. Bakken LR. Spreadsheets for gas kinetics [Internet] Ås; Norwegian University of Life Sciences; 2013 Dec 6 [2020 Aug 27; 2020 Sep 1]. Available from: https://www.nmbu.no/en/research/groups/nitrogen/spreadsheets-

54. Suenaga T, Hori T, Riya S, Hosomi M, Smets BF, Terada A. Enrichment, isolation, and characterization of high-affinity N2O-reducing bacteria in a gas-permeable membrane reactor. Environ Sci Tech. 2019;53(20):12101-12.

55. Monod J. From enzymatic adaptation to allosteric transitions. Nobel Lecture 1965: Science; 1966. p. 475-83.

56. Commichau FM, Gunka K, Landmann JJ, Stülke J. Glutamate metabolism in Bacillus subtilis: gene expression and enzyme activities evolved to avoid futile cycles and to allow rapid responses to perturbations of the system. J Bacteriol. 2008;190(10):3557-64.

57. Imlay JA. The molecular mechanisms and physiological consequences of oxidative stress: lessons from a model bacterium. Nat Rev Microbiol. 2013;11(7):443-54.

58. Qu Z, Bakken LR, Molstad L, Frostegård Å, Bergaust LL. Transcriptional and metabolic regulation of denitrification in Paracoccus denitrificans allows low but significant activity of nitrous oxide reductase under oxic conditions. Environ Microbiol. 2016;18(9):2951-63.

59. Højberg O, Binnerup SJ, Sørensen J. Growth of silicone-immobilized bacteria on polycarbonate membrane filters, a technique to study microcolony formation under anaerobic conditions. Appl Environ Microbiol. 1997;63(7):2920.

60. Hassan J, Qu Z, Bergaust LL, Bakken LR. Transient accumulation of NO2-and N2O during denitrification explained by assuming cell diversification by stochastic transcription of denitrification genes. PLoS Comput Biol. 2016;12(1):e1004621.

61. Lalucat J, Bennasar A, Bosch R, García-Valdés E, Palleroni NJ. Biology of Pseudomonas stutzeri. Microbiol Mol Biol Rev. 2006;70(2):510.

62.Stanier RY, Palleroni NJ, Doudoroff M. The aerobic pseudomonads a taxonomic study. Microbiology. 1966;43(2):159-271.

63. Chen H-B, Yang Q, Li X-M, Wang Y, Luo K, Zeng G-M. Post-anoxic denitrification via nitrite driven by PHB in feast–famine sequencing batch reactor. Chemosphere. 2013;92(10):1349-55.

64. Arntzen MØ, Karlskås IL, Skaugen M, Eijsink VGH, Mathiesen G. Proteomic investigation of the response of Enterococcus faecalis V583 when cultivated in urine. PLoS One. 2015;10(4):e0126694-e.

7. Appendix

7.1 Appendix A: Media for bacterial growth

All the compositions below are used for 1 X media.

7.1.1 Sistrom's medium

Table 7.1.1: The chemical composition of Sistrom's medium**.**

Chemical	**Weight/volume**
K_2HPO_4	3.48 g
or KH_2PO_4	2.72 g
$(NH_4)_2SO_4$	0.5 g
or NH_4Cl	0.195 g
Succinic acid	4.00 g
L – Glutamic acid	0.10 g
L – Aspartic acid	0.04 g
NaCl	0.5 g
Nitrilotriacetic acid	0.20 g
$MgSO_4$ x $7H_2O$	0.30 g
or $MgCl_2$ x $6H_2O$	0.244 g
$CaCl_2$ x $2H_2O$	0.0334 g
$FeSO_4$ x $7H_2O$	0.0020 g
$(NH_4)_6Mo_7O_{24}$ (1 % solution)	0.02 ml
Trace Elements Solution	0.1 ml
Vitamins Solution	0.1 ml
Distilled water	1000.00 ml

Table 7.1.2: The chemical composition of the trace elements solution used in Sistrom's medium and Sistrom's buffer.

Chemical	Weight/volume
EDTA	1.765 g
$ZnSO_4$ x $7H_2O$	10.95 g
$FeSO_4$ x $7H_2O$	5.0 g
$MnSO_4$ x H_2O	1.54 g
$CuSO_4$ x $5H_2O$	0.392 g
$Co(NO_3)_2$ x $6H_2O$	0.248 g
H_3BO_3	0.114 g
Distilled water	100 ml

Table 7.1.3: The chemical compositions of the vitamins solution for Sistrom's medium.

Chemical	Weight/volume
Nicotinic acid	1.0 g
Thiamine HCl	0.5 g
Biotin	0.010 g
Distilled water	100 ml

7.1.2 R2A medium

Table 7.1.4: The chemical composition of R2A medium.

Chemical	Weight/volume
Yeast extract	0.50 g
Proteose Peptone (Difco no. 3)	0.50 g
Casamino acids	0.50 g
Glucose	0.50 g
Soluble starch	0.50 g
Na-pyruvate	0.30 g
K2HPO4	0.30 g
MgSO4 x 7H2O	0.05 g
Distilled water	1000.00 ml

7.1.3 *Thauera* medium

Table 7.1.5: The chemical composition of *Thauera* medium (41).

Chemical	Weight/volume
20 x mineral solution	50 mL
KH_2PO_4	2.53 g
K_2HPO_4	14.2 g
Peptone from meat	5 g
Meat extract	3 g
Distilled water	1000.00 ml

7.1.4 Sistrom's buffer

Table 7.1.6: The chemical composition of buffer derived from Sistrom's medium.

Chemical	Weight/volume
K_2HPO_4	1.74 g
$(NH_4)_2SO_4$	0.25 g
NaCl	0.25 g
$MgSO_4$ x $7H_2O$	0.15 g
$CaCl_2$ x $2H_2O$	0.0167 g
$FeSO_4$ x $7H_2O$	0.0010 g
$(NH_4)_6Mo_7O_{24}$ (1 % solution)	0.01 ml
Trace Elements Solution	0.05 ml
Distilled water	1000.00 ml

7.1.5 Phosphate buffered saline (PBS)

Table 7.1.7: The chemical composition of phosphate buffered saline.

Chemical	Weight
NaCl	8.475 g
Na_2HPO_4 x $2H_2O$	1.093 g
NaH_2PO_4 x H_2O	0.276 g
Distilled water	1000.00 ml

7.2 Appendix B: R code for fitting a simple linear regression model in RStudio

```
library(readxl)
library(ggplot2)
OD_CFU <- read_excel("Master/OD_CFU.xlsx")
linear_regression <- lm(CFU ~ OD, data=OD_CFU)
summary(linear_regression)
```

Figure 7.2.1: Fitting a simple linear regression model for the relationship between OD and CFU.

```
Coefficients:
             Estimate Std. Error t value Pr(>|t|)
(Intercept)   1323671     430309   3.076  0.20010
OD          163304010    1310053 124.655  0.00511 **
---
Signif. codes:  0 ‘***’ 0.001 ‘**’ 0.01 ‘*’ 0.05 ‘.’ 0.1 ‘ ’ 1

Residual standard error: 540400 on 1 degrees of freedom
Multiple R-squared:  0.9999,    Adjusted R-squared:  0.9999
F-statistic: 1.554e+04 on 1 and 1 DF,  p-value: 0.005107
```

Figure 7.2.2: Output from fitting a simple linear regression model in RStudio. n = 3.

```
ggplot(data = OD_CFU, aes(x=OD, y=CFU)) + geom_point() +
  geom_abline(intercept = 1323671, slope=163304010, color="red") +
  labs(x= "OD600",y="CFU/ml")
```

Figure 7.2.3: Plotting values for OD (x-axis) and CFU (y-axis), with the estimated regression line from Figure 7.2.2.

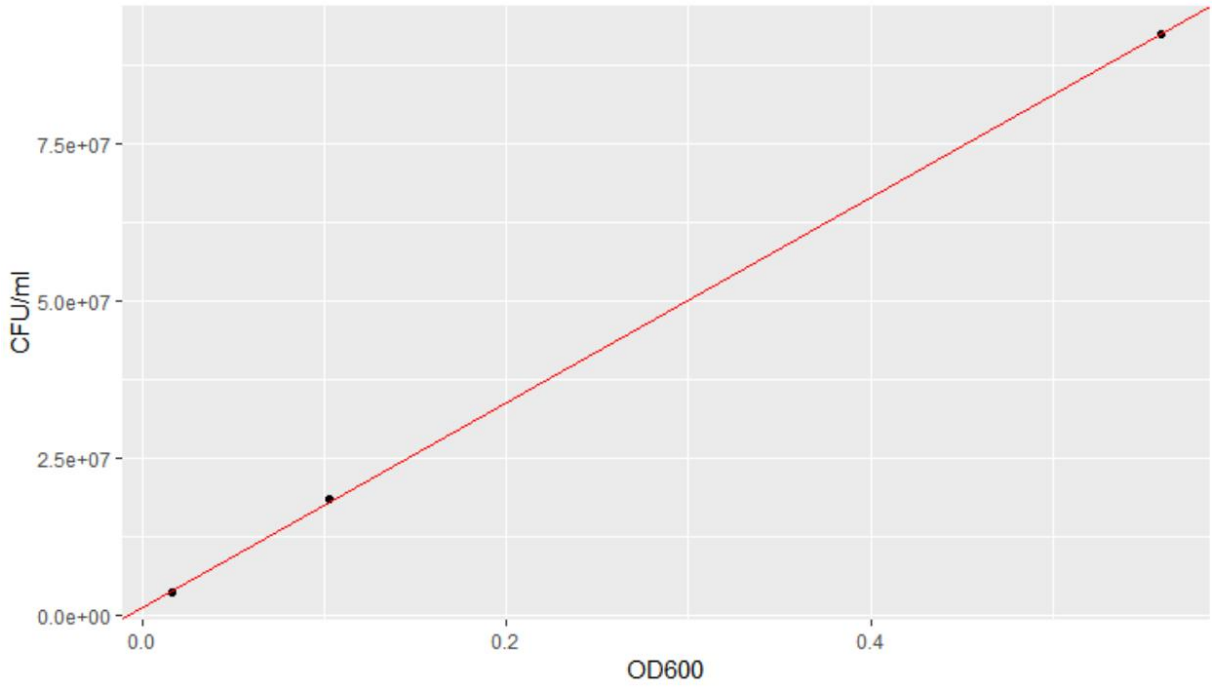

Figure 7.2.4: Estimated regression line. The linear relationship between OD_{600} and CFU/ml is presented in the standard curve. $R^2 = 0.9999$.

7.3 Appendix C: Proteomics

An attempt was made to determine the relative amounts of denitrification reductases during denitrification, by analysing the cell proteome. This was done for both well-fed and starved cultures of *P. stutzeri* JM300, and well-fed cultures of *T.* sp. 27. The samples were obtained by centrifuging entire incubation flasks (~50 ml liquid culture) and storing the cell pellets at –20 °C. The time points for sampling were determined by monitoring the gas kinetics in real time. Samples were taken in triplicates from the inoculum, during N_2O reduction and at the onset of nitrate reduction upon the depletion of N_2O. Two different methods for peptide extraction were used. Unfortunately, no results were obtained.

For cells of *P. stutzeri*, the extraction of the proteome did not go as planned. The well-fed cells excreted a large amount of exopolysaccharides (slime) that clogged the Strap filters used in the proteome extraction (see Appendix 7.3.2 for the protocol). This made following the protocol impossible. Although this was only the case for well-fed cells, and not starved cells, the proteome of well-fed cells was essential as a negative control. Had I had more time, I could have used a protocol developed by Arntzen et al (64) (Appendix 7.3.1). This protocol is

based on the separation of peptides using an SDS-gel, and is presumably not as sensitive towards slime. However, this is a rather time-consuming method, and previous attempts to use it were unsuccessful. Even though the extracted peptides were of high concentrations and quality (Table 7.3.1) only the longest peptides were successfully extracted.

The peptides from cells of *T.* sp. 27 were extracted according to the protocol in Appendix 7.3.2, seemingly without difficulties, and yielded high peptide concentrations (see Table 7.3.2). Despite this, the MS analysis did not give reliable chromatographic results, as they deviated between samples (Appendix 7.3.3). NosZ was not found among the extracted proteins, even though it is a periplasmic enzyme and N_2O was reduced by the cells. Additionally, the retention times for equal peptides varied with more than 60 seconds. All these factors made the results questionable. It was suggested that the problems were caused by the production of slime. This is possible, as anaerobic cells of *T.* sp. 27 seemed to aggregate (based on visual evaluations), which could be due to the production of slime. It was only the chromatograms of anaerobic cells that were problematic, further supporting that slime production was the culprit. Later studies should take the production of slime under consideration, and use a method less susceptible to slime. For future research, it may also be possible to remove the slime through enzymatic degradation.

7.3.1 Peptide extraction with gel separation

This protocol is developed by Arntzen et al (64). The cell pellets were dissolved in 300 µL lysis buffer and lysed by bead beating (0.2 g 106 micron glass beads) in a FastPrep for 2*45 seconds at 6.5 m/s. The protein concentration in the supernatant was determined by using a BCA protein assay. 5 µL supernatant was diluted in 45 µL ddH_2O and added to 1 mL BCA working solution. The samples were incubated at 60 °C for 30 minutes, and the absorbance at 562 nm was measured to determine the protein concentration. The samples were diluted, if necessary, to final concentrations of about 2 µg/µL. 20 µL of the sample was mixed with 7.5 µL Nupage 4x sample buffer and 3 µL Nupage 10x reducing agent, and incubated at 70°C for 10 minutes. Prior to gel application, the samples were spun down (1 min, 10 000g). 25 µL of the samples were applied in wells in an SDS-page gel. Each well was loaded with between

15-20 µg protein. The gel container was filled with TGS buffer to an appropriate volume, and the gel was run at 270 V for 4-5 minutes, until the bonds had travelled some centimetres. The gel was stained with Coomassie blue for 1 hour, and washed twice with ddH_2O before destaining. The gel was first destained twice for 20 minutes with a 100 % solution (ddH_2O, methanol and acetic acid in the ratio 50/40/10 [v/v/v]), and then ON in a 50 % solution.

After destaining, the gel bands were cut out of the gel into 1x1 mm cubes, and transferred to Eppendorf Protein LoBind tubes. 200 µL ddH_2O was added, and the samples were incubated for 15 minutes at RT in a thermo mixer (800 rpm). After incubation, the liquid was removed, and the samples were incubated with 200 µL ACN/AmBic (50 % acetonitrile (ACN)/25mM ammonium bicarbonate (AmBic)) for 15 minutes at RT in a thermo mixer (800 rpm). This step was repeated once. The samples were incubated for 5 minutes at RT with 100 µL 100% ACN in a thermo mixer (800 rpm). The liquid was removed, and the samples air dried for 1-2 minutes. The samples were then reduced by adding 50 µL DTT (dithiothreitol) solution (10 mM DTT/100 mM AmBic), and incubated for 30 minutes at 56 °C in a thermo mixer (800 rpm). After the samples had cooled down, and excess DTT was removed, 50 µL iodoacetamide (IAA) solution (55 mM IAA/100 mM AmBic) was added to alcylate the samples. The samples were incubated for 30 minutes at RT in the dark. Excess IAA was removed, and 200 µL 100 % ACN was added. The samples were incubated for 5 minutes at RT in a thermo mixer (800 rpm). Excess liquid was removed, and the samples were air dried for 1-2 minutes.

Digestion of the proteins was done by adding 30 µL Trypsin solution (10 ng/µL trypsin in trypsin buffer (25 mM AmBic/10 % ACN) and incubating for 30 minutes on ice. The gel pieces were covered with additional trypsin buffer and incubated ON at 37 °C in a thermo mixer (800 rpm). After incubation, 40 µL 1 % trifluoroacetic acid (TFA) was added to the samples, and they were sonicated on a water bath at RT for 15 minutes. To prepare the samples for MS, the last steps were performed using special tips (ZipTips). These were conditioned to enhance binding, and equilibrated between sample series. The equilibration was done by pipetting up 20 µL 100% MeOH, which was discarded to waste. 10 µL 70 % ACN/0.1 % TFA was pipetted up and discarded to waste, and the same was done with 10 µL

0.1 % TFA. To bind the samples, they were pipetted up and down 4 times using the equilibrated ZipTip. The tip was then cleaned with a tissue. The samples were washed by pipetting up 10 µL 0.1 % TFA, which was discarded to waste. The samples were eluted in an HPLC vial by pipetting up and down 4 times in 100 % ACN/0.1 % TFA. The samples in the HPLC vials were concentrated using a Speedvac, until they were dry. The peptides were dissolved in 10 µL 2 % ACN/0.1 % TFA. Before analysis, the peptides were sonicated for 5 minutes, and the peptide concentration was determined with Nanodrop at 205 nm (see Table 7.3.1). The samples were analysed using reverse phase chromatography, using a highly hydrophobic C18 column. MS/MS and QTOF was used. The analysis was operated in PASEF mode.

Table 7.3.1: Peptide concentration and qualities of samples from *P. stutzeri* JM300.

Sample	**Concentration [mg/ml]**	**A205**	**A280**
1.0.1	0.389	12.06	0.05
1.0.2	0.313	9.71	-0.07
1.0.3	0.355	11.0	0.02
2.0.1	0.338	10.47	-0.04
2.0.2	0.351	10.87	-0.02
2.0.3	0.358	11.09	0.01
2.2.1	0.359	11.12	0.00
2.2.2	0.290	8.98	0.07
2.2.3	0.367	11.38	0.04

7.3.2 Peptide extraction using STrap tips

This protocol for preparing samples for proteomic analyses is developed by Morten Skaugen (pers. com.). It uses STrap tips to extract the peptides from the lysed cells. The tips were prepared by stacking discs of Empore C18 (2 discs) and Munktell MK360 quartz filter (12 discs) in a Protein LoBind pipette tip and adding 270 µl STrapping solution (90 % methanol and 100 mM Tris pH 7.1). The tips were placed in LoBind eppendorf tubes for collection of the flow through, and turned 180° for each centrifugation step.

The cell pellets were dissolved in 500 µl lysis buffer (4 % SDS, 50 mM Tris-Cl (pH 7.9), 10 mM dithiothreitol (DTT)) and heat treated at 95 °C for 10 minutes. The cells were lysed through bead beating (0.2 g 106 micron glass beads) in a FastPrep for 3 x 45 seconds at 6.5 m/s. Thirty-six µl of the supernatant was alkylated with iodoacetamide (IAA) to a final concentration of 50 mM, and incubated in the dark for 20 minutes. After alkylation, the samples were acidified by adding 4 µl phosphoric acid (12.5 %). Twenty µl of the samples were loaded into the STrapping solution and spun down (10 min, 4000 g). The STrap tips were washed by spinning through 100 µl STrapping solution, whereupon 50 mM ammonium bicarbonate (AmBic) was added and spun down. The tips were transferred to a new Protein LoBind collection tube and the proteins, located in the filter, were digested by briefly spinning a trypsin solution (33 ng/µl trypsin in 50 mM AmBic) into the filters. The protein digestion was performed for 45-60 minutes at 47 °C.

After trypsination the trypsin was spun through the column, and 50 µl 0.5 % trifluoroacetic acid (TFA) was added to the flow through, which was spun through the column once more. The column was washed by spinning down 100 µl 0.1 % TFA, and the STrap tip was added to a new Protein LoBind collection tube. The peptides were eluted by shortly spinning an elution solution (80 % acetonitrile (ACN)/0.1 % TFA) into the column, and letting it sit for 2 minutes, before completing the elution by centrifugation for about 5 minutes at 2500 g.

The samples were dried using a SpeedVac and dissolved in 10 µl loading solution (2 % ACN/0.1 % formic acid). The samples were sonicated at RT for 10 minutes and the protein concentration was determined using Nanodrop (see Table 7.3.2). The samples were diluted in loading solution to 200 ng/µl if necessary and stored at 4 °C. They were analysed using reverse phase chromatography, using a highly hydrophobic C18 column. MS/MS and QTOF was used. The analysis was operated in PASEF mode.

Table 7.3.2: Peptide concentration and qualities of samples from *Thauera* sp. 27.

Sample	Oxic/Anoxic	Concentration [mg/ml]	A205	A280
T01	Oxic	0.292	9.25	1.23
T02	Oxic	0.246	7.63	0.07
T03	Oxic	0.359	11.13	0.10
T12	Anoxic	0.305	9.44	0.52
T13	Anoxic	0.298	8.97	0.28
T21	Anoxic	0.183	5.67	0.12
T22	Anoxic	0.296	9.18	0.35
T23	Anoxic	0.291	9.01	0.28
T31	Anoxic	0.323	10.01	0.30
T32	Anoxic	0.371	11.52	0.39
T33	Anoxic	0.361	11.19	0.40

7.3.3 Chromatograms

Three of the analysed samples from *T.* sp. 27 with peptides from cells grown under oxic conditions showed similar chromatograms which were reliable, even though the total ion current (TIC) was a little lower than expected. This could be caused by a low loading volume. A representative chromatogram for the three first samples is shown in Figure 7.3.1.

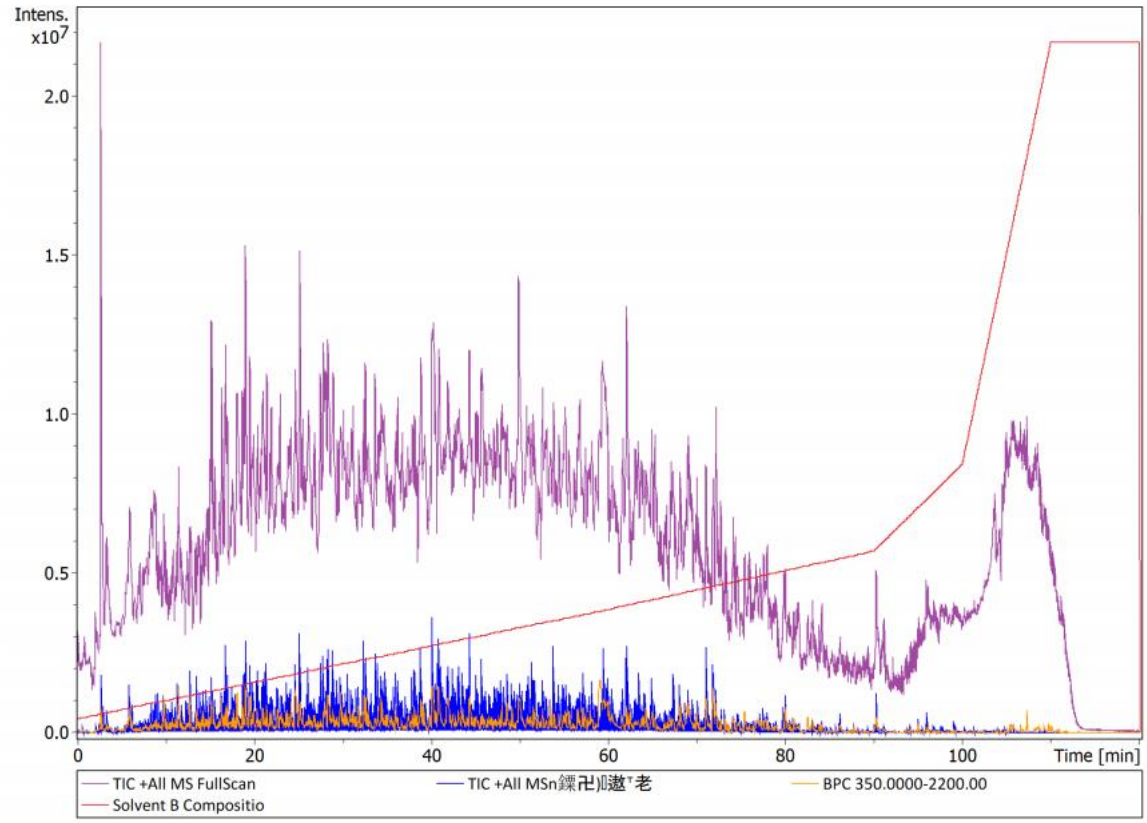

Figure 7.3.1: The chromatogram from sample T01 (*T.* sp. 27), with peptides from cells grown under oxic conditions. The total ion current is sensible, and peptides are eluted from the column during the entire run time (seen as purple peaks). The solvent is eluted at the end of the run (red signal).

The peptide samples from samples T12 and onwards showed non reliable chromatograms. These samples were obtained from cells grown under anoxic conditions. The TIC was very low for these samples, and almost all peptides were eluted at the end of the run, together with the solvent. A representative chromatogram is shown in Figure 7.3.2.

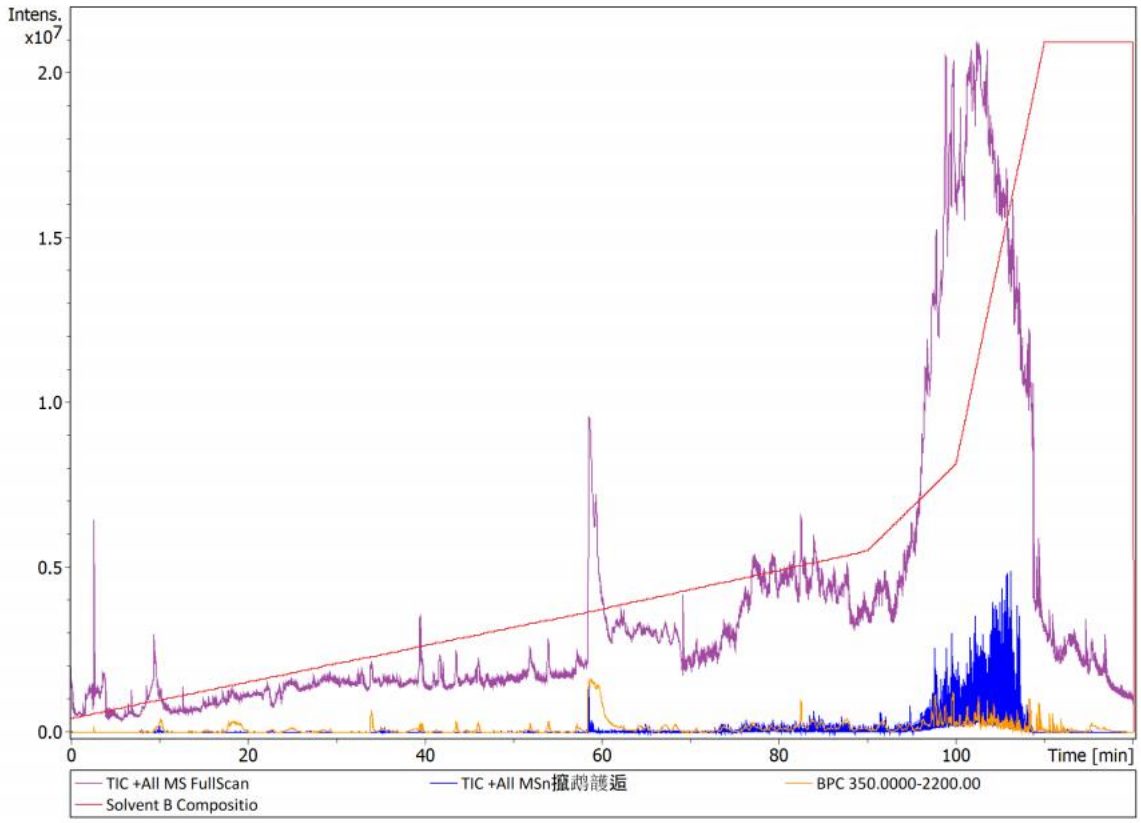

Figure 7.3.2: Chromatogram for peptides obtained from anaerobic cells of *T.* sp. 27. The TIC is very low throughout the runtime, and a majority of the peptides (purple peeks) are eluted together with the solvent (red).

7.4 Appendix D: Incubation of starved *P. stutzeri* JM300

When studying the 115 hours of oxic respiration in the starvation experiment of *P. stutzeri*, it seemed as if the cells were actively reducing N_2O, as the concentration of N_2O-N gradually decreased (Figure 7.4.1). However, just a fraction of the "reduced" N_2O was recovered as N_2-N, leading to the conclusion that N_2O was not removed through denitrification. The disappearance of N_2O was quickly assigned to headspace dilution during sampling, when He-gas replaces the sampled gas, leading to a constant dilution of the headspace. This dilution was evident in long-time incubations with little metabolic activity. Another indication that the decrease in N_2O-N was due to headspace dilution was seen when the cycle time for sampling was reduced (after ~ 40 hours). Up until this point, the decrease in N_2O-N was linear, but the rate decreased once the cycling time was increased, but remained linear. This was a strong indication that the decrease in N_2O-N was primarily caused by a constant dilution, and only to a very little degree microbial activity.

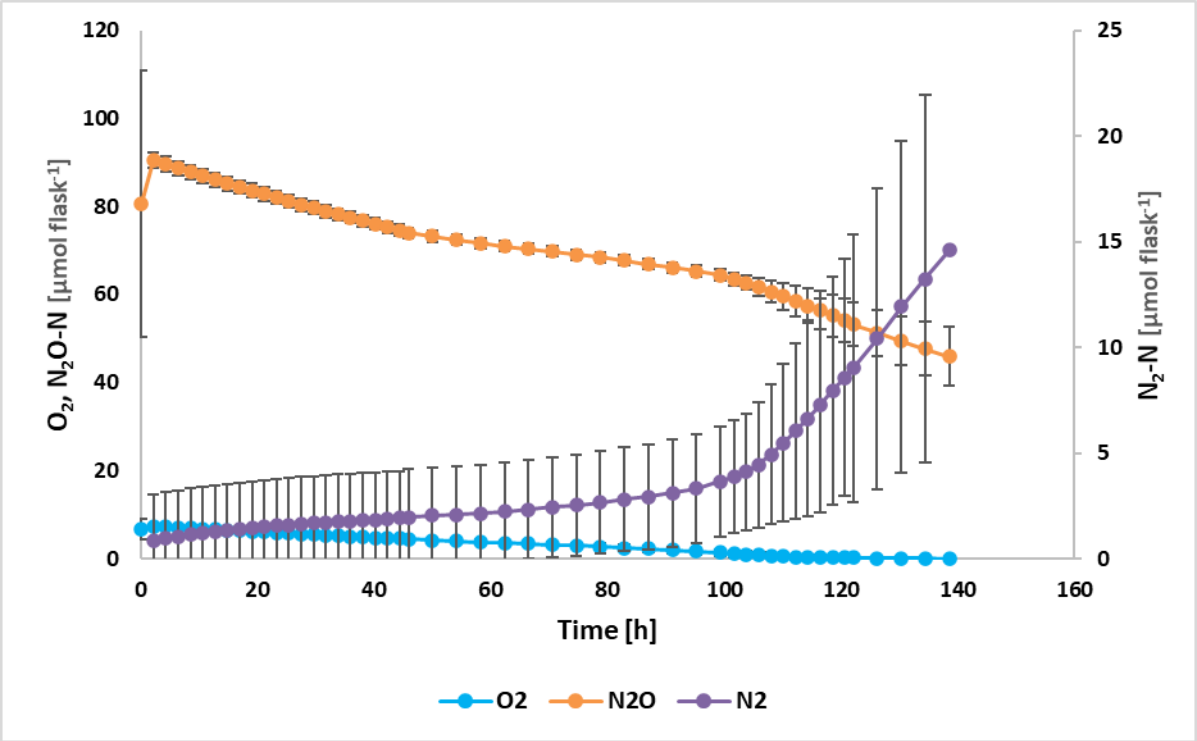

Figure 7.4.1: The complete incubation of starved *P. stutzeri*. Oxygen is gradually reduced during the first 100-120 hours. The concentration of N_2O-N shows a considerate decrease from the start of the incubation, but this is likely due to dilution of the headspace during sampling. The cycle time for sampling is reduced from 2 hours to 4 hours after 40 hours, and increased again when the concentration of N_2-N started to increase. Note that the concentration of N_2-N is given on the right-hand axis. Even though N_2-N increases throughout the incubation, the concentration of N_2-N is approximately 5 µmol flask^{-1} when the concentration of N_2O-N has decreased with approximately 20 µmol flask^{-1}. Standard deviations are given as vertical bars (n = 9).

7.5 Appendix E: Calculating cell specific electron flow

The calculations behind estimating cell specific electron flow rate were presented to me by Lars Bakken (pers.comm). They were based on the assumption that the cells grow exponentially when carbon sources are available. Based on this, an estimate of the exponential growth curve could be made. The estimate was based on the observed electron flow to the available electron acceptor per flask, from timepoint to timepoint. During exponential growth, the relationship between initial electron flow rate ($V(0)$) and growth rate (μ) can be summarized like this:

$$V(0)^{\mu * t}$$ Equation 7.5.1

V_{max} was set as $2*10^{-13}$ mol e $cell^{-1}$ h^{-1}. The relationship between growth yield (Y), growth rate (μ) and V_{max} is

$$Y = \frac{\mu}{V_{max}}$$ Equation 7.5.2

The initial cell number ($N(0)$) was calculated:

$$N(0) = \frac{V(0)}{V_{max}}$$ Equation 7.5.3

By using the parameters found from Equations 7.5.1, 7.5.2 and 7.5.3, the cell number throughout the incubation time ($N(t)$) was calculated, based on the electron flow to the available electron acceptor:

$$N(t) = N(0) + eflow * 10^6 * Y$$ Equation 7.5.4

The cell specific respiration at each timepoints was calculated, and given as % of V_{max}.

7.6 Appendix F: Gas kinetics of discarded *Thauera* strains

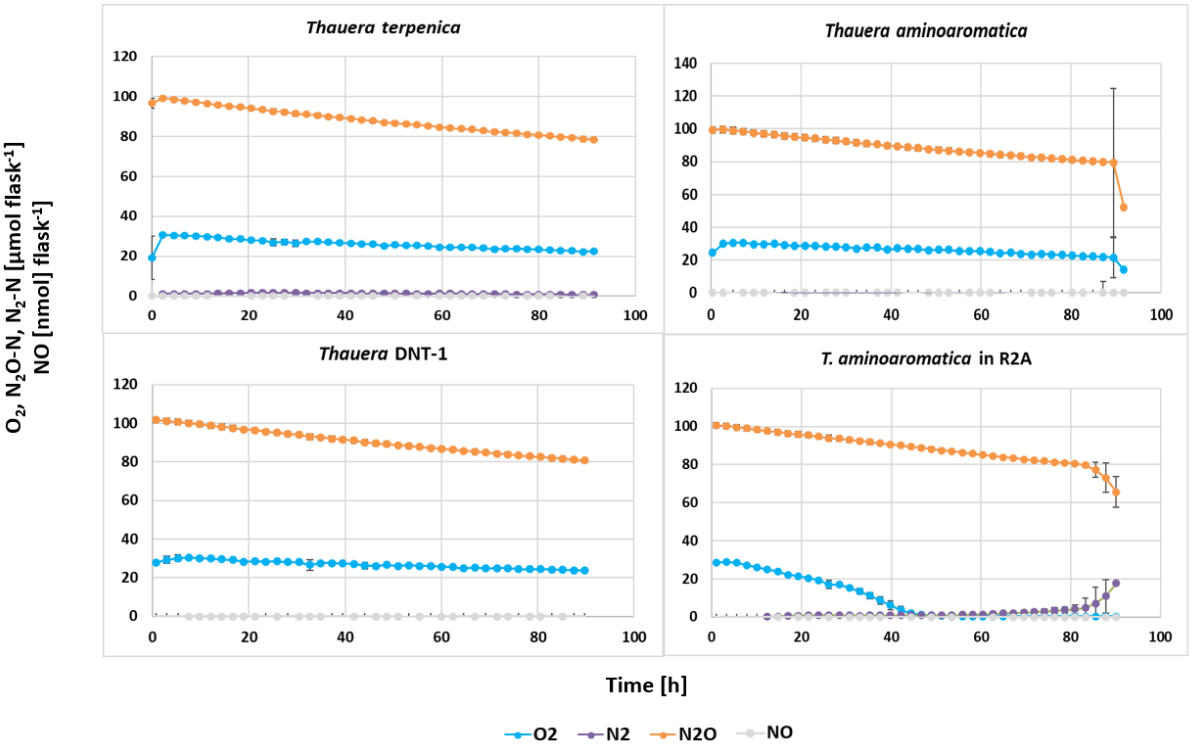

Figure 7.6.1: Gas kinetics of the three discarded *Thauera* strains. All cells were grown in *Thauera*-medium, except the culture which gas kinetics in shown in the bottom right corner. These cells were grown in R2A-medium. The strains were well-fed, and supplied with ~ 20 µmol O_2, ~ 100 µmol N_2O and 100 µmol NO_3^-. The decrease in N_2O for cultures grown in Thauera-medium is assigned to head space dilution during sampling. None of the cultures showed significant denitrification activity whilst grown in *Thauera*-medium. The culture grown in R2A-medium showed oxic respiration during the first 40 hours. No denitrification was seen before the cells had been incubated for 80 hours, when the reduction rate of N_2O increased and a production of N_2 was seen. Standard deviations are given as vertical bars, but are often too small to be seen (n=3).

7.7 Appendix G: Late expression of *narG* in *P. stutzeri* JM300

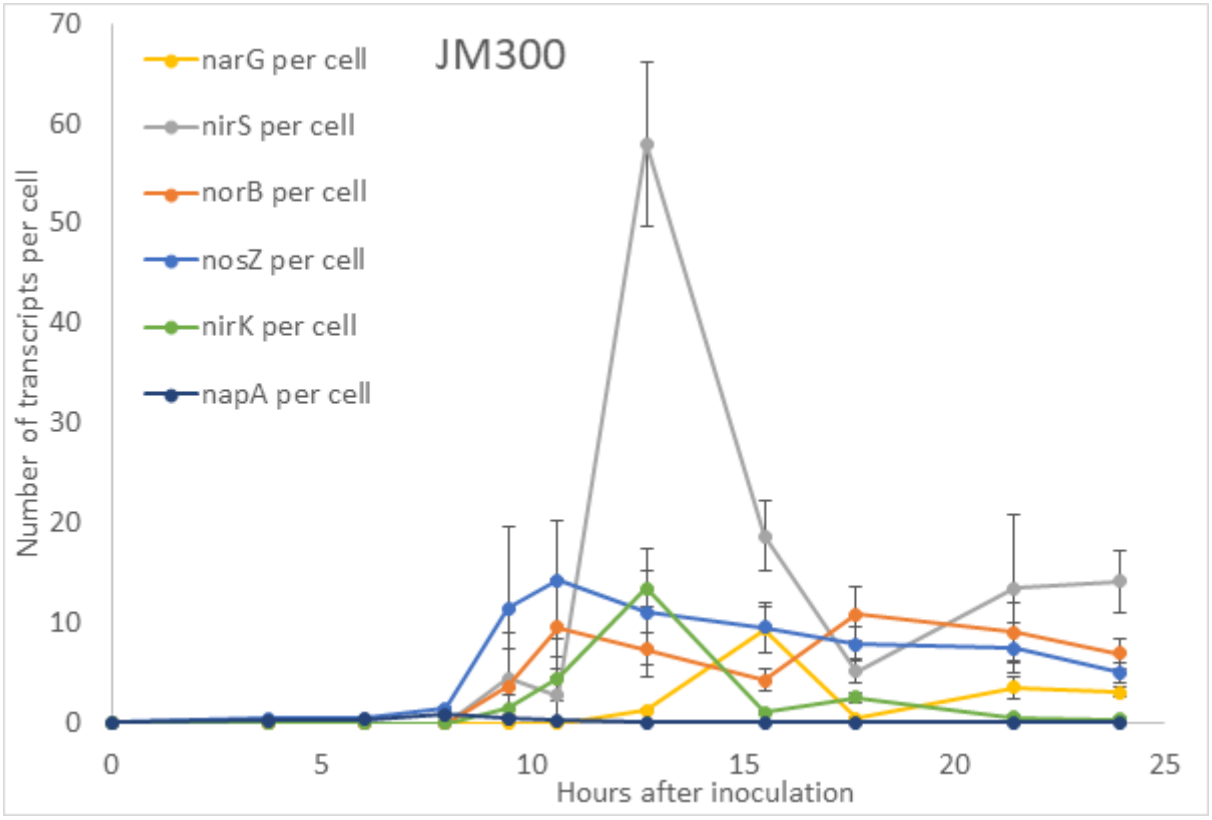

Figure 7.7.1: The transcription of different denitrification reductases in an incubation of *P. stutzeri* JM300 during the transition from oxic to anoxic conditions. *napA* is expressed in small amounts after 7 hours, together with *nosZ*. *narG* is not expressed until 12-13 hours after inoculation, with a peak of transcripts after 15 hours.

Norges miljø- og biovitenskapelige universitet
Noregs miljø- og biovitskapelege universitet
Norwegian University of Life Sciences

Postboks 5003
NO-1432 Ås
Norway